University of Massachusetts Boston
ScholarWorks at UMass Boston

Graduate Doctoral Dissertations | Doctoral Dissertations and Masters Theses

6-1-2014

Exploring the Link between Otolith Growth and Function along the Biological Continuum in the Context of Ocean Acidification

Eric D. Wilcox Freeburg
University of Massachusetts Boston

Follow this and additional works at: https://scholarworks.umb.edu/doctoral_dissertations

Part of the Environmental Sciences Commons, Geology Commons, Mineral Physics Commons, and the Oceanography Commons

Recommended Citation

Wilcox Freeburg, Eric D., "Exploring the Link between Otolith Growth and Function along the Biological Continuum in the Context of Ocean Acidification" (2014). *Graduate Doctoral Dissertations*. 164.
https://scholarworks.umb.edu/doctoral_dissertations/164

This Open Access Dissertation is brought to you for free and open access by the Doctoral Dissertations and Masters Theses at ScholarWorks at UMass Boston. It has been accepted for inclusion in Graduate Doctoral Dissertations by an authorized administrator of ScholarWorks at UMass Boston. For more information, please contact scholarworks@umb.edu.

EXPLORING THE LINK BETWEEN OTOLITH GROWTH AND FUNCTION ALONG THE BIOLOGICAL CONTINUUM IN THE CONTEXT OF OCEAN ACIDIFICATION

A Dissertation Presented

by

ERIC D. WILCOX FREEBURG

Submitted to the Office of Graduate Studies,
University of Massachusetts Boston
in partial fulfillment of the requirements for the degree of

DOCTOR OF PHILOSOPHY

June 2014

Environmental Sciences Program

© 2014 by Eric D. Wilcox Freeburg
All rights reserved

EXPLORING THE LINK BETWEEN OTOLITH GROWTH AND FUNCTION ALONG THE BIOLOGICAL CONTINUUM IN THE CONTEXT OF OCEAN ACIDIFICATION

A Dissertation Presented
by
ERIC D. WILCOX FREEBURG

Approved as to style and content by:

_____
Robyn Hannigan, Dean
Chairperson of Committee

_____
William E. Robinson, Professor
Member

_____
Meng Zhou, Professor
Member

_____
Solange Brault, Associate Professor
Member

_____
Ellen Douglas, Program Director
Environmental Sciences Program

_____
Robyn Hannigan, Dean
School for the Environment

ABSTRACT

EXPLORING THE LINK BETWEEN OTOLITH GROWTH AND FUNCTION ALONG THE BIOLOGICAL CONTINUUM IN THE CONTEXT OF OCEAN ACIDIFICATION

June 2014

Eric D. Wilcox Freeburg, B.A., Luther College
Ph.D., University of Massachusetts Boston

Directed by Professor Robyn Hannigan

Oceans are acidifying as atmospheric CO_2 is drawn down. This process, known as ocean acidification (OA), is well known and documented. Over the next 100 years, pH of the surface ocean is projected to decrease by up to 0.35 units. This CO_2 draw down has a direct effect on dissolved inorganic carbon (DIC) balance in the ocean. OA is expected to impact calcifying organisms that rely on constituencies of the DIC system, specifically carbonate ion $[CO_3^{2-}]$. It is clear that externally calcified structures, such as coral skeletons, bivalve shells, etc., will be significantly affected as pH, and consequently $[CO_3^{2-}]$, of the oceans decline. What is unclear, however, is how these changes will impact internally calcified structures, such as earstones (otoliths) of teleost fish. This dissertation examines the impacts of OA on otolith mineralization in larval reef fish (*Amphiprion clarkii* and *A. frenatus)*. This research included the development of a

laboratory controller system for control of experimental aquaria pH through pCO_2 dosing, exposure of larvae from hatch to settlement under various pCO_2 treatments and evaluation of otolith structure and morphology across treatments within a single genus.

No standard method for pH-stat CO_2 dosing controllers existed prior to this study. Incorporating low-cost, flexible hardware allowed high precision and accuracy pH controllers to be designed and implemented. Following system stability studies, we found that our system performed at or beyond the level of control exhibited in the literature.

Two species of clownfish, *Amphiprion clarkii* and *A. frenatus*, were exposed to different pCO_2 conditions, reared to settlement and otoliths extracted and studied. I found that the sagittae (largest of the 3 otolith types) of both species exhibited circularity changes towards more oblong otoliths under increased pCO_2. For *A. clarkii*, I found a significant negative relation between pCO_2 and lapilli otolith circularity, indicating a shift toward more circular lapilli under increased pCO_2. Since lapilli are critical to gravisensing in teleosts these results explain my anecdotal observations that, at high pCO_2, larvae exhibited lethargic, uncoordinated swim patterns. The core development of otoliths (sagittae, lapilli, and asterisci) from both species was analyzed using SEM imagery. Otolith images were scored by 6 independent readers for core development (poorly developed to well-developed). Otolith scores were regressed against aragonite saturation state (Ω_{Ar}). Results showed significant and strong relations between Ω_{Ar} and development score, indicating a shift toward protruding, unorganized crystal clusters within the core under high pH/low Ω_{Ar}.

This research is the first to comprehensively examine the impact of OA on the otolith system in larval fish. The research revealed direct impacts on otolith structure and morphology as well as mineralogy. These changes will directly impact survival of the larvae. It remains unknown whether the otolith system recovers post-settlement or whether the anecdotal observations on swimming behavior are directly related to otolith deformation. Future research will include exploration of these relations across genera as well as more deeply examine the recovery of the system and behavioral impacts of otolith deformation across life stages.

ACKNOWLEDGEMENTS

I would like to thank all of my friends and colleagues over the past years at both the University of Massachusetts - Boston, and Arkansas State University. Alan, Alex, Ashley, Jeremy, Katie, Nicole, Rob, Steve and others - you have been a major part of this endeavor. I would like to especially thank Bryanna for being there to help out, commiserate, and witness grumpy mornings and loopy overnight sessions. Working with all of you has been an honor and privilege.

I would also like to thank all of my undergraduate assistants over the years: Sonali, Lindsey, Jill, Dan, Allex and Matt. It has been fun to get to know each of you and to have you become an integral part of my research projects. I would like to especially thank Kristen, Shawna, Jackie, and Drew for being especially integral parts of running experiments and helping with the data processing. Without you, I would still be a long way off.

To my advisor, Robyn, thank you for giving me the long leash I needed to find my own voice and take ownership of my work. Thank you for being supportive, encouraging, and understanding. You have been a strong advocate over the years and I appreciate all that you have done and made possible for me. Also, thank you to my doctoral advisory committee. Dr. Bill Robinson, Dr. Meng Zhou, and Dr. Solange Brault have been a major part of the initial formation of this work as well as integral in the final push to completion. Thank you!

I would also like to give a special thank you to my parents. The foundations you instilled in me drive me to follow my curiosities, enjoying the ride as well as the outcome. To my grandfather, George Kasai, I was always intrigued by your quiet confidence and scientific background. Thank you for your inspiring example.

Most importantly, I would like to thank my wife, Emily. A PhD is a marathon, and I was never alone during the long run. You have stood by, assisted in research, proofread, and been my staunchest supporter through the entirety of the process. I love you and I thank you for everything you have done for me, whether I know of it or not.

TABLE OF CONTENTS

ACKNOWLEDGEMENTS vii

LIST OF FIGURES xii

LIST OF TABLES xvi

CHAPTER Page

1. INTRODUCTION 1
   - Development of the Experimental pH-stat System 12
     - Background 12
     - Experimental design 13
   - Otolith Morphological Studies 13
     - Background 13
     - Experimental Design 16
   - Otolith Mineralogy 17
     - Background 17
   - Significance of Study 23
   - Works Cited 24

2. COMPARISON OF TWO PH-STAT CARBON DIOXIDE DOSING SYSTEMS FOR OCEAN ACIDIFICATION EXPERIMENTS 35
   - Abstract 35
   - Introduction 36
   - Materials and Procedures 38
     - Omega Engineering (OE) system configuration 38
     - Digital Aquatics (DA) system configuration 42
   - Assessment 44
     - System Stability Tests 44
   - Cost analysis 50
   - Discussion 50
   - Comments and recommendations 52
   - References 54

CHAPTER Page

3. OCEAN ACIDIFICATION INDUCES MORPHOLOGICAL CHANGES IN LARVAL REEF FISH OTOLITHS 57
Introduction 57
Methods 61
Experimental pCO_2 Manipulation 61
Dissolved Carbonate Chemistry in Experimental Aquaria 62
Fish Collection and Otolith Preparation 62
Otolith Morphometrics 64
Results 67
Discussion 75
Conclusions 81
References 82
Supplemental information 89
MATLAB image analysis methodology 89

4. THE SHAPE OF THINGS TO COME: OCEAN ACIDIFICATION CAUSES FISH EARSTONE MINERALIZATION CHANGE 90
Abstract 90
Introduction 90
Materials and Methods 92
Results 94
Discussion and Conclusion 95
References and Notes: 104
Supplemental materials 108
A1: Experimental methods 108
A2: Otolith extraction method 109
A3: Otolith core score training guide 111
A4: Example image from core scoring website 126
A5: MATLAB image analysis toolset instructions 128
A6: MATLAB image analysis morphology toolset code 130
A7: MATLAB image analysis roughness toolset code 136

CHAPTER Page

5. SUMMARY, DISCUSSION, AND CONCLUSIONS 140
Summary 140
Discussion 142
Conclusions 144
Suggestions for Future Research 145
References 147

REFERENCES 149

LIST OF FIGURES

Figure Page

Chapter 1

1. DIC reactions and qualified kinetics of reactions (Robinson 2009, pers comm) 2

2. Calculated theoretical concentrations of carbonate species at changing pH values with modern ocean conditions highlighted (figure from Ridgwell and Zeebe, 2005) 3

3. A: A model larval fish otoconia, showing saggita and lapillus otoliths (Whitfield et al., 2002). B: A model showing otolith interior structure and sensory maculae (Fekete, 2003)....5

4. A. Sagittal otolith within the sacculus showing proposed chemical gradients modeled after *in situ* mRNA expression experiments of rainbow trout. B. Carbonate speciation along physiological pathways to the otolith crystallization site (Tohse et al., 2006). 6

5. Ecological continuum (figure from Hannigan 2010, pers comm). Proposed research will extrapolate from individual organisms to population level processes and predict underlying molecular regulation effects 11

6. Ocean Ω_{arag} featuring impacted reef dissolution areas and future modeled values (Pelejero et al., 2010)....15

7. Crystal structure of calcite (a), aragonite (c), and vaterite (e) with labeled unit cell length (Berman, 2008). 18

8. AFM imagery showing (a) phase image, (b) amplitude image indicating organic rich components (white arrows), and (h) crystal habit features (figure from Dauphin and Dufour, 2008). 20

9. Preliminary SEM results from two year old channel catfish otoliths. Each image was collected at different magnifications (green bar in each image noted with length) 21

10. TEM images of organic rich globules secreted by bacterium *D. lacustre* (figure from Aloisi et al., 2006)....22

Figure Page

Chapter 2

1. Top: Digital Aquatics, Inc. (DA) ReefKeeper Elite (RKE) setup, showing required duplication. Bottom: Omega Engineering (OE) setup, showing required duplication. Note that the OE sytem log is generated at each head unit box, but the temperature data is not logged as is possible with the DA system. OE logger (a), as shown, is a 4-port unit, and therefore a system must be deployed for every four tanks. Components are color coded as follows: red - controller, blue - gas dosing, orange - logger. 40

2. OE pH controller stability experiment time series using Thermo Scientific Ross combination pH electrodes. pH_T setpoints (mean ± SD) are shown 45

3. DA pH controller stability experiment time series using laboratory Ag/Ag-Cl refillable electrodes. pH_T setpoints (mean ± SD) are shown. Each setpoint consists of four experimental aquariums represented by contrasting colors. 45

4. Performance comparison between DA and OE systems for 5-day stability experiments. Error bars represent DA 95% CI (n = 4). OE standard deviation means do not fall within the DA 95% CI for treatment groups pH = 7.4 and 7.7 while the SD mean for OE pH=8.0 treatment group falls within the corresponding DA 95% CI. Precision of control appears to be comparable, therefore for pH = 8.0 treatment group only 46

5. Raw mV electrode potential output from pH electrodes as measured by Hach H107G with standard deviation across individual electrodes of same type. The mean of three aquaria setups per electrode type (mV) is represented by a horizontal line. Three replicate tanks for each probe as measured are represented with respect to time (mean ± SD): Fisher (-85.6 ± 1.8); DA (-86.3 ± 4.1); VWR (-78.3 ± 1.8); VWR-plug (-80.4 ± 1.5). 48

6. Electrode response comparisons (standard deviation of electrode response, N = 12) with 95% confidence interval bars. DA electrodes exhibited significantly higher variance in electrode response (Levene's Test, W = 52.40, $p < 0.001$, $\alpha = 0.05$, N = 12, k = 4). 48

7. Normalized response (pH/mV) highlighting DA SL2 ($R^2 = 0.947$) vs. SL1 ($R^2 = 0.627$) electrode calibration drift. Note that the slope of each line indicates SL2 units exhibit calibration drift 2.8x the rate of the SL1 units using same pH electrode (Fisher). 49

Figure Page

Chapter 3

1. Figure 1. Arrangement of removed otoliths showing positioning of otolith pairs. All photographs taken at 90x magnification. (LS – left sagitta, LL – left lapillus, LA – left asteriscus, R – right).....63

2. Theoretical comparison of true sample (A), photographic data (B), strict perimeter calculation (C, green), and model ellipsoid used in this study (D, red). 66

3. Standard length (SL) for *A. clarkii* with respect to pCO_2 (A) and Ω_{Arag} (B). Linear regression (black), 95% confidence interval (C.I.) (blue) and prediction interval (P.I.) (red) included for SL vs. pCO_2 ($R^2 = 0.20$, $p < 0.001$), and quadratic regression and intervals included for SL vs. Ω_{Arag} ($R^2 = 0.22$, $p < 0.001$). 69

4. Circularity indices of *A. clarkii* otoliths compared to Ω_{Arag} (linear regression line - black), 95% C.I.(blue) and P.I.(red) for each otolith type (side/type: L - left, R - right, S - sagitta, L - lapillus, A - asteriscus).....71

5. Normalized area measurements calculated by area/standard length. Represented are linear regression (black), 95% C.I.(blue) and P.I.(red) for each otolith type (side/type: L - left, R - right, S - sagitta, L - lapillus, A - asteriscus).....72

6. Normalized perimeter measurements calculated by perimeter/standard length. Represented are linear regression (black), 95% C.I.(blue) and P.I.(red) for each otolith type (side/type: L - left, R - right, S - sagitta, L - lapillus, A - asteriscus).....73

7. Scatterplot of standard length of individual vs. sagittal otolith circularity index by side (left, L; right, R) and grouped by treatment Ω_{Arag}. 75

Chapter 4

1. Somatic growth (standard length) and relation to modeled aragonite saturation state (Ω_{Ar}) comparisons between *A. clarkii* (A) and *A. frenatus* (B). Mean ± S.D. are included as dot and tails, respectively. Regression (black), 95% C.I. (blue), and 95% P.I. (red) are also included. *A. clarkii* exhibited a significant 2nd order relationship to Ω_{Ar} ($p < 0.0001$, $F_{2,203} = 27.8023$, $SL = 0.591*\Omega - 0.081*\Omega^2 + 5.779$, A). *A. frenatus* exhibited no significant linear correlation ($p = 0.427$, $F_{2,28} = 0.6503$, $SL = 0.043*\Omega + 7.0731$, B).....100

Figure Page

2. Circularity index and modeled aragonite saturation state (Ω_{Ar}) for *A. clarkii* for left (A) and right (B) and *A. frenatus* for left (C) and right (D) sagittal otoliths vs. Ω_{Ar}, including linear regression results exhibiting 95% confidence intervals (blue) and 95% prediction interval (red). *A. clarkii* results are significant (left: CircIndex = 0.0093*Ω + 0.0093, $p < 0.001$, $F_{2,215} = 14.55$; right: CircIndex = 0.0099*Ω + 0.7065, $p < 0.0001$, $F_{2, 215} = 23.6467$) while *A. frenatus* correlation are not ($p > 0.05$).....101

3. Core development score and modeled aragonite saturation state (Ω_{Ar}) linear regression results with embedded SEM imagery of otoliths for *A. clarkii* (A) and *A. frenatus* (B), including regression line (black). Examples are taken from each pCO_2 treatment group. All samples are of equal scale with the scale bar representing 150 µm. *A. clarkii* score regression was significant (score = $-0.6043*\Omega_{Ar} + 4.3813$, $F_{1,354} = 648.0753$, $p < 0.001$, A). *A. frenatus* score regression was also significant (score = $-0.7837*\Omega_{Ar} + 5.4391$, $F_{1,61} = 189.9739$, $p < 0.001$, B). Slopes were significantly different between species as well (ANCOVA, Ω_{Ar}-Species interaction term, $F_{3,411} = 7.788$ $p = 0.0055$)....102

4. Roughness assessment compared to modeled aragonite saturation state (Ω_{Ar}) output, including mean ± S.D (dot, tails), regression (black), 95% C.I. (blue), and 95% P.I.(red). The only regression that was significant was for the right sagittal otoliths (Roughness = $-0.0133*\Omega_{Ar} + 0.291$, $p = 0.00241$, $F_{2,103} = 5.2407$, D).....103

A2.1. Example photograph of crossed-polizer view of otoliths. Contrast is high in the photograph due to camera auto-exposure settings.....110

A2.2. Example photograph with superimposed otolith side and type. 110

A4.1. Website screenshot of otolith core scoring page.....127

A5.1. Example image, background subtraction, and final processed image proof (left to right).....129

LIST OF TABLES

Table Page

Chapter 2

1. Qualitative assessments of comparative strengths and weaknesses. Stability scores reflect system time between pH electrode calibrations. User customizable scores are determined by optional modules available for end user. Memory capacity scores reflect time between logger downloads. Memory capacity of the DA system is rated highly when using the RSS feed fetching script since it is only limited by computer hard disk space. User friendly scores are reflective of ease of deployment with provided product manuals. Cost scores are reflective of cost/aquarium deployment at larger scales. Overall performance scores represent the ability of the system to perform ocean acidification experimentation adequately. 42

Chapter 3

1. Aquaria carbonate chemistry showing average for triplicate replication for each treatment group (±SD, n=3) measured values (pH_T, S, T^oC, A_T) and model output from CO2SYS (DIC, pCO_2, Ω_{Arag}).....68

Chapter 4

1. Carbonate chemistry showing average (±SD where applicable) and model output from CO2SYS data output as collected over the period of the experiment. All water chemistry parameters were collected using standard methods (Dickson et al., 2007; Millero et al., 1993). pH was measured on the total scale using UV spectroscopy (Byrne, 1987). Salinity (S), temperature (T), pH_T, and total alkalinity (A_T) were measured directly. Using the CO2SYS excel macro (Pierrot et al., 2006), carbonate chemistry parameters were calculated using the above measurements. 99

CHAPTER 1

INTRODUCTION

Global climate change is having and will continue to have significant global ecological impacts. Increased atmospheric CO_2 has broad-reaching implications for global ecosystems and has associated implications in ocean chemistry and therefore marine ecology. Additionally, rapid changes in global average temperature are affecting local habitats, changing the range of some species [e.g. (Walther et al., 2002; Sorte et al., 2013)] while doing tremendous harm to sessile communities including most of the world's coral reef habitats [e.g. (Hughes et al., 2003)].

The ocean is a significant sink of CO_2, drawing down about 30% of the anthropogenic production between 1800-1994 (Sabine et al., 2004). Dissolved inorganic carbon (DIC) species are derived from conversion of dissolved CO_2 (Fig. 1). These components serve as the foundational units with which marine organisms create organic matter and skeletal structures.

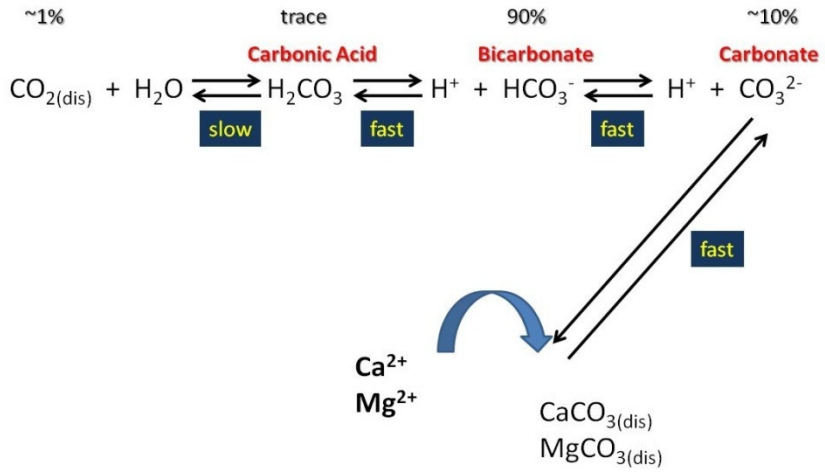

Figure 1. DIC reactions and qualified kinetics of reactions (figure from Robinson 2009, pers comm).

As atmospheric CO_2 increases, oceans are acidifying through the conversion of CO_2 to carbonic acid $[H_2CO_3]$ and resultant dissociation to H^+, bicarbonate $[HCO_3^-]$ and carbonate $[CO_3^{2-}]$ ions (Fig. 1). Under the business-as-usual carbon emission model, it is predicted that ocean pH will decrease by up to 0.35 pH units by 2100 (IPCC, 2007). This pH change drives a subsequent shift in ocean water carbonate series speciation, reducing $[CO_3^{2-}]$ while increasing $[HCO_3^-]$ and pCO_2 (Fig. 2).

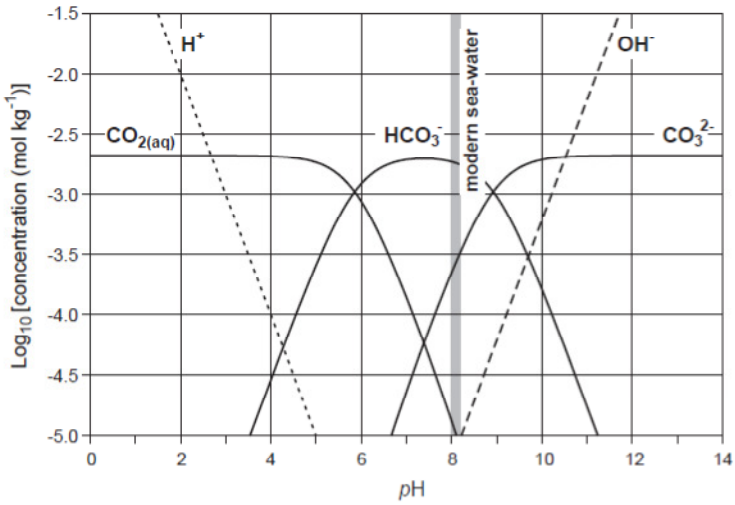

Figure 2. Calculated theoretical concentrations of carbonate species at changing pH values with modern ocean conditions highlighted (figure from Ridgwell and Zeebe, 2005).

Calcium carbonate minerals are used by some marine organisms to create hard structures, such as shells (such as those found in calcareous plankton), teeth (such as those found in some echinoderms), etc. Mineralization of these structures is driven by saturation state (Ω_{CaCO_3}, Equation 1):

$$\Omega_{CaCO_3} = \frac{\alpha Ca^{2+} \times \alpha CO_3^{2-}}{K_{sp}} \qquad \textit{Equation 1.}$$

The relationship between atmospheric CO_2 and Ω_{CaCO_3} has been thoroughly studied, specifically with regards to CO_2 flux between the atmosphere and ocean as well as the associated pH and carbon cycling [e.g. (Ridgwell and Zeebe, 2005) and references therein]. However, research related to the ecological effects specific to ocean

acidification have mainly dealt with exoskeletal calcifiers [e.g. (Iglesias-Rodriguez et al., 2008; Langdon et al., 2003; Shi et al., 2010)].

The research presented here focuses on a large gap in our understanding of the impact of ocean acidification on bony fish (Infraclass Teleostei, Class Actinopterygii). Teleosts include around 20,000 extant species comprising most of the fish in today's oceans (Miller et al., 2007). These fish represent significant economic and ecologic wealth. From an economic standpoint, fin-fisheries represent a central food source for humans as well as providing other fish-based products such as fertilizers, etc. In addition to subsistence benefits, the US marine ornamental trade represents a large source of economic activity with imports of over 1,800 species documented in 2005 (Rhyne et al., 2012). Understanding the impacts of global climate change, specifically ocean acidification, on fin-fish is therefore extremely important for sustainable management of fisheries.

Within each ear of teleost fish resides the otoconia. The otoconia is comprised of three calcium carbonate (aragonite) ear stones (otoliths). The otoliths, 3 on each side, act under the influence of acceleration in a straight line to stimulate macular hair cells by their movement relative to fluid (endolymph) in the saccule and utricle. The otoliths (sagitta, lapillus, asteriscus) are located on each side of the head proximally ventral to the brain (Fig. 3A). As sensory structures the otoliths provide information for hearing and balance via the otoconic sensory maculae [Fig. 3B, (Fekete, 2003)]. Each otolith is located in a semicircular canal (Fig. 3A) filled with a fluid (endolymph).

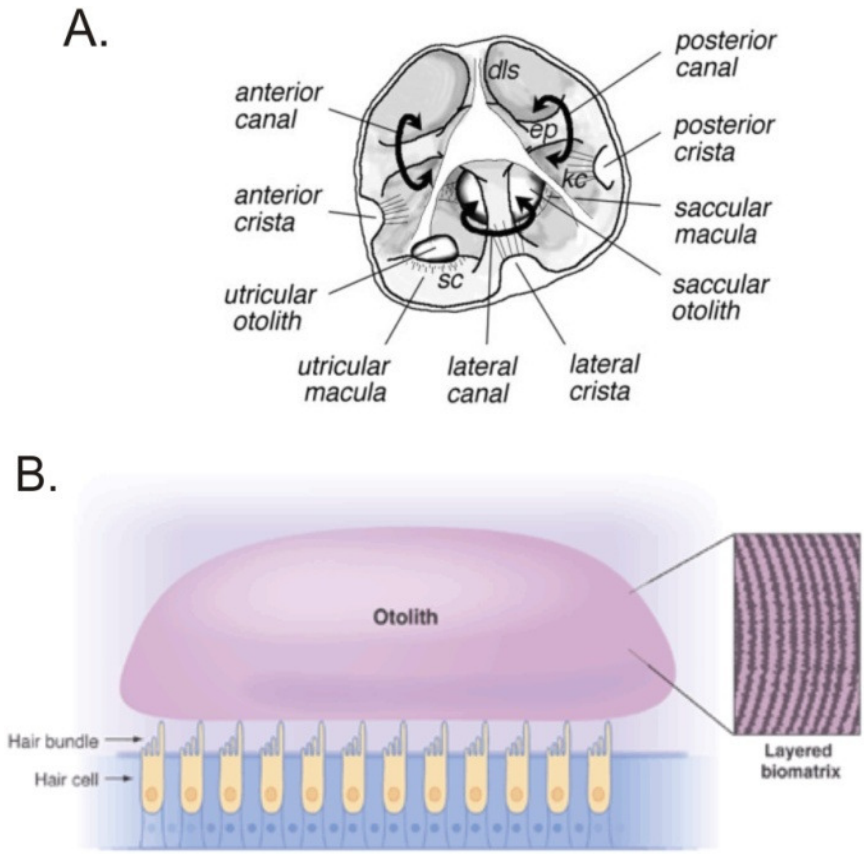

Figure 3. A: A model larval fish otoconia, showing saggita and lapillus otoliths (Whitfield et al., 2002). B: A model showing otolith interior structure and sensory maculae (Fekete, 2003).

The otolith grows daily, utilizing a web-like matrix of extracellular proteins, (Kang et al., 2008; Takagi et al., 2005; Murayama et al., 2002; Tohse et al., 2008), upon which mineralized calcium carbonate precipitates. The otoliths form over the lifetime of the individual, continually mineralizing new growth over the previous, growing such that a structure similar to an onion is revealed in thin section (Fig. 2B). The otolith grows continuously on all sides of the otolith, with one side growing much faster (the

"crystallization front"). At the crystallization front, the calcite saturation state of the endolymph is greater than 1 (supersaturated) (Eq. 1). This supersaturation is thought to be maintained by proton pumps in the epithelial cells adjacent to the site of crystallization (Borelli et al., 2003; Ishimatsu et al., 2008), which maintain the pH gradient required for carbonate-bicarbonate balance (Fig. 4A). Locally, the carbonate sequence is shifted towards carbonate ion availability (Fig. 4B, 5) and increased saturation state (Ω, Eq. 1) along the crystallization front (Tohse et al., 2006). Mineralization at the crystallization front, therefore, is accelerated compared to the opposite side.

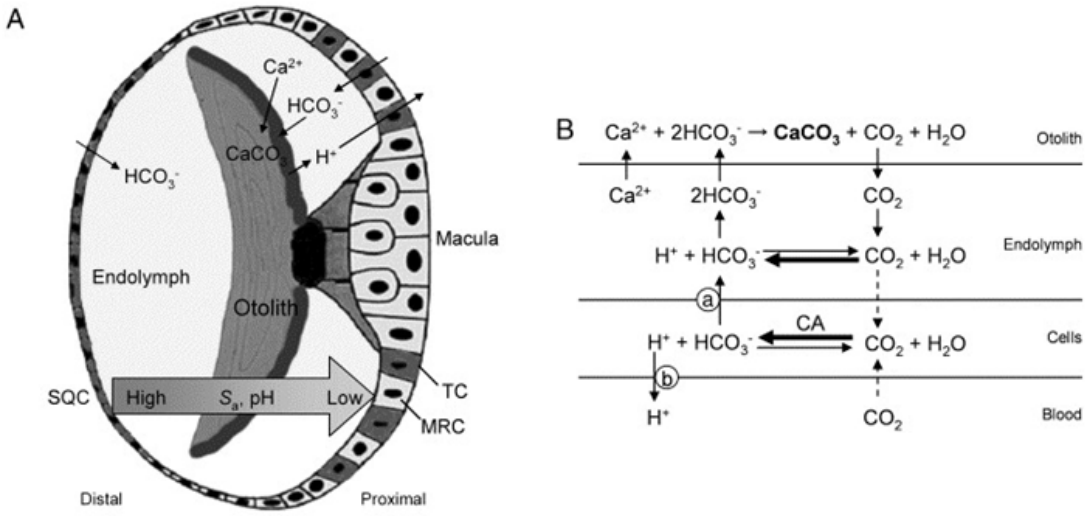

Figure 4. A. Sagittal otolith within the sacculus showing proposed chemical gradients modeled after *in situ* mRNA expression experiments of rainbow trout. B. Carbonate speciation along physiological pathways to the otolith crystallization site (Tohse et al., 2006).

Since the otolith contains neither vasculature nor cellular inclusions, previous deposition remains unchanged throughout the life of the organism. Even under extreme stress fish do not resorb material mineralized onto the otolith (Campana and Thorrold, 2001). Since resorbtion does not occur, the chemical composition of the otolith remains intact over the life of the fish. Chemical markers are recorded in response to environmental conditions at the time of formation, such as trace element and stable isotopic composition. These markers are used to reconstruct environmental life history of individual fish. Over the past few decades, extensive studies utilizing otoliths as a source of information for identifying individual life history characteristics such as: age and growth studies yielding population structure [e.g. (Dulcic, 1995; Fekete, 2003; Gauldie, 1999; Mc Dougall, 2004; Ponton, 2006)], trace element proxies for connectivity and habitat identification [e.g. (Arai et al., 2007; Bath et al., 2000; Campbell et al., 2002; Chittaro et al., 2006; Coghlan et al., 2007; Gemperline et al., 2002; Gillanders, 2005; Gillanders and Kingsford, 2003; Kalish, 1993; Miller and Kent, 2009; Thorrold et al., 1998)], and isotopic proxies for water temperature, fish metabolism, and age [e.g. (Ghosh et al., 2007; Thorrold et al., 1997; Walther and Thorrold, 2009)].

Related to metabolism, layers of protein are laid daily upon the otolith in a mesh-like fashion (Dauphin and Dufour, 2003; Murayama et al., 2005; Murayama et al., 2002; Sumanas et al., 2003). Over this protein matrix, calcium carbonate mineralizes. Several studies have shown that aragonite comprises the dominant inorganic phase of the otolith, while vaterite, calcite, and high-Mg calcite are found in increasingly lesser proportions [e.g. (Carlström, 1963; Dauphin and Dufour, 2008; Falini et al., 2005)]. These metastable

aragonite crystals have a higher solubility than true calcite [e.g. (Zhong and Mucci, 1989)] and their formation is controlled by extracellular endolymph proteins (Murayama et al., 2005; Murayama et al., 2002; Tohse et al., 2008).

Calcium carbonate deposition is controlled by saturation state (Ω) of the mineral phase (Eq. 1). Solubility product (K_{sp}) is dependent on variables within the depositional environment and differs between each mineral polymorph. Under standard temperature and pressure conditions, applicable to surface water, K_{sp} of calcite is approximately $10^{-8.35}$, while K_{sp} of aragonite is approximately $10^{-8.22}$. Calcite, therefore, is thermodynamically favored over aragonite since aragonite has a higher solubility. Over the past million years, ocean Ca^{2+} concentrations have been relatively constant (Pelejero et al., 2010), suggesting the controlling factor of calcium carbonate deposition to be carbonate ion concentration (CO_3^{2-}). In times of "aragonite seas", such as the Jurassic, magnesium concentrations in the ocean are high, suppressing the rate of calcite precipitation (Stanley et al., 2010; Zhang and Dawe, 2000). During these times, aragonite both forms faster and dissolves more slowly. In times of acidification, carbonate series speciation shifts away from carbonate and towards carbonic acid, lowering the thermodynamically controlling component of calcium carbonate mineralization (Fig. 1 - 2, Eq. 1).

It is currently unclear what effects ocean acidification will have on marine teleosts. Marine calcifiers show a direct response to increased pCO_2 [e.g. (Checkley et al., 2009; Iglesias-Rodriguez et al., 2008; Ries et al., 2009; Stanley et al., 2010)]. Marine fish

are calcium carbonate biocalcifiers that use carbonate in both otolith formation and in the gut (Checkley et al., 2009; Wilson et al., 2009).

Checkley et al. (2009) found that sagittal otoliths from larval bass increased in size with increasing aquaria pCO_2. The authors stated that area had increased, but did not provide direct mass measurements, ignoring the mineralogy of the otolith completely. Though the Checkley et al. (2009) study exposed a large gap in our understanding of otolith-environment interactions, it did very little to explain the causes of morphological changes or the ramifications of such changes. Two additional studies of otolith growth in response to OA have been published. Munday et al. (2011) found little morphological change in sagittal otoliths of orange clownfish (*Amphiprion percula*) in response to OA. Bignami et al. (2013) found a significant change in sagitta in the cobia (*Rachycentron canadum*). These studies were performed under different conditions (specifically aquaria dosing of CO_2, pH maintenance, and other methodological differences) making it difficult to compare results directly. Image analysis of SEM micrographs (Checkley et al., 2009; Munday et al., 2011) are insufficient to provide data on polymorph heterogeneity to enable comparison to changes in average density (Bignami et al., 2013). Since density of the otolith is tied to its functional response to gravimetric and acceleration stimuli, such density changes may impact function. Without density measurements, it is impossible to estimate overall mass of the otolith and therefore assess the rate of otolith mineralization. However, SEM image analysis can be used for morphological assessments though this approach suffers some disadvantages as a two-dimensional tool used to assess a three-dimensional structure. Regardless, a change to

otolith size, density, or shape will change navigational signals. These changed navigational signals may manifest in behavioral change such as the listless or kinetotic behavior seen in fish grown in micro and hypergravity (Anken et al., 1998; Anken and Rahmann, 1999; Beier, 1998; Hilbig et al., 2002).

Ocean acidification also shows impacts on other organ systems within teleost fish. Recent studies showed a direct negative effect on olfactory sensing in clownfish from increasing levels of aquaria acidification (Munday et al., 2009; Munday et al., 2010; Nilsson et al., 2012). It is clear that a neurophysiological change is responsible for loss of olfaction sense. Gravitation sense and general visual stimuli may allow fish to overcome olfactory inhibition. For this reason, I believe it is important to focus studies on otolith function. Tying the data from the above studies to direct evidence derived from otolith studies will assist in understanding the question of impacts on survival and ultimately how individual impacts scale along the biological continuum (Fig. 5).

Much work has been completed regarding otolith growth (Beier, 1998; Campana and Thorrold, 2001; Checkley et al., 2009; Morales-Nin, 2000; Murayama et al., 2002) and otolith function (Anken et al., 1998; Lychakov and Rebane, 2005; Riley and Moorman, 2000). Currently, the only studies linking otolith growth and morphology to OA show little change in otolith shape (Munday et al., 2011) or very large changes in calculated otolith density (Bignami et al., 2013). In the latter study, these density data were used to model sound sensitivity changes. The current body of literature does not include gravity sense functional studies. The research presented in this dissertation can be extrapolated to predict changes along the biological continuum (Fig. 5) and may lead to

more thoroughly understand controlling factors in gravity sensing and tie these results to observed decreased fish somatic growth and survival (Munday et al., 2009; Dixson et al., 2010), observed enhanced otolith growth (Checkley et al., 2009), unchanged morphology (Munday et al., 2011), and significantly changed density (Bignami et al., 2013) with response to ocean acidification.

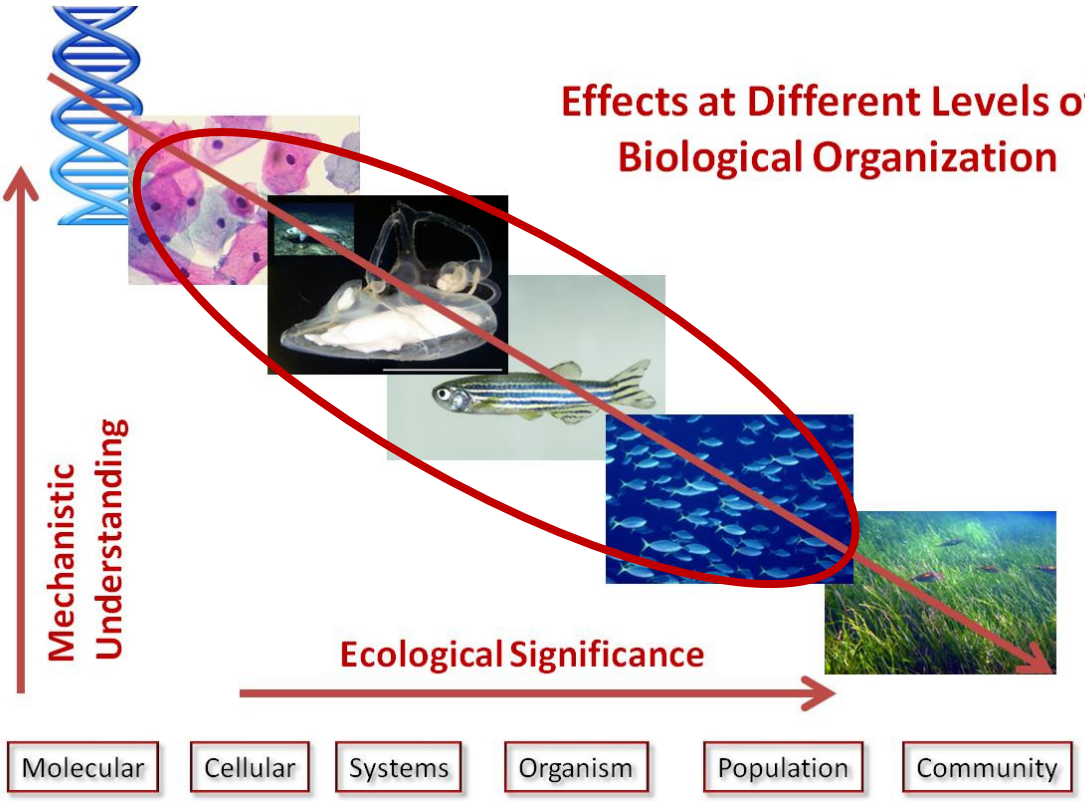

Figure 5. Ecological continuum (figure from Hannigan 2010, pers comm). Proposed research will extrapolate from individual organisms to population level processes and predict underlying molecular regulation effects (circled above).

The research presented here was centered on determining the relation between ocean acidification, otolith morphology, mineral polymorph composition and crystal form (habit) change. For more than a decade, ocean acidification has been the focus of a

multitude of research projects, focusing on topics such as the physics and chemistry of CO_2 flux between the atmosphere and ocean [e.g. (Ridgwell and Zeebe, 2005)], impact on calcification rates of calcareous plankton and coccolithophorids [e.g. (Iglesias-Rodriguez et al., 2008; Shi et al., 2010)], the impact on marine fish homing ability *in vivo* (Munday et al., 2009), and others. As pH of the ocean decreases, carbonate ion availability will invariably be greatly reduced as the speciation changes to a new equilibrium (Fig. 4). Though this has already been shown to have direct effects on exoskeletal calcifiers (Ries et al., 2009), it is unknown how this new equilibrium will affect biomineral structures found within endoskeletal organisms such as the otoconic organ of teleost fish.

Development of the Experimental pH-stat System

Background

An exhaustive search of the literature yielded no complete methods in pCO_2 manipulation for use in OA experimentation. While existing literature does discuss, briefly, what controller was used, little detail or system characterization is presented. For this reason, it was important to my research to (1) fully describe and characterize a viable system for OA pCO_2 manipulation, (2) increase pH data density to more fully understand variance in the controlled aquariums, and (3) engineer a cost-effective alternative to large scale industrial aquarium systems. Additionally, because pH electrodes offer a generally stable signal over time and are desirable over more expensive and sensitive pCO_2 ion selective electrodes, I tested a number of electrode types in developing a stable, low-cost pH-stat system.

Experimental design

Standard 40 L glass aquaria were used for the study for ease of replication. To keep the cost of the system low, I used a hobbyist reef tank controller system, Reef Keeper Elite (Digital Aquatics, Woodinville, WA). This system is modular so it can be expanded significantly. Using widely available electronics, replication of hardware is both simple and cost effective. The system I developed used standard solenoid valves for gas delivery and I added a flasher system for intermittent dosing for slower gas introduction.

The use of high precision pH electrodes was also important since small changes in pH correspond to large changes in pCO_2. I therefore tested electrodes from several manufacturers to evaluate performance and recalibration intervals. Electrode stability data was assessed for drift using regression analysis. Electrode response were normalized to mV readout collected using an independent meter. Additionally, stability of system pH was assessed using one-way ANOVA comparing each aquarium controller. These standard deviations on the means were then be compared to existing literature.

Otolith Morphological Studies

Background

Though each calcium carbonate polymorph (calcite, aragonite, vaterite) has an independent K_{sp}. The generalized formula for saturation state of a polymorph (Equ. 1) assists in understanding the dynamics of mineralization in the context of pH change. The saturation state (Ω) will, by definition, be $\geq$ one (1) under mineral forming conditions. Under carbonate mineral formation conditions in the open ocean, $[Ca^{2+}]$ is assumed

constant since the concentrations of this ion have been relatively constant over long time scales greater than 1 million years (Pelejero et al., 2010). Under steady-state conditions, K_{sp} is constant, leaving the controlling variable $[CO_3^{2-}]$. It is logically possible, therefore, that as pH declines thereby decreasing $[CO_3^{2-}]$, calcium carbonate mineralization processes will be slowed or reversed. This was shown to be true of many exoskeletal species and inorganic precipitation processes, as stated above. A few studies show increased mineralization, implying some confounding factor for mineralization of the fish otolith structures (Checkley et al., 2009) and some shellfish (Ries et al., 2009). Though it is known that otoliths are, at least for one species, affected by acidified waters, it is not fully known how the organ system itself is functionally impacted.

Oceans are becoming increasingly undersaturated with respect to aragonite (Ω_{arag}) due to the increasing flux of CO_2 from the atmosphere into the ocean, acidifying and shifting carbonate series equilibrium (Pelejero et al., 2010). Consequently, biomineralizers are expected to be severely impacted, especially those that produce aragonitic structures like calcareous plankton, etc. Though otoliths are isolated from the environment in which the fish swims, passive gas diffusion and active ion transport may also result in impacted mineralization under OA conditions. Large areas of the ocean are expected to reach values well below $\Omega_{arag} = 1$ [Fig. 6,]. This being the case, widespread mineral dissolution will likely occur. Since the otolith structure is protected from direct interaction with ocean water, the degree to which mineralization or function will be impacted is not known.

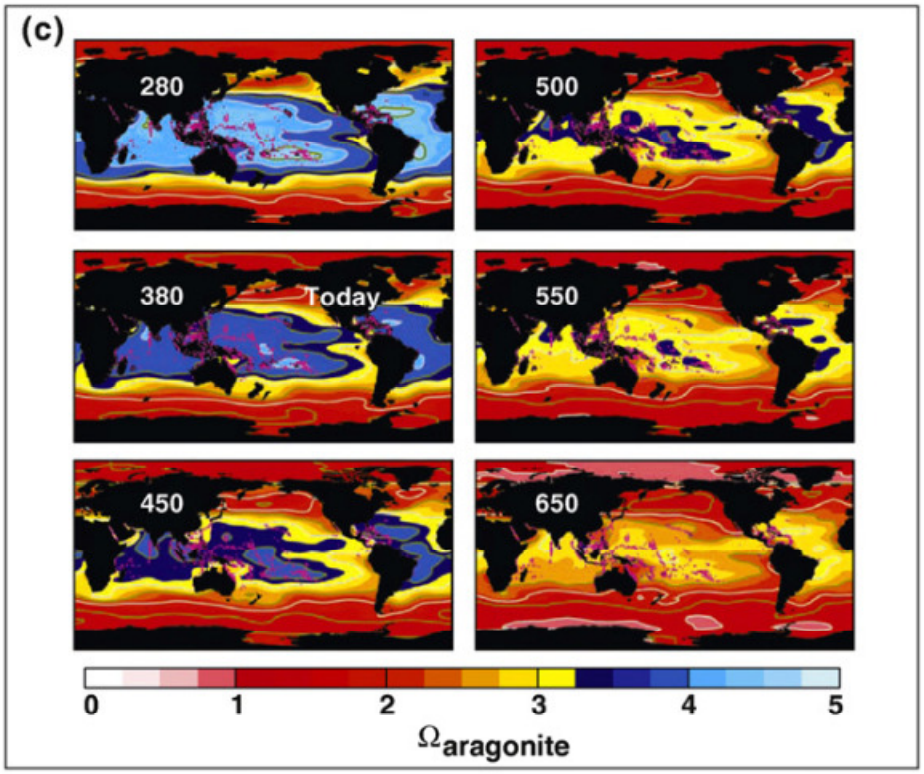

Figure 6. Ocean Ω_{arag} featuring impacted reef dissolution areas and future modeled values (Pelejero et al., 2010).

The mechanism for otolith deposition requires bicarbonate at the crystallization site (Fig. 3). Using inorganic precipitation as a model, the system is controlled by bicarbonate ion content within the endolymph. This increased bicarbonate ion concentration is facilitated by the active transfer of bicarbonate through the otoconic membrane while pH and $[CO_3^{2-}]$ gradients are maintained through Cl^-/HCO_3^- and Na^+/H^+ exchangers (Payan et al., 1997; Ishimatsu et al., 2008). It is hypothesized that active bicarbonate ion transfer coupled with localized pH increase may facilitate supersaturation of carbonate ion in the endolymph and thus increase the saturation state of aragonite

(Ω_{arag}>>1). It is difficult to directly measure pCO_2 of the endolymph of larval fish as at least 100 µL is required for the measurement. The object of my research was to study the effect of OA on early life stages which is viewed as particularly vulnerable stage. As such direct measurement of the endolymph was not possible. Instead, the research related otolith morphology to modeled pCO_2 and $\Omega_{arag.}$

Experimental Design

Species selection: *Amphiprion clarkii* and *Amphiprion frenatus*

The marine ornamental fish trade is significant in the US. In 2005, it is estimated that over 1,800 species of fish were imported (Rhyne et al., 2012). Of imports, the taxonomic family *Pomacentridae*, which includes the genus *Amphiprion*, is responsible for over half of the number of imported individual fish. *Amphiprion percula* ranks number five among the top imported species of fish. Of importance are also close relatives *A. clarkii* and *A. frenatus*, the latter representing the 18th most commonly imported marine ornamental species (Rhyne et al., 2012). Since the orange clownfish, *Amphiprion percula*, has been the subject of many studies in the past few years (Munday et al., 2011; Munday et al., 2009; Munday et al., 2010; Dixson et al., 2010; Nilsson et al., 2012), Clark's clownfish, *Amphiprion clarkii,* and the tomato clownfish, *Amphiprion frenatus*, were selected to study intragenus responses. Both species of fish exhibit a pelagic larval stage followed by a demersal juvenile stage. The nature of the pelagic larval stage causes these fishes to be particularly vulnerable to predation and environmental change. As such, the correct mineralization of the otolith and thereby function of the otoconia, is paramount to the continued success of reef fishes.

Studying these closely related species provides the first data regarding intraspecies impacts of OA in teleosts. As increased demand of wild capture fish increases, understanding the impacts of ocean acidification to natural reef systems may help inform more responsible harvesting of wild fish populations and assist in sustainable management of this important fishery.

Otolith Mineralogy

Background

The mineralogy of the otolith has been studied [e.g. (Dauphin and Dufour, 2008; Gauldie, 1999)], though much remains unknown. 98% of the otolith is comprised of calcium carbonate (Campana et al., 1997), with the remainder organic constituents. Three polymorphs comprise the most commonly found forms within the otolith: calcite, aragonite, and vaterite. The high solubility polymorph, high magnesium calcite, has not been reported. Sagittal otoliths have been found to be mostly aragonitic with some vaterite character (Campana and Thorrold, 2001; Dauphin and Dufour, 2008; Falini et al., 2005). Polymorph selection has an effect on total otolith density since each have a different packing pattern. Calculated polymorph densities are as follows: calcite (2.71 g/cm^3), aragonite (2.93 g/cm^3), and vaterite (2.66 g/cm^3). Important features distinguishing calcite from other polymorphs include the existence of a three-fold c-axis and close packed molecular structure. To obtain the perfect faces required for the classification of a three-fold c-axis, the unit cell is comparatively large (17.06 Å) whereas

the unit cell c-axis for aragonite (5.47 Å) and vaterite (8.47 Å) are comparatively short (Fig. 7).

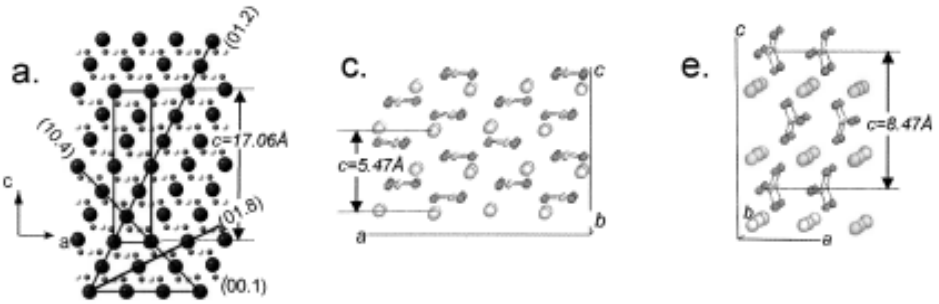

Figure 7. Crystal structure of calcite (a), aragonite (c), and vaterite (e) with labeled unit cell length (Berman, 2008).

Interstitial mineral spaces allow for elemental incorporation including ions of larger ionic radius. The increased distance between carbonate and calcium coordination, allow for ions such as Sr^{2+} and Ba^{2+} to replace Ca^{2+}, and ions such as Pb^{2+} to be incorporated in the interstitial crystal spaces with minimal distortion from polyhedral rearrangement (Melancon et al., 2005; Casanova et al., 2004). Vaterite coordination also allows incorporation of large ionic radius ions as well (Berman, 2008). Although aragonite has the largest calculated interstitial space of 2.53 Å and vaterite is calculated to have 2.46 Å, Melancon et al. (2005) found that otoliths with both crystal polymorphs fractionated trace metals. In the presence of both polymorphs, larger cations, such as Sr^{2+} (1.32 Å), Ba^{2+} (1.49 Å), and Rb^{2+} (1.66 Å) were preferentially deposited within the aragonite fractions (Melancon et al., 2005). Polymorphism within the otolith itself, therefore, may have a distinct role in the passive capture of trace elements from the endolymph. Life history analyses of otoliths have relied on incorporation of such

elements as indicative of environmental and biological variables. Understanding controlling factors of polymorphism, therefore, is critical to our understanding of coincident variables tied to life history analyses.

Polymorphism within the otoliths may also have a functional role. Since the otolith itself acts as a bouy-like structure, density and shape have a profound effect on the ability of the individual to sense motion and gravity (Anken et al., 1998; Beier, 1998; Hardison et al., 2005; Hilbig et al., 2002).

Additionally, crystal habit of previously precipitated minerals may change over time. Many studies show the rapid transformation of inorganically precipitated vaterite to calcite under changing experimental conditions (Andreassen and Hounslow, 2004; Nehrke and Van Cappellen, 2006; Spanos and Koutsoukos, 1998). This has also been shown in transitions from aragonite to calcite in laboratory precipitates (Nan et al., 2008a) in corals (Yoshioka et al., 1986), as well as calcite to aragonite in laboratory precipitates (Nan et al., 2008b). No studies are found in the literature addressing polymorph and subsequent crystal habit change in the otolith.

The mechanisms by which the otolith is constructed is still unknown. Though it has been shown that normal otolith mineralization requires specific proteins (Murayama et al., 2005; Takagi et al., 2005), the function of these proteins remains theoretical. In addition to evidence, both microscopic and biological, studies have shown that the proteins found within the otolith will induce specific polymorph deposition *in vitro.* Zhuo et al. (2010, *accepted*) show that proteins extracted from sagittal and lapillar otoliths induced the formation of aragonitic and vateritic minerals, respectively. It is currently

believed that the otolith proteins produce a web-like matrix on which calcium carbonate minerals form. Give the evidence shown in Dauphin and Dufour (2008), it may be possible that small mineral packets are being chaperoned to their host site. The complex nanostructures exposed through atomic force microscopy imaging show protein deposition to be ubiquitous. AFM imaging (Fig. 8a, b) of cod otoliths suggests an organic rich "envelope" surrounding the calcium carbonate mineral units (Dauphin and Dufour, 2008).

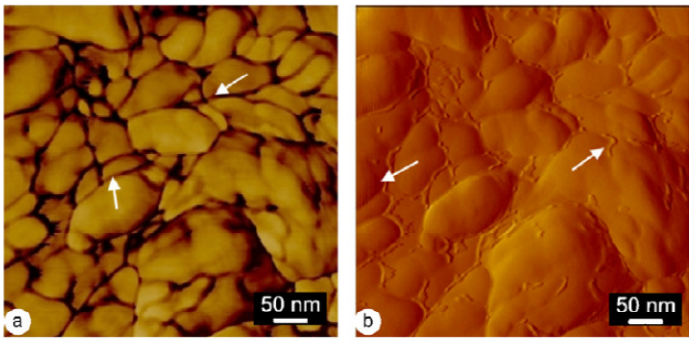

Figure 8. AFM imagery showing (a) phase image, (b) amplitude image indicating organic rich components (white arrows), and (h) crystal habit features (figure from Dauphin and Dufour, 2008).

Additionally, the habit of the deposited crystals within the otolith can be observed under optical light microscopy, SEM, or AFM imagery (Fig. 8h). The long needle-like projections may be considered acicular, though other habits exist for aragonite, including pseudo-hexagonal twinning. Aragonite is a metastable mineral in high pressure, low temperature conditions, such as ocean sediments. Deposited crystals are spontaneously replaced with calcite, the thermodynamically favorable phase, at surface ocean conditions.

Preliminary data gathered on adult *Ictalurus punctatus*, or the channel catfish, otoliths show dramatic changes in polymorph selection (Fig. 9). Two different crystal habits of aragonite can be seen: columnar habit (Fig. 9C) and distinct plate-like habit (Fig. 9B). Additionally, images taken in actively growing sites show similar "globules" (Fig. 9D) as found in Aloisi et al. (2006) (Fig. 10).

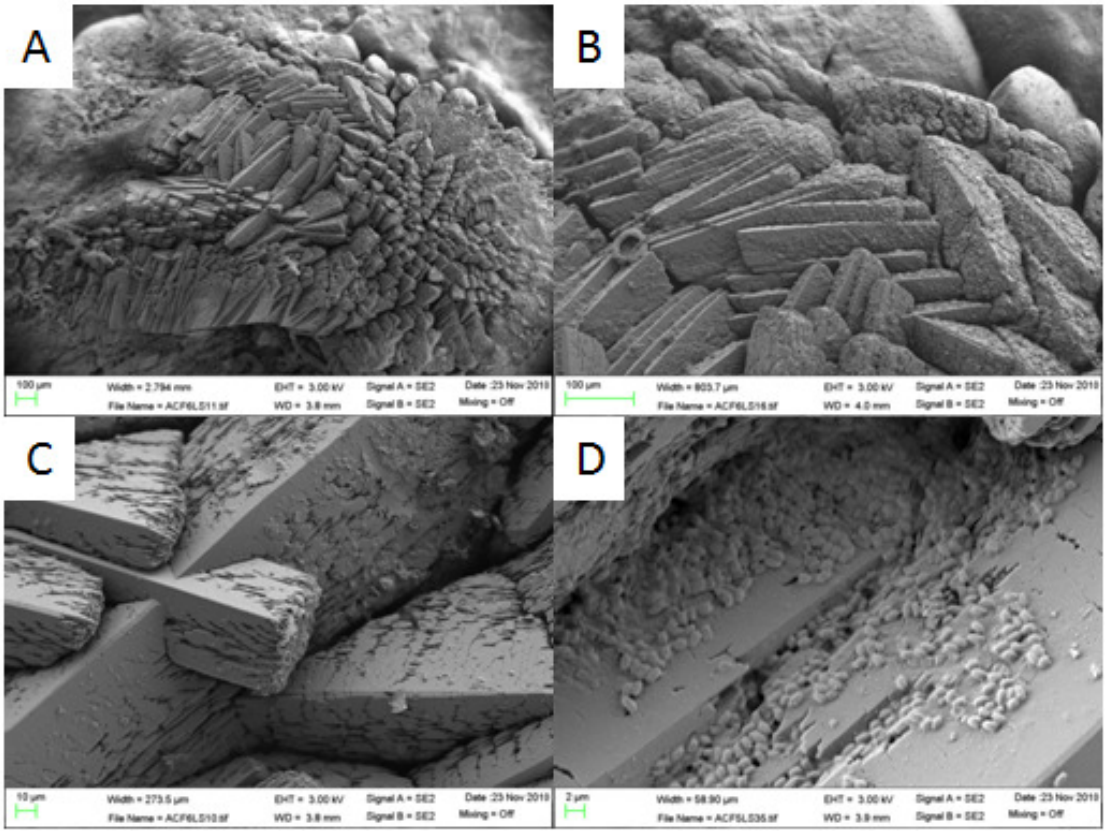

Figure 9. Preliminary SEM results from two year old channel catfish otoliths. Each image was collected at different magnifications (green bar in each image noted with length).

Calcium carbonate was found to precipitate on extracellular globules secreted by *D. lacustre* (Fig. 10). These bacteria induce calcium carbonate formation when appropriate media is applied. Similarly, proteins found within the endolymph may induce precipitation as seen here in channel catfish.

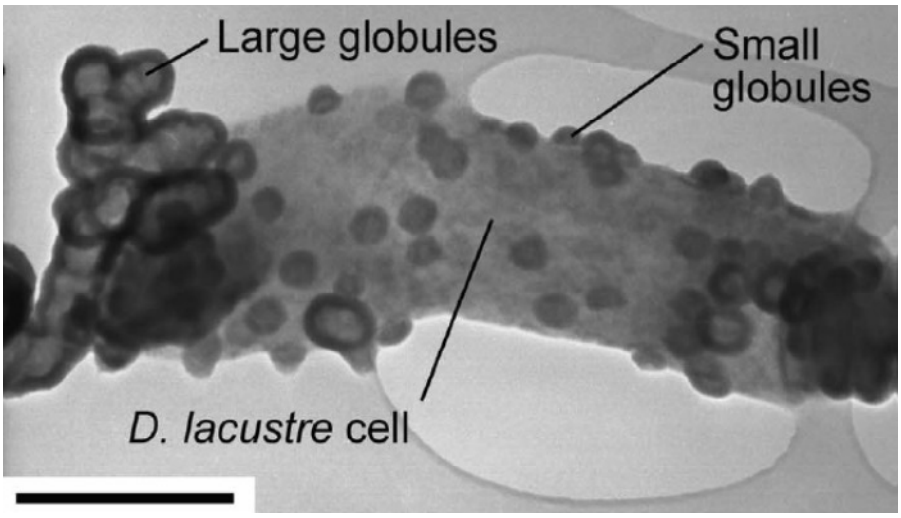

Figure 10. TEM images of organic rich globules secreted by bacterium *D. lacustre* (figure from Aloisi et al., 2006).

These preliminary results show a clear indication of polymorph transformation. The results presented in this dissertation provide opportunity for further analysis of active crystallization. In addition, core crystal habit is very important to the function of the otoconic organ. As the otolith mineralizes, transforming amorphous grains must form structure that compliments the hair cell maculae on which the otolith lies. As such, development of the core is paramount to the persistence of fishes.

Significance of Study

This research is essential to the understanding of ocean acidification on calcium carbonate biomineralization in marine teleosts. Though there are many reports of impacts on exoskeletal calcifiers [e.g. (Iglesias-Rodriguez et al., 2008; Riebesell et al., 2000; Ries et al., 2009; Shi et al., 2010), et al.], few reports focus on biocalcification in fish (Checkley et al., 2009; Wilson et al., 2009). Additionally, the otolith chemistry (Bath et al., 2000; Coghlan et al., 2007; Gillanders, 2005; Kalish, 1993; Melancon et al., 2005; Payan et al., 1997; Campana et al., 1997; Thresher, 1999), and mineralogy/morphology (Carlström, 1963; Dauphin and Dufour, 2008; Falini et al., 2005; Gauldie, 1999; Hüssy, 2008; Melancon et al., 2005; Morales-Nin, 2000; Ponton, 2006) are well studied. While Checkley et al. (2009) shows a connection between pCO_2 and otolith growth, mineralogy and behavioral studies are lacking, exposing a hole in our understanding of the system. Beier (1998), however, shows a link between otolith asymmetry and quantifiable behavior. This research sought to increase our understanding of the otolith and its response to climate change in terms of both ocean acidification and warming of surface ocean waters and can be extrapolated to population level effects.

Works Cited

Aloisi, G., Gloter, A., Kruger, M., Wallmann, K., Guyot, F., and Zuddas, P., 2006, Nucleation of calcium carbonate on bacterial nanoglobules: Geology, v. 34, no. 12, p. 1017–1020, doi: 10.1130/g22986a.1.

Andreassen, J.-P., and Hounslow, M.J., 2004, Growth and aggregation of vaterite in seeded-batch experiments: AIChE Journal, v. 50, no. 11, p. 2772–2782, doi: 10.1002/aic.10205.

Anken, R.H., Ibsch, M., and Rahmann, H., 1998, Neurobiology of fish under altered gravity conditions: Brain Research Reviews, v. 28, no. 1-2, p. 9–18.

Anken, R.H., and Rahmann, H., 1999, Effect of Altered Gravity on the Neurobiology of Fish: Naturwissenschaften, v. 86, no. 4, p. 155–167, doi: 10.1007/s001140050591.

Arai, T., Hirata, T., and Takagi, Y., 2007, Application of laser ablation ICPMS to trace the environmental history of chum salmon Oncorhynchus keta: Marine Environmental Research, v. 63, no. 1, p. 55–66.

Bath, G.E., Thorrold, S.R., Jones, C.M., Campana, S.E., McLaren, J.W., and Lam, J.W.H., 2000, Strontium and barium uptake in aragonitic otoliths of marine fish: Geochimica et Cosmochimica Acta, v. 64, no. 10, p. 1705–1714.

Beier, M., 1998, On the influence of altered gravity on the growth of fish inner ear otoliths: Acta Astronautica, v. 44, no. 7-12, p. 585–591.

Beier, M., and Anken, R., 2006, On the role of carbonic anhydrase in the early phase of fish otolith mineralization: Advances in Space Research, v. 38, no. 6, p. 1119–1122, doi: http://dx.doi.org/10.1016/j.asr.2005.10.027.

Beier, M., Anken, R.H., and Rahmann, H., 2002, Susceptibility to abnormal (kinetotic) swimming fish correlates with inner ear carbonic anhydrase-reactivity: Neuroscience Letters, v. 335, no. 1, p. 17–20, doi: http://dx.doi.org/10.1016/S0304-3940(02)01151-5.

Berman, A., 2008, Biomineralization of Calcium Carbonate: The Interplay with Biosubstrates, *in* Sigel, A., Sigel, H., and Sigel, R.K.O. eds., Metal Ions in Life Sciences, Wiley, West Sussex PO19 8SQ, England, p. 167–205.

Bignami, S., Spongaugle, S., and Cowen, 2013, Response to ocean acidification in larvae of a large tropical marine fish , Rachycentron canadum: Global Change Biology, v. 19, p. 996–1006, doi: 10.1111/gcb.12133.

Borelli, G., Guibbolini, M.E., Mayer-Gostan, N., Priouzeau, F., De Pontual, H., Allemand, D., Puverel, S., Tambutte, E., and Payan, P., 2003, Daily variations of endolymph composition: relationship with the otolith calcification process in trout: J Exp Biol, v. 206, no. 15, p. 2685–2692, doi: 10.1242/jeb.00479.

Broecker, W.S., Peng, T.-H., and Beng, Z., 1982, Tracers in the Sea: Lamont-Doherty Geological Observatory, Columbia University.

Byrne, R.H., 1987, Standardization of standard buffers by visible spectrometry: Analytical Chemistry, v. 59, no. 10, p. 1479–1481, doi: 10.1021/ac00137a025.

Campana, S.E., and Thorrold, S.R., 2001, Otoliths, increments, and elements: keys to a comprehensive understanding of fish populations?: Canadian Journal of Fisheries and Aquatic Sciences, v. 58, no. 1, p. 30–38.

Campana, S.E., Thorrold, S.R., Jones, C.M., Günther, D., Tubrett, M., Longerich, H., Jackson, S., Halden, N.M., Kalish, J.M., Piccoli, P., Pontual, H. de, Troadec, H., Panfili, J., Secor, D.H., et al., 1997, Comparison of accuracy, precision, and sensitivity in elemental assays of fish otoliths using the electron microprobe, proton-induced X-ray emission, and laser ablation inductively coupled plasma mass spectrometry:.

Campbell, J.L., Babaluk, J.A., Cooper, M., Grime, G.W., Halden, N.M., Nejedly, Z., Rajta, I., and Reist, J.D., 2002, Strontium distribution in young-of-the-year Dolly Varden otoliths: Potential for stock discrimination: Nuclear Instruments and Methods in Physics Research Section B: Beam Interactions with Materials and Atoms, v. 189, no. 1-4, p. 185–189.

Carlström, D., 1963, A crystallographic study of vertebrate otoliths: Biol Bull, v. 125, p. 441–463.

Casanova, D., Cirera, J., Llunell, M., Alemany, P., Avnir, D., and Alvarez, S., 2004, Minimal distortion pathways in polyhedral rearrangements: Journal of the American Chemical Society, v. 126, no. 6, p. 1755–1763.

Chappard, D., Degasne, I., Hure, G., Legrand, E., Audran, M., and Basle, M.F., 2003, Image analysis measurements of roughness by texture and fractal analysis correlate with contact profilometry: Biomaterials, v. 24, no. 8, p. 1399–1407.

Checkley, D.M., Dickson, A.G., Takahashi, M., Radich, J.A., Eisenkolb, N., Asch, R., and Checkley, D.M., 2009, Elevated CO2 enhances otolith growth in young fish: Science, v. 324, no. 5935, p. 1683, doi: 324/5935/1683 [pii] 10.1126/science.1169806.

Chittaro, P.M., Usseglio, P., Fryer, B.J., and Sale, P.F., 2006, Spatial variation in otolith chemistry of Lutjanus apodus at Turneffe Atoll, Belize: Estuarine, Coastal and Shelf Science, v. 67, no. 4, p. 673–680.

Coghlan, S.M., Lyerly, M.S., Bly, T.R., Williams, J., Bowman, D., and Hannigan, R., 2007, Otolith Chemistry Discriminates among Hatchery-Reared and Tributary-Spawned Salmonines in a Tailwater System:.

Dauphin, Y., and Dufour, E., 2003, Composition and properties of the soluble organic matrix of the otolith of a marine fish: Gadus morhua Linne, 1758 (Teleostei, Gadidae): Comp Biochem Physiol A Mol Integr Physiol, v. 134, no. 3, p. 551–561, doi: S1095643302003586 [pii].

Dauphin, Y., and Dufour, E., 2008, Nanostructures of the aragonitic otolith of cod (Gadus morhua): Micron, v. 39, no. 7, p. 891–896.

Dickson, A.G., Sabine, C.L., and Christian, J.R., 2007, Guide to best practices for ocean CO2 measurements:.

Dixson, D.L., Munday, P.L., and Jones, G.P., 2010, Ocean acidification disrupts the innate ability of fish to detect predator olfactory cues: Ecology Letters, v. 13, no. 1, p. 68–75, doi: 10.1111/j.1461-0248.2009.01400.x.

Dulcic, J., 1995, Estimation of age and growth of sardine, Sardina pilchardus (Walbaum, 1792), larvae by reading daily otolith increments: Fisheries Research, v. 22, no. 3-4, p. 265–277.

Fabry, V.J., Seibel, B.A., Feely, R.A., and Orr, J.C., 2008, Impacts of ocean acidification on marine fauna and ecosystem processes: ICES Journal of Marine Science: Journal du Conseil , v. 65 , no. 3 , p. 414–432, doi: 10.1093/icesjms/fsn048.

Falini, G., Fermani, S., Vanzo, S., Miletic, M., and Zaffino, G., 2005, Influence on the formation of aragonite or vaterite by otolith macromolecules: European Journal of Inorganic Chemistry, , no. 1, p. 162–167, doi: DOI 10.1002/ejic.200400419.

FAO, 2010, FAO yearbook. Fishery and aquaculture statistics:.

Feely, R.A., Alin, S.R., Newton, J., Sabine, C.L., Warner, M., Devol, A., Krembs, C., and Maloy, C., 2010, The combined effects of ocean acidification, mixing, and respiration on pH and carbonate saturation in an urbanized estuary: Estuarine, Coastal and Shelf Science, v. 88, no. 4, p. 442–449, doi: http://dx.doi.org/10.1016/j.ecss.2010.05.004.

Feely, R.A., Sabine, C.L., Hernandez-Ayon, J.M., Ianson, D., and Hales, B., 2008, Evidence for Upwelling of Corrosive "Acidified" Water onto the Continental Shelf: Science , v. 320 , no. 5882 , p. 1490–1492, doi: 10.1126/science.1155676.

Feely, R.A., Sabine, C.L., Lee, K., Berelson, W., Kleypas, J., Fabry, V.J., and Millero, F.J., 2004, Impact of Anthropogenic CO2 on the CaCO3 System in the Oceans: Science , v. 305 , no. 5682 , p. 362–366, doi: 10.1126/science.1097329.

Fekete, D.M., 2003, Developmental biology. Rocks that roll zebrafish: Science, v. 302, no. 5643, p. 241–242, doi: 10.1126/science.1091171 302/5643/241 [pii].

Gauldie, R.W., 1999, Ultrastructure of lamellae, mineral and matrix components of fish otolith twinned aragonite crystals: implications for estimating age in fish: Tissue Cell, v. 31, no. 2, p. 138–153, doi: S0040-8166(99)90030-7 [pii] 10.1054/tice.1999.0030.

Gemperline, P.J., Rulifson, R.A., and Paramore, L., 2002, Multi-way analysis of trace elements in fish otoliths to track migratory patterns: Chemometrics and Intelligent Laboratory Systems, v. 60, no. 1-2, p. 135–146.

Ghosh, P., Eiler, J., Campana, S.E., and Feeney, R.F., 2007, Calibration of the carbonate [`]clumped isotope' paleothermometer for otoliths: Geochimica et Cosmochimica Acta, v. 71, no. 11, p. 2736–2744.

Gillanders, B.M., 2005, Using elemental chemistry of fish otoliths to determine connectivity between estuarine and coastal habitats: Estuarine, Coastal and Shelf Science, v. 64, no. 1, p. 47–57.

Gillanders, B.M., and Kingsford, M.J., 2003, Spatial variation in elemental composition of otoliths of three species of fish (family Sparidae): Estuarine, Coastal and Shelf Science, v. 57, no. 5-6, p. 1049–1064.

Grant, J.A., Bishop, N.E., Götzen, N., Sprecher, C., Honl, M., and Morlock, M.M., 2007, Artificial composite bone as a model of human trabecular bone: The implant–bone interface: Journal of biomechanics, v. 40, no. 5, p. 1158–1164.

Hardison, A.L., Lichten, L., Banerjee-Basu, S., Becker, T.S., and Burgess, S.M., 2005, The zebrafish gene claudinj is essential for normal ear function and important for the formation of the otoliths: Mechanisms of Development, v. 122, no. 7-8, p. 949–958.

Hauri, C., Gruber, N., Vogt, M., Doney, S.C., Feely, R.A., Lachkar, Z., Leinweber, A., McDonnell, A.M.P., Munnich, M., and Plattner, G.-K., 2013, Spatiotemporal variability and long-term trends of ocean acidification in the California Current System: Biogeosciences, v. 10, no. 1, p. 193–216, doi: 10.5194/bg-10-193-2013.

Hilbig, R., Anken, R.H., Sonntag, G., Höhne, S., Henneberg, J., Kretschmer, N., and Rahmann, H., 2002, Effects of altered gravity on the swimming behaviour of fish: Advances in Space Research, v. 30, no. 4, p. 835–841.

Hughes, T.P., Baird, A.H., Bellwood, D.R., Card, M., Connolly, S.R., Folke, C., Grosberg, R., Hoegh-Guldberg, O., Jackson, J.B.C., Kleypas, J., Lough, J.M., Marshall, P., Nystrom, M., Palumbi, S.R., et al., 2003, Climate Change, Human Impacts, and the Resilience of Coral Reefs: Science, v. 301, no. 5635, p. 929–933, doi: 10.1126/science.1085046.

Hughes, I., Blasiole, B., Huss, D., Warchol, M.E., Rath, N.P., Hurle, B., Ignatova, E., David Dickman, J., Thalmann, R., Levenson, R., and Ornitz, D.M., 2004, Otopetrin 1 is required for otolith formation in the zebrafish Danio rerio: Developmental Biology, v. 276, no. 2, p. 391–402, doi: http://dx.doi.org/10.1016/j.ydbio.2004.09.001.

Hüssy, K., 2008, Otolith shape in juvenile cod (Gadus morhua): Ontogenetic and environmental effects: Journal of Experimental Marine Biology and Ecology, v. 364, no. 1, p. 35–41.

Iglesias-Rodriguez, M.D., Halloran, P.R., Rickaby, R.E.M., Hall, I.R., Colmenero-Hidalgo, E., Gittins, J.R., Green, D.R.H., Tyrrell, T., Gibbs, S.J., von Dassow, P., Rehm, E., Armbrust, E.V., and Boessenkool, K.P., 2008, Phytoplankton Calcification in a High-CO2 World: Science, v. 320, no. 5874, p. 336–340, doi: 10.1126/science.1154122.

IPCC, 2007, Climate Change 2007: Synthesis Report: Intergovernmental Panel on Climate Change, Geneva.,.

Ishimatsu, A., Hayashi, M., and Kikkawa, T., 2008, Fishes in high-CO2, acidified oceans: Mar Ecol Prog Ser, v. 373, p. 295–302.

Kalish, J.M., 1993, Fish Otolith Chemistry: Science, v. 260, no. 5106, p. 279, doi: 260/5106/279 [pii] 10.1126/science.260.5106.279.

Kang, Y., Stevenson, A., Yau, P., and Kollmar, R., 2008, Sparc Protein is required for normal growth of zebrafish otoliths: J Assoc Res Otolaryngol, v. 9, no. 4, p. 436–451.

Kroeker, K.J., Micheli, F., Gambi, M.C., and Martz, T.R., 2011, Divergent ecosystem responses within a benthic marine community to ocean acidification: Proceedings of the National Academy of Sciences , v. 108 , no. 35 , p. 14515–14520, doi: 10.1073/pnas.1107789108.

Langdon, C., Broecker, W.S., Hammond, D.E., Glenn, E., Fitzsimmons, K., Nelson, S.G., Peng, T., Hajdas, I., and Bonani, G., 2003, Effect of elevated CO2 on the community metabolism of an experimental coral reef: Global Biogeochemical Cycles, v. 17, no. 1, p. 14, doi: 10.1029/2002GB001941.

Lombarte, A., and Castellón, A., 1991, Interspecific and intraspecific otolith variability in the genus Merluccius as determined by image analysis: Canadian journal of zoology, v. 69, no. 9, p. 2442–2449.

Lychakov, D. V, and Rebane, Y.T., 2005, Fish otolith mass asymmetry: morphometry and influence on acoustic functionality: Hear Res, v. 201, no. 1-2, p. 55–69, doi: S0378-5955(04)00283-7 [pii] 10.1016/j.heares.2004.08.017.

Lychakov, D. V, and Rebane, Y.T., 2000, Otolith regularities: Hearing Research, v. 143, no. 1–2, p. 83–102, doi: http://dx.doi.org/10.1016/S0378-5955(00)00026-5.

Lychakov, D. V, Rebane, Y.T., Lombarte, A., Fuiman, L.A., and Takabayashi, A., 2006, Fish otolith asymmetry: morphometry and modeling: Hear Res, v. 219, no. 1-2, p. 1–11, doi: S0378-5955(06)00117-1 [pii] 10.1016/j.heares.2006.03.019.

Mc Dougall, A., 2004, Assessing the use of sectioned otoliths and other methods to determine the age of the centropomid fish, barramundi (Lates calcarifer) (Bloch), using known-age fish: Fisheries Research, v. 67, no. 2, p. 129–141.

Melancon, S., Fryer, B.J., Ludsin, S.A., Gagnon, J.E., and Yang, Z., 2005, Effects of crystal structure on the uptake of metals by lake trout (Salvelinus namaycush) otoliths: Canadian Journal of Fisheries & Aquatic Sciences, v. 62, no. 11, p. 2609–2619, doi: 10.1139/f05-161.

Miller, J.A., and Kent, A.J.R., 2009, The determination of maternal run time in juvenile Chinook salmon (Oncorhynchus tshawytscha) based on Sr/Ca and 87Sr/86Sr within otolith cores: Fisheries Research, v. 95, no. 2-3, p. 373–378.

Miller, Stephen, and Harley, 2007, Zoology: McGraw-Hill Higher Education, New York.

Millero, F.J., Zhang, J.-Z., Fiol, S., Sotolongo, S., Roy, R., Lee, K., and Mane, S., 1993, The use of buffers to measure the pH of seawater: Marine Chemistry, v. 44, p. 143–152, doi: 10.1016/0304-4203(93)90199-X.

Morales-Nin, B., 2000, Review of the growth regulation processes of otolith daily increment formation: Fisheries Research, v. 46, no. 1-3, p. 53–67.

Munday, P.L., Dixson, D.L., Donelson, J.M., Jones, G.P., Pratchett, M.S., Devitsina, G. V, and Døving, K.B., 2009, Ocean acidification impairs olfactory discrimination and

homing ability of a marine fish: Proceedings of the National Academy of Sciences, v. 106, no. 6, p. 1848–1852, doi: 10.1073/pnas.0809996106.

Munday, P.L., Dixson, D.L., McCormick, M.I., Meekan, M., Ferrari, M.C.O., and Chivers, D.P., 2010, Replenishment of fish populations is threatened by ocean acidification: Proceedings of the National Academy of Sciences, v. 107, no. 29, p. 12930–12934, doi: 10.1073/pnas.1004519107.

Munday, P.L., Hernaman, V., Dixson, D.L., and Thorrold, S.R., 2011, Effect of ocean acidification on otolith development in larvae of a tropical marine fish: Biogeosciences, v. 8, no. 6, p. 1631–1641, doi: 10.5194/bg-8-1631-2011.

Murayama, E., Herbomel, P., Kawakami, A., Takeda, H., and Nagasawa, H., 2005, Otolith matrix proteins OMP-1 and Otolin-1 are necessary for normal otolith growth and their correct anchoring onto the sensory maculae: Mechanisms of Development, v. 122, no. 6, p. 791–803.

Murayama, E., Takagi, Y., Ohira, T., Davis, J.G., Greene, M.I., and Nagasawa, H., 2002, Fish otolith contains a unique structural protein, otolin-1: Eur J Biochem, v. 269, no. 2, p. 688–696, doi: 2701 [pii].

Nan, Z., Chen, X., Yang, Q., Wang, X., Shi, Z., and Hou, W., 2008a, Structure transition from aragonite to vaterite and calcite by the assistance of SDBS: Journal of Colloid and Interface Science, v. 325, no. 2, p. 331–336.

Nan, Z., Shi, Z., Yan, B., Guo, R., and Hou, W., 2008b, A novel morphology of aragonite and an abnormal polymorph transformation from calcite to aragonite with PAM and CTAB as additives: Journal of Colloid and Interface Science, v. 317, no. 1, p. 77–82.

Nehrke, G., and Van Cappellen, P., 2006, Framboidal vaterite aggregates and their transformation into calcite: A morphological study: Journal of Crystal Growth, v. 287, no. 2, p. 528–530.

Nilsson, G.E., Dixson, D.L., Domenici, P., McCormick, M.I., Sørensen, C., Watson, S.-A., and Munday, P.L., 2012, Near-future carbon dioxide levels alter fish behaviour by interfering with neurotransmitter function: Nature Climate Change, v. 2, p. 201–204, doi: 10.1038/nclimate1352.

Nolf, D., 1985, Otolithi piscium, *in* Handbook of Paleoichthyology, Gustav Fischer Verlag, Stuttgart.

Payan, P., Kossmann, H., Watrin, A., Mayer-Gostan, N., and Boeuf, G., 1997, Ionic composition of endolymph in teleosts: origin and importance of endolymph alkalinity: J Exp Biol, v. 200, no. Pt 13, p. 1905–1912.

Pelejero, C., Calvo, E., and Hoegh-Guldberg, O., 2010, Paleo-perspectives on ocean acidification: Trends Ecol Evol,, doi: S0169-5347(10)00044-3 [pii] 10.1016/j.tree.2010.02.002.

Pickering, A.D., 1993, Growth and stress in fish production: Aquaculture, v. 111, no. 1–4, p. 51–63, doi: http://dx.doi.org/10.1016/0044-8486(93)90024-S.

Pierrot, D., Lewis, E., and Wallace, D., 2006, Program developed for CO2 system calculations: Carbon Dioxide Information Analysis Center, Oak Ridge National Laboratory, U.S. Department of Engergy, Oak Ridge, Tennessee.

Ponton, D., 2006, Is geometric morphometrics efficient for comparing otolith shape of different fish species?: J Morphol, v. 267, no. 6, p. 750–757, doi: 10.1002/jmor.10439.

Rhyne, A.L., Tlusty, M.F., Schofield, P.J., Kaufman, L., Morris Jr, J.A., and Bruckner, A.W., 2012, Revealing the appetite of the marine aquarium fish trade: the volume and biodiversity of fish imported into the United States: PloS one, v. 7, no. 5, p. e35808.

Ridgwell, A., and Zeebe, R.E., 2005, The role of the global carbonate cycle in the regulation and evolution of the Earth system: Earth and Planetary Science Letters, v. 234, no. 3-4, p. 299–315.

Riebesell, U., Zondervan, I., Rost, B., Tortell, P.D., Zeebe, R.E., and Morel, F.M.M., 2000, Reduced calcification of marine plankton in response to increased atmospheric CO2: Nature, v. 407, no. 6802, p. 364–367.

Ries, J.B., Cohen, A.L., and McCorkle, D.C., 2009, Marine calcifiers exhibit mixed responses to CO2-induced ocean acidification: Geology, v. 37, no. 12, p. 1131–1134.

Riley, N.A., 1941, Projection sphericity: Journal of Sedimentary Research , v. 11 , no. 2 , p. 94–95, doi: 10.1306/D426910C-2B26-11D7-8648000102C1865D.

Riley, B.B., and Moorman, S.J., 2000, Development of utricular otoliths, but not saccular otoliths, is necessary for vestibular function and survival in zebrafish: Journal of Neurobiology, v. 43, no. 4, p. 329–337.

Sabine, C.L., Feely, R.A., Gruber, N., Key, R.M., Lee, K., Bullister, J.L., Wanninkhof, R., Wong, C.S., Wallace, D.W.R., Tilbrook, B., Millero, F.J., Peng, T.-H., Kozyr, A., Ono, T., et al., 2004, The Oceanic Sink for Anthropogenic CO2: Science, v. 305, no. 5682, p. 367.

Shi, D., Xu, Y., Hopkinson, B.M., and Morel, F.M., 2010, Effect of ocean acidification on iron availability to marine phytoplankton: Science, v. 327, no. 5966, p. 676–679, doi: science.1183517 [pii] 10.1126/science.1183517.

Söllner, C., Burghammer, M., Busch-Nentwich, E., Berger, J., Schwarz, H., Riekel, C., and Nicolson, T., 2003, Control of Crystal Size and Lattice Formation by Starmaker in Otolith Biomineralization: Science , v. 302 , no. 5643 , p. 282–286, doi: 10.1126/science.1088443.

Sorte, C.J.B., Etter, R.J., Spackman, R., Boyle, E.E., and Hannigan, R.E., 2013, Elemental Fingerprinting of Mussel Shells to Predict Population Sources and Redistribution Potential in the Gulf of Maine: PloS one, v. 8, no. 11, p. e80868.

Spanos, N., and Koutsoukos, P.G., 1998, The transformation of vaterite to calcite: effect of the conditions of the solutions in contact with the mineral phase: Journal of Crystal Growth, v. 191, no. 4, p. 783–790.

Stanley, S.M., Ries, J.B., and Hardie, L.A., 2010, Increased Production of Calcite and Slower Growth for the Major Sediment-Producing Alga Halimeda as the Mg/Ca Ratio of Seawater is Lowered to a “Calcite Sea” Level: Journal of Sedimentary Research, v. 80, no. 1, p. 6–16, doi: 10.2110/jsr.2010.011.

Stupp, S.I., and Ciegler, G.W., 1992, Organoapatites: materials for artificial bone. I. Synthesis and microstructure: Journal of biomedical materials research, v. 26, no. 2, p. 169–183.

Sumanas, S., Larson, J.D., and Miller Bever, M., 2003, Zebrafish chaperone protein GP96 is required for otolith formation during ear development: Developmental Biology, v. 261, no. 2, p. 443–455.

Takagi, Y., Tohse, H., Murayama, E., Ohira, T., and Nagasawa, H., 2005, Diel changes in endolymph aragonite saturation rate and mRNA expression of otolith matrix proteins in the trout otolith organ: Marine Ecology-Progress Series, v. 294, p. 249–256.

Thorrold, S.R., Jones, C.M., and Campana, S.E., 1997, Response of otolith microchemistry to environmental variations experienced by larval and juvenile Atlantic croaker (Micropogonias undulatus): Limnology and Oceanography, v. 42, no. 1, p. 102–111.

Thorrold, S.R., Jones, C.M., Campana, S.E., McLaren, J.W., and Lam, J.W.H., 1998, Trace element signatures in otoliths record natal river of juvenile American shad (Alosa sapidissima):.

Thresher, R.E., 1999, Elemental composition of otoliths as a stock delineator in fishes: Fisheries Research, v. 43, no. 1-3, p. 165–204.

Tohse, H., Murayama, E., Ohira, T., Takagi, Y., and Nagasawa, H., 2006, Localization and diurnal variations of carbonic anhydrase mRNA expression in the inner ear of the rainbow trout Oncorhynchus mykiss: Comparative Biochemistry and Physiology Part B: Biochemistry and Molecular Biology, v. 145, no. 3-4, p. 257–264.

Tohse, H., Takagi, Y., and Nagasawa, H., 2008, Identification of a novel matrix protein contained in a protein aggregate associated with collagen in fish otoliths: FEBS J, v. 275, no. 10, p. 2512–2523, doi: EJB6400 [pii] 10.1111/j.1742-4658.2008.06400.x.

Tuset, V.M., Rosin, P.L., and Lombarte, A., 2006, Sagittal otolith shape used in the identification of fishes of the genus Serranus: Fisheries Research, v. 81, no. 2–3, p. 316–325, doi: http://dx.doi.org/10.1016/j.fishres.2006.06.020.

De Vries, H., 1950, The Mechanics of the Labyrinth Otoliths: Acta Oto-laryngologica, v. 38, no. 3, p. 262–273, doi: 10.3109/00016485009118384.

Walther, G.-R., Post, E., Convey, P., Menzel, A., Parmesan, C., Beebee, T.J.C., Fromentin, J.-M., Hoegh-Guldberg, O., and Bairlein, F., 2002, Ecological responses to recent climate change: Nature, v. 416, no. 6879, p. 389–395.

Walther, B.D., and Thorrold, S.R., 2009, Inter-annual variability in isotope and elemental ratios recorded in otoliths of an anadromous fish: Journal of Geochemical Exploration, v. In Press, .

Whitfield, T.T., Riley, B.B., Chiang, M.-Y., and Phillips, B., 2002, Development of the zebrafish inner ear: Developmental Dynamics, v. 223, no. 4, p. 427–458.

Widdicombe, S., and Needham, H.R., 2007, Impact of CO~ 2-induced seawater acidification on the burrowing activity of Nereis virens and sediment nutrient flux: MARINE ECOLOGY-PROGRESS SERIES-, v. 341, p. 111.

Wilcox-Freeburg, E., Rhyne, A., Robinson, W.E., Tlusty, M., Bourque, B., Hannigan, R.E., and Wilcox Freeburg, E., 2013, A comparison of two pH-stat carbon dioxide dosing systems for ocean acidification experiments: Limnology and Oceanography Methods, v. 11, p. 485–494.

Wilson, R.W., Millero, F.J., Taylor, J.R., Walsh, P.J., Christensen, V., Jennings, S., and Grosell, M., 2009, Contribution of Fish to the Marine Inorganic Carbon Cycle: Science, v. 323, no. 5912, p. 359–362, doi: 10.1126/science.1157972.

Yoshioka, S., Ohde, S., Kitano, Y., and Kanamori, N., 1986, Behaviour of magnesium and strontium during the transformation of coral aragonite to calcite in aquatic environments: Marine Chemistry, v. 18, no. 1, p. 35–48.

Zhang, Y., and Dawe, R.A., 2000, Influence of Mg2+ on the kinetics of calcite precipitation and calcite crystal morphology: Chemical Geology, v. 163, no. 1-4, p. 129–138.

Zhong, S., and Mucci, A., 1989, Calcite and aragonite precipitation from seawater solutions of various salinities: Precipitation rates and overgrowth compositions: Chemical Geology, v. 78, no. 3-4, p. 283–299.

CHAPTER 2

COMPARISON OF TWO PH-STAT CARBON DIOXIDE DOSING SYSTEMS FOR OCEAN ACIDIFICATION EXPERIMENTS

(This Chapter was published in Limnology and Oceanography Methods and is reformatted for this dissertation. Original Citation: Wilcox-Freeburg, Eric, et al. "A comparison of two pH-stat carbon dioxide dosing systems for ocean acidification experiments." Limnol. Oceanogr: Methods 11 (2013): 485-494.)

Abstract

As the oceans acidify due to increasing atmospheric CO_2, there is a growing need to understand the impact of this process on marine organisms. Field observations are difficult because of multiple covarying factors (e.g., temperature, salinity). As such, there is interest in conducting controlled, laboratory experiments in order to best understand how changes in acidity will affect marine organisms. We tested two intermittent CO_2 dosing systems, a “home aquarium hobby” grade pH controller and an industrial process control platform. We assessed stability, accuracy, and precision over 7-day experimental periods as well as relative cost of the two configurations. We also compared three laboratory grade pH electrodes to the hobbyist electrode to further evaluate electrode

quality on system-controlled pH stability and drift. While the industrial system offered some benefit with regard to autonomy, our results show that the low-cost hobbyist system can be modified appropriately to provide comparable pH control. We provide a detailed list of procedures and software developed for the implementation of a cost-effective, precision controlled CO_2 dosing system to support laboratory-based ocean acidification experiments.

Introduction

The pH of the ocean is declining in response to increased concentrations of atmospheric carbon dioxide, [CO_2]. This process, known as ocean acidification, consequently changes carbonate system equilibria resulting in greatly declining carbonate ion availability. Calcium carbonate mineralization is thermodynamically limited by carbonate ion activity (αCO_3^{2-}). Therefore, ocean acidification is expected to severely limit growth of calcified structures. Organismal response (by calcifiers and non-calcifiers) to ocean acidification is the subject of many recent studies (Widdicombe and Needham, 2007; Checkley et al., 2009; Ries et al., 2009; Wilson et al., 2009; Cummings et al., 2011; Kroeker et al., 2011; Munday et al., 2011; Doropoulos et al., 2012; Ferrari et al., 2012; and references therein). The results of these studies demonstrate that the impact of ocean acidification on marine life is not restricted to calcified structures. Other physiological responses range from changes in growth rate and morphology to changes in gene expression. While there remains a vast knowledge gap with respect to impacts of ocean acidification on marine biota, entry into this area of research may be hampered due

to prohibitive cost and lengthy method development required to precisely control aquaria pH in the laboratory.

It is possible to control seawater pH in the laboratory through a variety of means. For example, synthetic seawater can be produced and tailored to desired dissolved inorganic carbon (DIC), total alkalinity (A_T), and pH levels. These parameters can be maintained by minimizing gas exchange and evaporation (Gattuso et al., 1998). The pH of natural waters can be adjusted with mineral acids and bases to simulate historic and modeled pH (Riebesell et al., 2000; Spero et al., 1997). This approach, however, is generally avoided because of its impact on alkalinity and total organic carbon (Dickson et al., 2007). More recently, adjustments of pH using continuous dosing of natural waters with premixed specialty CO_2 enriched air mixtures (CO_2 + air) enable a broad array of laboratory experiments. Indeed this approach is used successfully in conjunction with moderate- to large-scale recirculating flow-through seawater systems (Checkley et al., 2009; Ries et al., 2009) as well as static exposures (Iglesias-Rodriguez et al., 2008). This approach is simple and should, in theory, reduce variability in set pH values over an extended period of time. While this method allows for little deviation in tank pH, specialty mixed gases can be costly. Mass flow controllers may be used to mix incoming air to a desired pCO_2 (de Putron et al., 2011; Edmunds et al., 2012). While this method assures a constant pCO_2 value entering the aquaria, equilibrium pH within the aquaria may shift depending on biological activity and/or passive gas exchange. An alternative gas dosing approach uses intermittent dosing with pure CO_2 gas along with continuous aeration of tanks with ambient air. This approach can be used to control pH in individual

aquaria, as static or static renewal exposures (Gazeau et al., 2007; Waldbusser et al., 2011), or with header tanks that provide flow-through to one or more individual aquaria (Berge et al., 2006; Munday et al., 2009; Munday et al., 2011).

We assessed two approaches to intermittent CO_2 dosing of static aquaria. Specifically, we evaluated two of the many available dosing systems with respect to stability, accuracy, precision, dependability and cost, as well as pH electrode performance, and describe their deployment in detail. We chose to compare an industrial system manufactured by Omega Engineering (Stamford, CT) and a hobbyist system manufactured by Digital Aquatics (Woodinville, WA.). Both systems monitor the pH of aquaria using a pH probe and have a controller for which a specific target pH value can be set. In both systems, continuous aeration of the aquaria using ambient air leads to outgassing of CO_2, causing an increase in pH. Once the upper pH threshold is met, the controller opens a gas solenoid valve, allowing CO_2 gas from a pressurized cylinder to be bubbled into the aquarium water, thereby lowering pH.

Materials and Procedures

Omega Engineering (OE) system configuration

The Omega Engineering single setpoint proportional pH controller (PHCN-901) is an industrial process management platform that has a splash and corrosive resistant enclosure. This unit has a standard connection for pH electrodes and allows for a broad performance range of electrodes. Additionally, the unit sends data to an external logger over analog amperage output. The controller houses all functions required for control of

one aquarium, and therefore is replicated for each additional tank. pH calibration is done prior to sealing the housing, using a two-point calibration method. Calibration dials (analog potentiometers) consist of an “offset” and “slope” set. Any set of pH calibration standards may be used, allowing the system to use either National Bureau of Standards (NBS) standard pH scale buffers (pH_{NBS}) or synthetic seawater pH buffer solutions (pH_T) (Byrne, 1987; Millero et al., 1993a; Millero et al., 1993b).

In experimental aquaria (Figure 1), pH is maintained at the given setpoint by CO_2 dosing when the pH of the aquaria drifts above the setpoint value by approximately 0.01 - 0.02 pH units. A dosing schedule circuit within the controller allows optimization of system hysteresis and offers the ability to dose intermittently via a gas solenoid valve (Omega SV3204) that is plumbed to a CO_2 cylinder. Multiple controllers can feed into the same data logger. We used an Omega four channel 25 mA current data logger (omega.com; OM-CP-QUADPROCESS-25MA). Data collection and storage times depend on the choice of polling rate. In our study, we used a 5 min polling rate allowing for collection of 4 channels of data for more than 2 weeks. We downloaded data every 3 – 4 days corresponding to the schedule of water changes for the aquaria. Multiple gas solenoid valves can be plumbed to the CO_2 cylinder using standard gas connections. A step down regulator (swagelok.com, KPR1DFC412A20000), attached as a ‘third stage’ to a standard two-stage laboratory CO_2 regulator, was set to 2-7 psi in order to lower flow rates delivered to the aquaria.

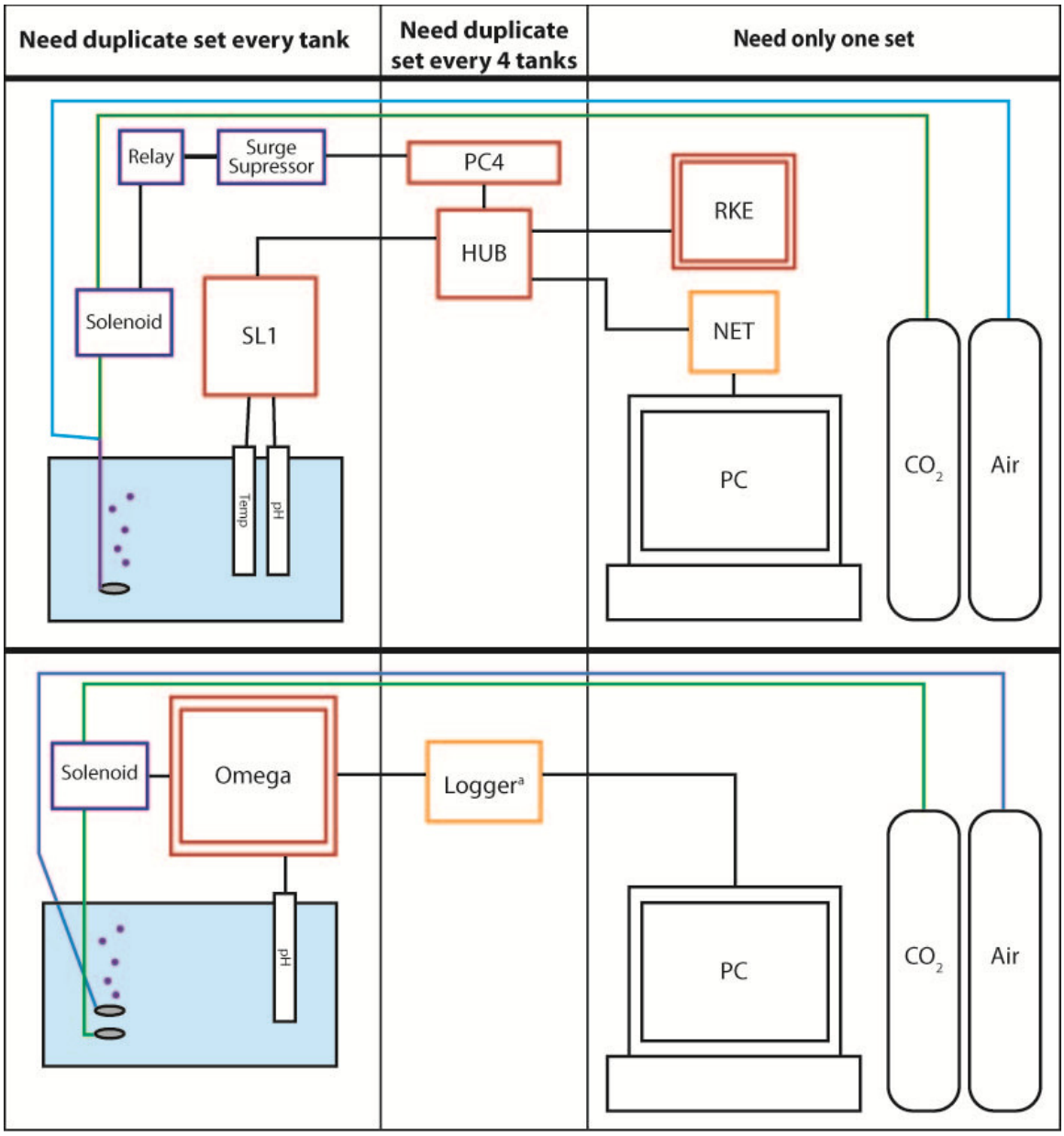

Fig. 1. Top: Digital Aquatics, Inc. (DA) ReefKeeper Elite (RKE) setup, showing required duplication. Bottom: Omega Engineering (OE) setup, showing required duplication. Note that the OE sytem log is generated at each head unit box, but the temperature data is not logged as is possible with the DA system. OE logger (a), as shown, is a 4-port unit, and therefore a system must be deployed for every four tanks. Components are color coded as follows: red - controller, blue - gas dosing, orange - logger.

The output line from the gas solenoid was connected via an in-line check valve to a standard aquarium airstone placed directly below the continuously flowing ambient air airstone at the bottom of the aquarium. This tiered airstone setup promotes water circulation in the aquarium and assists in efficient gas diffusion. We used commercially-available software (omega.com, OM-CP-IFC200) specific for the data logger to manually control start and stop of data logging. We found that connecting a laptop computer via a USB port to the four-channel Omega data logger resulted in a 0.90 mA voltage drop in the recorded signal. Hence, we connected the computer to the system for short periods of time and stopped data logging until the data could be downloaded. The computer was not connected to the data logger during electrode calibration or long-term monitoring of aquaria pH. During electrode calibration we found that the data polling rate had to be changed to allow sufficient time for the data logger to record mA output during each calibration step to externally verify pH calibration. The data polling rate was set to two second intervals during pH calibration. Afterwards, we reset the polling rate to 5 min intervals for long-term pH monitoring. We regressed calibration data logs offline to convert mA output to pH. We optimized hysteresis compensation using the two analog potentiometers ("Proportional Settings"). Adjusting these settings changes the total on/off time per dose as well as frequency of the cycle. Manual adjustment of CO_2 dose can be done, as well, by changing the gas pressure to the solenoids using the 'third stage' gas regulator as mentioned above.

Digital Aquatics (DA) system configuration

The Digital Aquatics (DA) ReefKeeper Elite controller (RKE) is an aquarium hobbyist system (Table 1). The RKE platform allows control/monitoring of several water quality variables depending on the choice of an appropriate module from a host of add-on modules. Indeed, this controller is most often used in a hobbyist reef tank system and is capable of automating most reef tank functions (pH, temperature, oxidation reduction potential, and salinity). Specifically, lab modules (SL1 or SL2) monitor pH over a BNC connection, allowing flexibility in pH electrode selection. In addition to pH electrodes, temperature, ORP, and salinity probes are available and can be attached to the lab units. The DA system is highly modular, as one controller unit (RKE) can address 255 peripheral units.

Table 1. Qualitative assessments of comparative strengths and weaknesses. Stability scores reflect system time between pH electrode calibrations. User customizable scores are determined by optional modules available for end user. Memory capacity scores reflect time between logger downloads. Memory capacity of the DA system is rated highly when using the RSS feed fetching script since it is only limited by computer hard disk space. User friendly scores are reflective of ease of deployment with provided product manuals. Cost scores are reflective of cost/aquarium deployment at larger scales. Overall performance scores represent the ability of the system to perform ocean acidification experimentation adequately.

	OE	DA
Out-of-the-box	+	-
Stability	+	+
User Customizable	-	+
Memory Capacity	+	+
User Friendly	-	-
Cost	-	+
Overall Performance	+	+

Similar to the OE controller, calibration of pH uses a two point calibration where the user is able to digitally set each calibration target. This allows for the use of synthetic seawater buffers (Dickson et al., 2007) for enhanced pH accuracy. pH is controlled by programming a "function" for each individual power outlet of a 4-port power module (PC4) by comparison to the measured pH of the SL1 or SL2 lab module. Assigning a simple “function” allows the user to select power on/off criteria for the 120V AC relay wired to a 120V AC gas solenoid valve. pH is controlled through direct injection of CO_2 from a compressed gas tank into the experimental aquaria.

In our configuration, each system lab unit included an external flasher relay (i.e. grainger.com; cat# 5JJ48) fed into a 120V, normally closed, gas solenoid valve (alliedelect.com; cat# VX2330-02T-3CR1). This allowed for the opening/closing of the gas solenoid. The flasher relay was set to a rate of 0.25 s on, 3 s off. The voltage drop associated with turning on the solenoid valve produced a power surge that resulted, at times, in a software restart and accompanying loss of pH control. To remedy this problem, single outlet surge suppressors (amazon.com; cat# B00006B81E, B000EWVSZK) were wired between the external flasher relay and the outlet in the PC4 strip serving each aquarium. CO_2 gas routing was identical to the OE system. A web interface unit (NET) delivered data via an ethernet connection to attached computer. Data was logged externally over RSS feeds provided by the NET interface at 1s intervals. Data was backed up to external and cloud storage for off-site verification at 1 hr intervals. The Perl and batch scripts we used are available in the supplemental materials.

Assessment

System Stability Tests

We completed a 7-day pH stability test on each system using comparable pH electrodes (OE: Ross Combination pH electrode, Thermo Scientific, cat# 8256BN; DA: Orion PerpHecT combination pH electrode, Thermo Scientific, cat# 13-642-559). During this test, we set the pH controller systems at specific pH levels and held the pH for the duration of the experiment. For the OE system stability experiment we used filtered (1.0µm) and UV sterilized seawater from Savin Hill Cove, Boston, MA. We set the OE controllers to a 1 control and 3 experimental pH values (pH_T = 8.0, 7.7, and 7.4). We downloaded data logs weekly. Due to the cost of OE controllers, we did not replicate aquaria (Figure 2). For the DA experiments, we used filtered (1.0 µm) and UV sterilized seawater collected from Mt. Hope Bay, RI. Due to the lower cost of the DA units we replicated the aquaria (n=4). DA systems were set to control pH as in the OE experiment. RSS feed provided for continuous data downloading (Figure 3).

For stability comparisons we compared pH data collected every 5 minutes across 5 days by both systems. Using the value of observed pH – expected pH we compared the data such that positive values indicate the system is reading higher than expected and negative values correspond to lower than expected. To assess the variability in reading, we calculated the standard deviation for each replicate. The DA replicates were tested for statistical similarity with a one-way ANOVA, and the standard deviation value for each OE replicate was compared to the 95% CI for the corresponding DA pH treatment group. There was no significant difference in the standard deviation between DA replicate

aquaria at the different pH treatments ($F_{2,9} = 3.13$, $p > 0.05$). The standard deviations of the OE treatments were within the 95% CI for the DA treatments (Figure 4)

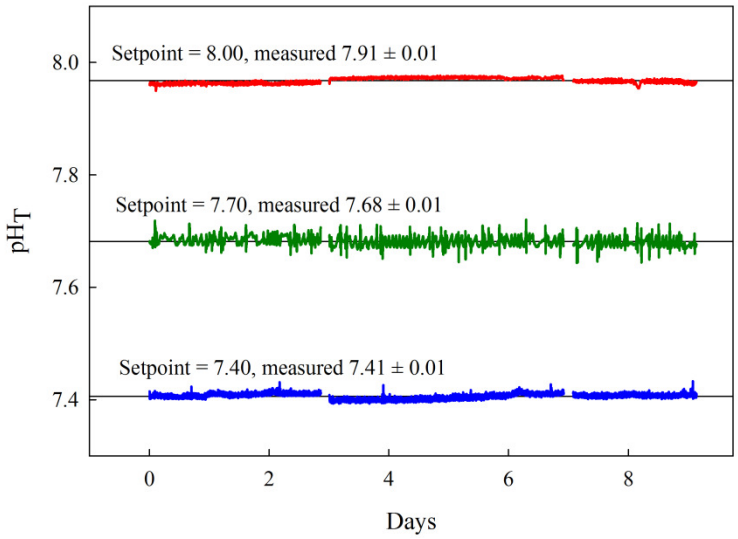

Fig. 2. OE pH controller stability experiment time series using Thermo Scientific Ross combination pH electrodes. pH_T setpoints (mean ± SD) are shown.

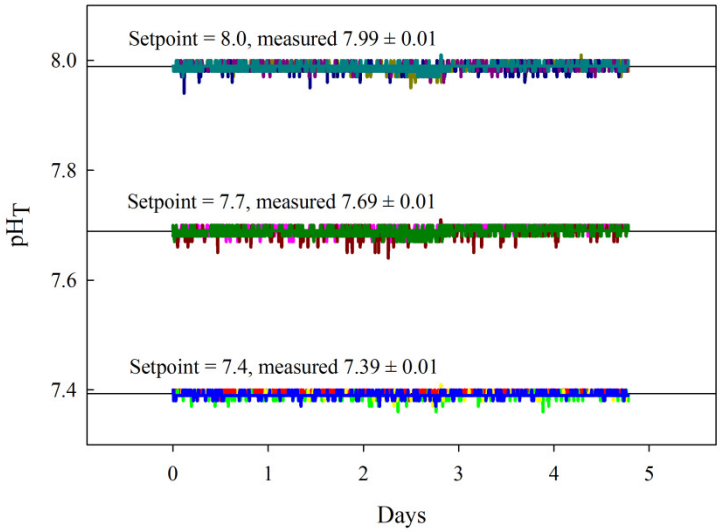

Fig. 3. DA pH controller stability experiment time series using laboratory Ag/Ag-Cl refillable electrodes. pH_T setpoints (mean ± SD) are shown. Each setpoint consists of four experimental aquariums represented by contrasting colors.

pH electrode stability tests

Since our goal was to identify cost-effective alternatives to support ocean acidification experiments, we assessed the stability of a range of pH electrodes with the DA controller. For electrode testing, we used filtered (1.0 µm) and UV treated seawater from Mt. Hope Bay, RI. We buffered total alkalinity (A_T) to 2500 µmol/kg using sodium carbonate to minimize pH change over the study period. We verified A_T following standard methods (Dickson, 1981). We added the buffered seawater to 40 L glass aquaria and aerated the aquaria with house compressed air. Twice daily we verified controller pH using an independent hand-held pH meter (Hach H170G). We calibrated both the DA system and the Hach meter on the total hydrogen concentration scale (pH_T) using colorimetrically calibrated synthetic seawater buffers (Byrne, 1987). In the case of the Hach handheld meter, which collects mV readings, we calculated pH offline due to software restrictions. We measured pH_T directly twice a day over each 7- day experiment.

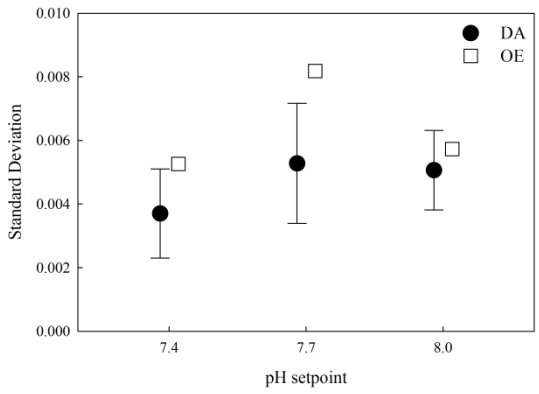

Fig. 4. Performance comparison between DA and OE systems for 5-day stability experiments. Error bars represent DA 95% CI (n = 4). OE standard deviation means do not fall within the DA 95% CI for treatment groups pH = 7.4 and 7.7 while the SD mean for OE pH=8.0 treatment group falls within the corresponding DA 95% CI. Precision of control appears to be comparable, therefore for pH = 8.0 treatment group only.

We tested pH electrodes available from Digital Aquatics (DA), Inc. (sealed, non-refillable epoxy-body electrodes). We also compared calibration drift of the DA electrodes to laboratory-grade Ag/Ag-Cl combination pH electrodes (Fisher Scientific, Cat#: 13-642-559; VWR International, Cat#: 14002-780) . Since the refillable electrodes from VWR exhibited rapid reference solution evaporation, we tested an additional set of VWR pH electrodes fitted with a cotton pad covering the electrode vent (VWR-plug). We tested each electrode (DA, Fisher, VWR, VWR-plug) on two separate metering devices (DA digital readout and Hach H107G handheld meter). This allowed for comparison between replicate tanks with the same meter, between different meters, and between electrode manufacturer (e.g. VWR, VWR-plug). DA electrodes had a larger mV reading range (10.4 mV) than did the laboratory grade electrodes (Fisher = 6.6 mV, VWR = 6.3 mV, VWR-plug = 3.7 mV) (Figure 5). Since repeatability in replicate electrode response indicated comparable precision, a test for Equal Variances showed not all electrodes exhibited comparable variance (Figure 6) (Levene's Test, $p < 0.001$, $W = 52.40$, $\alpha = 0.05$, $N = 12$, $k = 4$) .

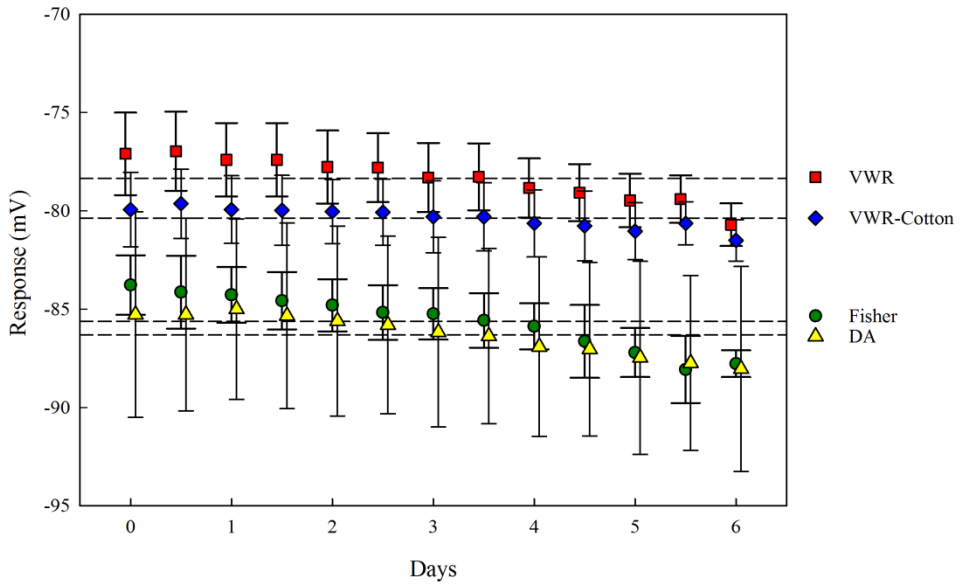

Fig 5. Raw mV electrode potential output from pH electrodes as measured by Hach H107G with standard deviation across individual electrodes of same type. The mean of three aquaria setups per electrode type (mV) is represented by a horizontal line. Three replicate tanks for each probe as measured are represented with respect to time (mean ± SD): Fisher (-85.6 ± 1.8); DA (-86.3 ± 4.1); VWR (-78.3 ± 1.8); VWR-plug (-80.4 ± 1.5).

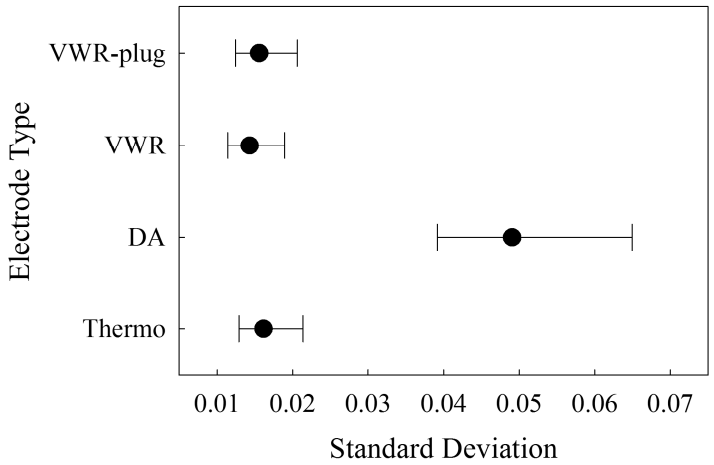

Figure 6. Electrode response comparisons (standard deviation of electrode response, N = 12) with 95% confidence interval bars. DA electrodes exhibited significantly higher variance in electrode response (Levene's Test, $W = 52.40$, $p < 0.001$, $\alpha = 0.05$, $N = 12$, $k = 4$).

Once calibrated, the relationship between pH readout and electrode potential should remain constant. However, normalizing the SL1 pH readings to mV readout indicated a pH/mV ratio shift independent of calibration procedures on all units (Figure 7). When comparing SL2 unit performance under identical data collection conditions, calibration drift was more pronounced than that of SL1 units. Since we accounted for electrode drift in the data normalization procedure, we suggest that differences in slope were likely caused by the electronics used in the lab unit. Linear regression of normalized values indicated that the calibration of the SL2 drifts at a significantly faster rate than that of the SL1 unit (ANOVA, $F_{1,24} = 36.34$, $p < 0.001$) (Figure 7).

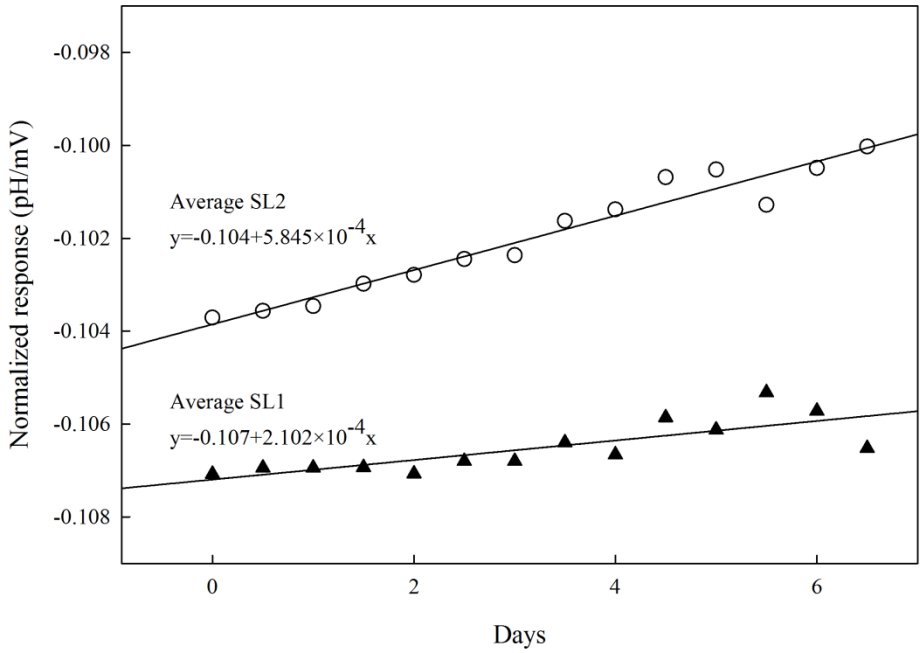

Figure 7. Normalized response (pH/mV) highlighting DA SL2 ($R^2 = 0.947$) vs. SL1 ($R^2 = 0.627$) electrode calibration drift. Note that the slope of each line indicates SL2 units exhibit calibration drift 2.8x the rate of the SL1 units using same pH electrode (Fisher).

Cost analysis

Digital Aquatics, Inc. (DA) ReefKeeper Elite-based systems offered a cost effective alternative to industrial controllers such as those offered by Omega Engineering (OE). The cost for a single tank at the time of this study was $1057 for the DA system, and $1180 for the Omega system. However, replication favored the DA system as each additional tank was $408 for the DA system but $906 for the Omega system.

Discussion

Over the period of the experimental trial, we scored each system for a handful of qualitative parameters (Table 1). The low gas flow rate required for ocean acidification experiments to rear sensitive marine larvae makes control of aquaria pH very difficult. The dosing and sensor equipment can be costly, and thus we compared two systems. Each system offered unique advantages and disadvantages. While precision of the pH control by the "out of the box" DA hobbyist system was less than that of the OE industrial system, we found that the addition of external components to the DA system, such as flasher relays and individual surge protectors, yielded precision control on par with the more costly OE system. This, along with the cost savings, suggests the DA system is a viable option for ocean acidification studies. The biggest strength of the OE system over the DA system was its variable dosing schedule. The OE system was able to pulse-dose the aquaria with variable on and off times through the proportional control knob-driven potentiometers. Without external control, the DA systems dosed continuously until the aquarium pH dipped below the target pH set point, resulting in excessive system pH lag and subsequent hysteresis. By adding variable timer relays

between the power outlet and solenoid valve to the DA system, OE pulse dosing could be mimicked by the DA system.

Power interruption impacted the DA system. Preliminary DA data logs contained gaps ranging from 30 minutes to several hours which were likely a result of power surges and/or power loss. Locally stored data logs appeared to be corrupted during such events. Upon power loss, SL2 units took up to 15 minutes to read correct pH, whereas the SL1 units recovered nearly immediately. We ruled out slow electrode response as the issue since we tested electrodes using an external handheld meter (Hach H107G). These tests showed equilibration of signal readings within 5-10 seconds. To remedy data corruption and electrode stability problems, we placed the systems on uninterruptable power supplies with battery backup and line conditioning and connected to power lines with emergency generator power. We enabled the NET unit RSS feed feature and collected data at 1s intervals using a Perl script. Using this approach we recorded three months of uninterrupted data, including data logs recorded during brownouts, blackouts, and line surges associated with Hurricane Sandy.

Calibration of electrodes on the DA system revealed some issues with the SL2 unit. Calibration of all electrode on SL2 units was slow and cumbersome due to the slow response of the electronics (20 minutes/tank). We could, conversely, complete calibration on the SL1 units in a time frame comparable to the OE system (< 4 - 5 min per controller). We evaluated electrode equilibration using a Hach pH meter and found equilibration time to be within expected limits (5-10 s). This indicated that response time was due to the SL2 electronics not the pH electrodes, themselves. Stability results show

that while the SL2 systems maintained setpoint pH, calibration needs to be monitored and updated daily (Figure 7). When using SL1 units, we increased the calibration cycle to three days of operational accuracy (a set point of 0.02 pH units). In contrast, the OE system did not require pH calibration adjustments over 7 – 10 day periods.

Importantly, DA system calibration must be run manually on each tank, one tank at a time. This is in contrast to the OE system with its dedicated controllers for each tank. The OE setup allowed for simultaneous calibration of multiple tanks and therefore significantly reduced system downtime during calibration.

Comments and recommendations

Systems provided an exceptionally stable platform for relatively automated experiments with minimal modification. With the modifications presented here, we found the DA system provided comparable precision and accuracy of control. Additionally, the modular nature of the DA system allows for a great amount of user customizability whereas the OE system allows for a set number and type of data to be collected.

In designing systems, power backup and data logging must be addressed, and the approach will depend on the specifics of the laboratory location. While OE controllers offer more independent control with high "out-of-the-box" stability, the relative expense of such industrial controllers may prohibit purchase. Researchers will have to balance the relative costs and benefits of the OE and DA systems to determine the best fit for their research needs. The DA system, through modification and regular monitoring of performance, offers a cost-effective alternative to expensive pH controller infrastructure, and can, as shown here, produce results comparable to the OE system.

The cost to set up the first tank, using either system, is nearly identical. However, OE systems become more expensive, averaging almost double the cost per tank when replicating over eight systems. Since true replication to assess pH/pCO_2 effects requires individually controlled tanks, cost of the experimental system heavily favors the DA controller. Although the statistical results show significant differences in tank pH control, the observed differences are outside of the precision range of the pH metering system. DA SL1 performance, including calibration drift, is better than that of the SL2 units. Based on our results we recommend using the SL1 units when employing the DA system.

Appropriate selection of pH electrode is important since it determines pH measurement precision. We found no statistically significant difference in accuracy on the OE or DA systems using laboratory grade Ag/Ag-Cl combination pH electrodes. However, the DA hobbyist electrode was not as precise as the laboratory grade electrodes. Therefore, we suggest that laboratory grade electrodes be used, although it is unnecessary to use electrodes with higher precision than ±0.01 pH units.

In DA system experiments, we encountered calibration drift that required recalibration every three days. For this reason, if using a DA system, we suggest that pH be confirmed with an externally calibrated meter daily to monitor for drift. Since refillable electrodes suffer from solution evaporation over time, the observed drift in these electrodes on the DA system could be exacerbated by particularly warm or dry conditions and so users should develop a drift monitoring protocol for their laboratory conditions. For our purposes, a pH calibration divergence of 0.02 units prompted a recalibration procedure. We found it necessary to recalibrate the electrodes every five

days on average. In our study, we also added precautionary protocols to replace all pH buffers after being used for system calibration due to the heavy use required (12 aquaria). We observed marked improvement in calibration accuracy following this protocol change and suggest this as an ongoing adaptation, regardless of pH/CO_2 control platform.

We developed a scalable, cost-effective and modular system that accurately and precisely controls pH to allow for ocean acidification experiments in the case of the DA system. Modifications are also available to support combined parameter experiments due to the modular base system. This system will open up new avenues of investigation into one of the most significant threats to marine organisms, allowing more researchers to enter into this important area of study.

References

Berge, J.A., Bjerkeng, B., Pettersen, O., Schaanning, M.T., and Øxnevad, S., 2006, Effects of increased sea water concentrations of CO_2 on growth of the bivalve *Mytilus edulis* L: Chemosphere, v. 62, p. 681-687.

Byrne, R.H., 1987, Standardization of Standard Buffers by Visible Spectrometry: Analytical Chemistry, v. 1987, p. 1479-1481.

Checkley, D.M., Jr., Dickson, A.G., Takahashi, M., Radich, J.A., Eisenkolb, N., and Asch, R., 2009, Elevated CO_2 enhances otolith growth in young fish: Science, v. 324, p. 1683.

Cummings, V., Hewitt, J., Van Rooyen, A., Currie, K., Beard, S., Thrush, S., Norkko, J., Barr, N., Heath, P., Halliday, N.J., Sedcole, R., Gomez, A., McGraw, C., and Metcalf, V., 2011, Ocean Acidification at High Latitudes: Potential Effects on Functioning of the Antarctic Bivalve Laternula elliptica: PLoS ONE, v. 6, p. e16069.

de Putron, S.J., McCorkle, D.C., Cohen, A.L., and Dillon, A., 2011, The impact of seawater saturation state and bicarbonate ion concentration on calcification by new recruits of two Atlantic corals: Coral Reefs, v. 30, p. 321-328.

Doropoulos, C., Ward, S., Diaz-Pulido, G., Hoegh-Guldberg, O., and Mumby, P.J., 2012, Ocean acidification reduces coral recruitment by disrupting intimate larval-algal settlement interactions: Ecology Letters, v. 15, p. 338-346.

Dickson, A. G., 1981, An exact definition of total alkalinity and a procedure for the estimation of alkalinity and total inorganic carbon from titration data: Deep Sea Research Part A. Oceanographic Research Papers, v. 28, p. 609-623.

Dickson, A.G., Sabine, C.L., and Christian, J.R., 2007, Guide to best practices for ocean CO_2 measurements.

Edmunds, P.J., Brown, D., and Moriarty, V., 2012, Interactive effects of ocean acidification and temperature on two scleractinian corals from Moorea, French Polynesia: Global Change Biology, v. 18, p. 2173-2183.

Ferrari, M.C.O., Manassa, R.P., Dixson, D.L., Munday, P.L., McCormick, M.I., Meekan, M.G., Sih, A., and Chivers, D.P., 2012, Effects of Ocean Acidification on Learning in Coral Reef Fishes: PLoS ONE, v. 7, p. e31478.

Gattuso, J.P., Frankignoulle, M., Bourge, I., Romaine, S., and Buddemeier, R.W., 1998, Effect of calcium carbonate saturation of seawater on coral calcification: Global and Planetary Change, v. 18, p. 37-46.

Gazeau, F., Quiblier, C., Jansen, J.M., Gattuso, J.-P., Middelburg, J.J., and Heip, C.H.R., 2007, Impact of elevated CO_2 on shellfish calcification: Geophys. Res. Lett., v. 34, p. L07603.

Iglesias-Rodriguez, M.D., Halloran, P.R., Rickaby, R.E.M., Hall, I.R., Colmenero-Hidalgo, E., Gittins, J.R., Green, D.R.H., Tyrrell, T., Gibbs, S.J., von Dassow, P., Rehm, E., Armbrust, E.V., and Boessenkool, K.P., 2008, Phytoplankton Calcification in a High-CO_2 World: Science, v. 320, p. 336-340.

Kroeker, K.J., Micheli, F., Gambi, M.C., and Martz, T.R., 2011, Divergent ecosystem responses within a benthic marine community to ocean acidification: Proceedings of the National Academy of Sciences, v. 108, p. 14515-14520.

Millero, F.J., Zhang, J.-Z., Fiol, S., Sotolong, S., Roy, R.N., and Lee, K., 1993a, The use of buffers to measure the pH of seawater: Marine Chemistry, p. 143-152.

Millero, F.J., Zhang, J.-Z., Lee, K., and Campbell, D.M., 1993b, Titration alkalinity of seawater: Marine Chemistry, v. 44, p. 153-165.

Munday, P.L., Dixson, D.L., Donelson, J.M., Jones, G.P., Pratchett, M.S., Devitsina, G.V., and Døving, K.B., 2009, Ocean acidification impairs olfactory discrimination and homing ability of a marine fish: Proceedings of the National Academy of Sciences, v. 106, p. 1848-1852.

Munday, P.L., Hernaman, V., Dixson, D.L., and Thorrold, S.R., 2011, Effect of ocean acidification on otolith development in larvae of a tropical marine fish: Biogeosciences, p. 1631-1641.

Riebesell, U., Zondervan, I., Rost, B., Tortell, P.D., Zeebe, R.E., and Morel, F.M.M., 2000, Reduced calcification of marine plankton in response to increased atmospheric CO_2: Nature, v. 407, p. 364-367.

Ries, J.B., Cohen, A.L., and McCorkle, D.C., 2009, Marine calcifiers exhibit mixed responses to CO_2-induced ocean acidification: Geology, v. 37, p. 1131-1134.

Spero, H.J., Bijma, J., Lea, D.W., and Bemis, B.E., 1997, Effect of seawater carbonate concentration on foraminiferal carbon and oxygen isotopes: Nature, v. 390, p. 497-500.

Waldbusser, G., Voigt, E., Bergschneider, H., Green, M., and Newell, R., 2011, Biocalcification in the Eastern Oyster (*Crassostrea virginica*) in Relation to Long-term Trends in Chesapeake Bay pH: Estuaries and Coasts, v. 34, p. 221-231.

Widdicombe, S., and Needham, H.R., 2007, Impact of CO_2-induced seawater acidification on the burrowing activity of *Nereis virens* and sediment nutrient flux: Marine Ecology Progress Series, v. 341, p. 111-122.

Wilson, R.W., Millero, F.J., Taylor, J.R., Walsh, P.J., Christensen, V., Jennings, S., and Grosell, M., 2009, Contribution of Fish to the Marine Inorganic Carbon Cycle: Science, v. 323, p. 359-362.

CHAPTER 3

OCEAN ACIDIFICATION INDUCES MORPHOLOGICAL CHANGES IN LARVAL REEF FISH OTOLITHS

Introduction

Atmospheric CO_2 is causing dissolved inorganic carbon (DIC) equilibrium changes resulting in a pH decline in the global ocean. This process of ocean acidification (OA), is a of concern for marine calcifiers (Feely et al., 2004). These calcifiers require a favorable environment in which to mineralize carbonate-based structures. Such an environment is commonly considered correlated to high aragonite saturation state ($\Omega_{Ar,}$ Eq. 1).

$$\Omega_{Ar} = \frac{\alpha Ca^{2+} \times \alpha CO_3^{2-}}{K_{sp}} \qquad \text{Eq. 1}$$

This state is dependent on the solubility constant, K_{sp}, which is mainly controlled by temperature and pressure. Calcium ion activity, αCa^{2+}, is regulated by large scale weathering processes and its residence time, 1.1 million years (Broecker et al., 1982), is long enough to consider αCa^{2+} constant over times scales relevant to OA processes. For these reasons, it is expected that saturation state is proportional to the activity of carbonate, αCO_3^{2-} (Eq. 2). The carbonate anion activity is controlled be the exchange of atmospheric $CO_{2(g)}$ into water as $CO_{2(aq)}$ which then reacts with water to form carbonic

acid (H_2CO_3) which dissociates to bicarbonate anion (HCO_{3-}) and then to carbonate anion (Eq. 3). Ultimately the activity of CO_3^{2-} is directly related to its concentration (γCO_3^{2-} x $[CO_3^{2-}] = aCO_3^{2-}$) which is, in turn, related to the partial pressure of atmospheric CO_2 (pCO_2). The equilibrium of the carbonate system shifts with increasing pCO_2 leading to increased CO_2(aq) and HCO_3^- and decreases in CO_3^{2-} ultimately leading to decreased Ω_{Arag}. Commensurate with the decline in CO_3^{2-} is an increase in hydrogen ion content (H^+; pH = -log(aH^+)) leading to acidification of the ocean. Both the acidification by hydrogen ion and the decreasing concentrations of carbonate anion as well as decreased saturation state of aragonite impact marine calcifiers in a number of complex ways (Frommel et al., 2010; Fabry et al., 2008; Riebesell et al., 2000; Munday et al., 2009; Hoegh-Guldberg et al., 2007; Walther et al., 2002).

$$\Omega_{Ar} \propto \alpha CO_3^{2-} \qquad \text{Eq. 2}$$

$$CO_{2(atm)} \leftrightarrow CO_{2(aq)} + H_2O \leftrightarrow H_2CO_3 \leftrightarrow H^+ + HCO_3^- \leftrightarrow 2H^+ + CO_3^{2-} \qquad \text{Eq. 3}$$

Experimental studies describe a range of calcification responses among a variety of species as a result of declining Ω_{Arag} (Checkley et al., 2009; Fabry et al., 2008; Kroeker et al., 2011; Ries et al., 2009; Widdicombe & Needham, 2007). Net calcification is, in external calcifiers such as bivalves, negatively impacted by increased pCO_2 (Ries et al., 2009, (Comeau et al., 2014; Cummings et al., 2011). This is expected given carbonate equilibrium thermodynamics (Eq. 1). However, this relation does not

necessarily hold for internal calcifiers such as teleost fish (Bignami et al., 2013; Checkley et al., 2009; Munday et al., 2011, (Wilcox-Freeburg et al., 2013)).

Teleost fish have 2 pairs (left and right inner ear) of 3 otoliths (aragonite; $CaCO_3$). The otoliths form the vestibular system of the fish and provide for both hearing and gravisensing (Riley and Moorman, 2000; Fekete, 2003; Beier et al., 2002). The system responds to changes in body orientation by movement of the otolith within the endolymphatic fluid of the inner ear and the interaction of the otoliths with hair cell maculae (Lychakov et al., 2006; Cruz et al., 2009; Hardison et al., 2005). For this reason, otolith morphology (e.g., asymmetry) is very important to the function of the vestibular system (Lychakov & Rebane, 2005) as the contact between the otolith surface and maculae provide the sensory information needed for correct spatial orientation of the body. Indeed, removal of otoliths is linked to loss of navigation capacity (B. B. Riley & Moorman, 2000). Incorrect formation of otoliths is also associated with behavioral abnormalities associated with vestibular malfunction (Hardison, Lichten, Banerjee-Basu, Becker, & Burgess, 2005). Since the otolith is a predominantly aragonite (98%; (Campana and Thorrold, 2001)) it is expected that mineralization will be affected by changes in ocean carbonate chemistry [i.e., (Ries et al., 2009)]. Given the potential negative impacts on otolith morphology induced by increased atmospheric CO_2 and associated changes in activity of carbonate anion and ocean pH (here forward referred to as ocean acidification, OA), our study focused on a comprehensive assessment of otolith morphology of larval reef fish under ocean acidification conditions. It is the first such

study to examine impacts on all three otoliths and extends the results to explore potential impacts on the vestibular system.

Recent otolith studies show mixed responses to OA. These responses range from dramatic changes in overall area (Checkley et al., 2009) and density (Bignami et al., 2013), to little change in morphology (Munday et al., 2011). Otolith morphology is strongly related to function (Fekete, 2003; Lychakov, Rebane, Lombarte, Fuiman, & Takabayashi, 2006). Changes in otolith morphology may lead, ultimately, to behavioral changes. Unfortunately, there is no way to compare otolith morphology changes across published studies as they lack common morphological metrics. Moreover, the methods for pCO_2 dosing of experimental aquaria differ among these studies. Species and life history differences also make comparison across studies difficult. There is ample evidence that otolith morphology is genera and, sometimes, species-specific [e.g., (Lombarte & Castellón, 1991; Tuset, Rosin, & Lombarte, 2006)] and so it is inappropriate, if only for this reason, to interpret the results of previous studies in the context of all teleosts. By establishing a common suite of morphometrics and experimental methods, it may be possible to compare experimental results with wild caught fish data and also enable cross-study comparison and evaluation of genera and species-specific OA impacts on the otolith system.

Here we present otolith morphometric data from Clark's clownfish (*Amphiprion clarkii*) reared under different pH conditions. We selected a species of *Amphiprion* to enable comparison of our results to those published by Munday et al. (2011). In addition to otolith morphometrics we examined impacts of OA on somatic growth. Somatic

growth is negatively impacted in aquacultured fish when population density is high resulting in higher dissolved concentrations of CO_2 (Pickering, 1993). High concentrations of dissolved CO_2 leads to blood acidosis, as well (Ishimatsu et al., 2008). The relation between the CO_2(aq) and pH combined with the fact that blood and endolymph should be in equilibrium (Payan et al., 1997; Payan et al., 1999; Borelli et al., 2003) further supports the expectation that OA will impact otolith growth.

Methods

Experimental pCO_2 Manipulation

Clownfish eggs were laid on porcelain tiles placed in the brood stock aquaria. Eggs were left in the aquaria until the day of hatch and then placed in a 200 L aquarium at ambient pH (~8.3). Eggs were gently aerated to assure sufficient oxygen diffusion without excess agitation. Upon hatch, larvae were distributed randomly into 40-L replicate experimental aquaria using sterilized 100 mL beakers while maintaining minimal agitation. Larvae were reared in pH-controlled aquaria using a pH-stat CO_2 dosing controller (Wilcox-Freeburg et al., 2013). We used four replicate tanks of four pH (pCO_2) treatments [pH_T =8.16 (300), 7.80 (800), 7.60 (1400), 7.30 (3000)] with each aquarium independently held at the pH set-point (Wilcox-Freeburg et al., 2013). We provided a native diet of copepods (*Pseudodiaptomus sp.*) in a background of algae (*Isochrysis sp.*) at 20,000 cells/mL. We held prey item density constant over the study period (4:1 nauplii:adult per mL) to allow *ad libitum* feeding. The experiment ended

after 8 days coincident with the beginning of settlement coloration and behavior in the control tanks.

Dissolved Carbonate Chemistry in Experimental Aquaria

We collected water from each tank twice daily and analyzed samples, using standard methods (Dickson et al., 2007; Millero et al., 1993) immediately following collection. pH was measured on the total scale (pH_T) by UV spectroscopy (Byrne, 1987). We measured salinity (S) and temperature (T) using a YSI laboratory salinity and temperature probe (YSI 3200). Measurement of total alkalinity (A_T) followed standard methods for seawater alkalinity titration (Dickson and Goyet, 1994). Using the CO2SYS excel macro and the measured data, we modeled the saturation state of aragonite and other carbonate chemistry parameters (Pierrot, Lewis, & Wallace, 2006). Tank effects on carbonate chemistry were assessed using Analysis of Variance (ANOVA).

Fish Collection and Otolith Preparation

Fish were euthanized in tricaine methanesulfonate. We photographed individually identified fish on a 1 mm grating. Fish were then immediately rinsed and stored in 95% ethanol. We measured individual standard length (SL) using ImageJ (vers 1.47, Java Runtime Environment). Tank effects on somatic growth, measured as SL, modeled pCO_2 and Ω_{Arag} were assessed using Analysis of Variance (ANOVA). Correlations were assessed using linear regression and analysis of covariance (ANCOVA) on linear regression coefficients.

We dissected fish under 10-90x magnification (Olympus SZX10) using microdissection tools. Left and right sagittae, lapilli, and asterisci were placed into a dry petri dish. We added 18 MΩ water to cover the otoliths and arranged then on the left and right of the dish in order from sagittae (top) to asterisci (bottom) (Fig. 1). We gently removed visible tissue from the otoliths but minor tissue did remain as the otoliths, particularly the lapilli and asteriscii, are very small and fragile. We photographed each set of otoliths at a calibrated magnification of 90x.

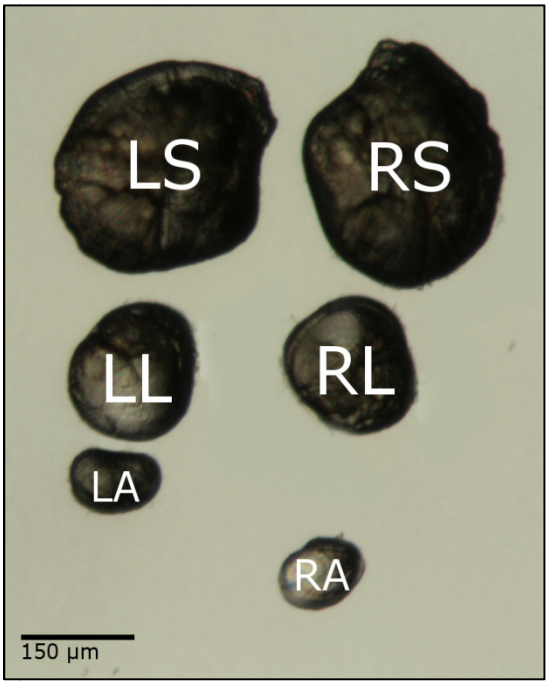

Figure 1. Arrangement of removed otoliths showing positioning of otolith pairs. All photographs taken at 90x magnification. (LS – left sagitta, LL – left lapillus, LA – left asteriscus, R – right).

Otolith Morphometrics

We developed a MATLAB image item morphology algorithm to automate collection of measurement data directly from the photomicrographs. The algorithm automatically subtracted background, added the otolith sample name to the image as well as labeled left and right, and otolith type. Once labeled and digitized for processing we manually "cleaned" the image to remove any remaining tissue residue. MATLAB scripts provided morphological data (major axis, minor axis, circularity index, perimeter, and area) and integrated measurement data with sample metadata for storage in a database which could be used for comparison to experimental treatment parameters as well as comparison between sides and otolith types.

To enable inter-study comparison between this work and that of Munday et al. (2011), we compared otolith circularity using the circularity index. In sedimentary petrology studies, circularity index is a commonly acquired grain morphology metric. Circularity index is defined by the ratio of the largest fully inscribed circle area to the smallest fully circumscribed circle area (Riley, 1941). To apply this metric to otoliths, we used model ellipse parameters. MATLAB's built in functions calculated the model ellipse which, by definition, has the same normalized second central moments as the region of interest. By calculating the major and minor axes, we developed a modified Riley circularity index. The circularity index used here is calculated as the ratio of the area of the circle generated by the minor axis to the area of the circle generated by the major axis (Eq. 3). A value of 1 indicates a circular structure. As the value approaches 0 the structure is more elliptical

$$Circularity\ Index = \frac{\pi*(minor\ axis/2)^2}{\pi*(major\ axis/2)^2} \quad \text{Eq. 3}$$

We explored the relation between circularity index to Ω_{Arag} by otolith type and side of head using linear regression. Analysis of Covariance (ANCOVA) was used for comparison of regression coefficients between otoliths of same type, but opposite side of the head (i.e. left sagittal to right sagittal otolith). To evaluate the interaction of somatic growth (SL) and otolith growth we treated SL as a covariate. While Ω_{Arag} is used widely as an indicator for water chemistry-mineralization interactions, we argue a more accurate factor for somatic growth is pCO_2, since this is more closely tied to blood gas content (Esbaugh et al., 2012; Cech et al., 2002).

Circularity index, here, is considered a standarizable morphometric for otolith studies. To explore the potential of this metric for interstudy comparison we normalized otolith perimeter and area to SL and regressed these values against Ω_{Arag}. We compared these regression results to those of SL and otolith circularity index to Ω_{Arag} to measure general somatic growth changes and otolith morphology changes and determine trend correlations.

Morphometric data was acquired using MATLAB image processing tools with photomicrographs imported into the software. Edge fidelity can be lost as images are imported and edge detection routines are employed (Fig 2A). We used interpolation to restore edge fidelity (Fig 2B). Due to the loss of edge fidelity otolith perimeter, which is dependent on the identification of true edges, is not an appropriate metric to compare across studies as each software package used will identify edges using slightly different

algorithms for interpolation (Figure 2C). Automated perimeter traces may incorporate jagged edges that artificially increase the perimeter to area ratios used by others [i.e. perimeter^2/area (Bignami et al., 2013; Munday et al., 2011)]. Smoothed or interpolated perimeter traces may reduce some of the overestimation of changes in morphology. In this study, we used an ellipsoid model to circumvent the need for such perimeter traces (Fig 2D). This approach means that our perimeter measures are not directly comparable to those of other published studies. Rather our perimeter measures provide for guidance in the development of a common perimeter acquisition method that will enable comparison across future studies.

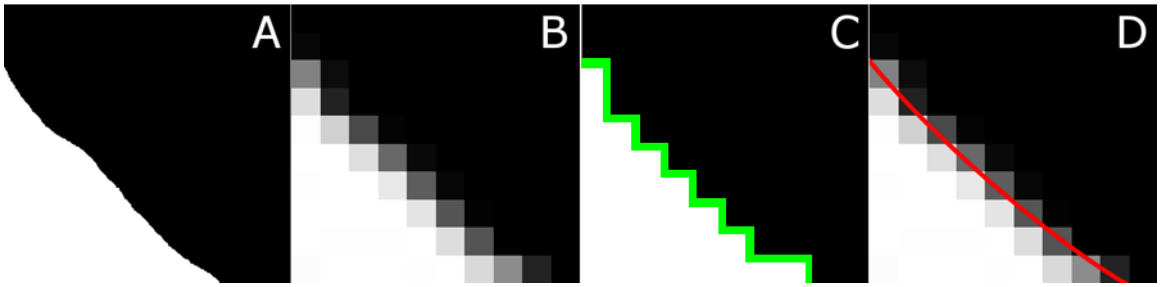

Figure 2. Theoretical comparison of true sample (A), photographic data (B), strict perimeter calculation (C, green), and model ellipsoid used in this study (D, red).

The current version of the MATLAB scripts are available through Github (github.com/edfreeburg/MATLAB-Image-Analysis) and will be continuously updated and refined for the purposes of automated morphometric analysis.

Results

Total pH (pH_T) represents pH measurements of waters, done twice daily (Table 1). Controller pH was within 0.01 of measured pH throughout the experiment. Salinity remained stable across all aquaria at (35.0 =/- 0.01 (n=7), Table 1). Total alkalinity was found to be within 1 standard deviation across all aquaria, A_T, (Table 1). Total alkalinity remained constant as the result of charge balance (Eq. 4). CO_2 incorporation increases the overall carbon load in the system leading to increased dissolved inorganic carbon concentrations (Table 1). Conversely, carbonate equilibrium shifts away from CO_3^{2-} at high pCO_2, resulting in decreased Ω_{Arag}. These relations are reflected in the model results provided by CO2SYS (Table 1).

Mortality variance (mean(stdev)) was very high (Control - 2.20 ± 2.39, pH = 7.8 - 5.20 ± 4.38, pH = 7.6 - 2.20 ± 1.79, pH = 7.3 - 3.40 ± 2.70) with no detectable difference between treatment groups (ANOVA: $F_{3,14} = 1.14$, $p = 0.365$, pooled standard deviation = 2.974). However, mortality was assessed during water changes when fish bodies were discovered. Final counts on each aquarium did not match mortality counts. We found no detectable difference between treatment groups and final population counts (ANOVA: $F_{3,8} = 2.26$, $p = 0.158$).

Table 1. Aquaria carbonate chemistry showing average for triplicate replication for each treatment group (±SD, n=3) measured values (pH_T, S, T^oC, A_T) and model output from CO2SYS (DIC, pCO_2, Ω_{Arag}).

pH_T	S ppt	T °C	A_T µmol kg^{-1}	DIC µmol kg^{-1}	pCO_2 µatm	Ω_{Ar}
8.16 (0.04)	35	28.2(0.4)	2440(147)	2018	299.4	4.84
7.80 (0.01)	35	28.2(0.4)	2440(152)	2237	825.5	2.54
7.60 (0.01)	35	28.3(0.4)	2432(140)	2318	1384.3	1.70
7.30 (0.01)	35	28.2(0.4)	2418(140)	2415	2897.0	0.89

Tank replicate did not affect pH, as measured by an independent meter (ANOVA: control - F2,37 = 1.1, p = 0.351; pH = 7.8 - F2,36 = 0.63, p = 0.648; pH = 7.6 - F2,35 = 2.15, p = 0.095; pH = 7.3 - F2,37 = 0.82, p = 0.519) while treatment group pH was significantly different (ANOVA: F2,155 = 2458.49, p < 0.001). Tank replicate did not affect somatic growth (ANOVA: control - F2,46 = 0.60, pH = 7.8 - F2,50 = 3.28, pH = 7.6 - F2,61 = 0.03, pH = 7.3 - F2,37 - 3.07). However, standard length (SL) was different across treatment groups (ANOVA: F3,202=18.45, p < 0.001). Though pCO2 impacted somatic growth (y = -0.0002x + 6.8491, n = 206, R2 = 0.2003, F = 51.09, p < 0.001, Fig 3A), pCO2 accounts for only 20% of the variance in SL. Interestingly ΩArag accounts for 21% of the variance in SL (y = -0.0814x2 + 0.5911x + 5.7792, n = 206, R2 = 0.2150, F = 27.8023, p < 0.0001, Fig 3B).

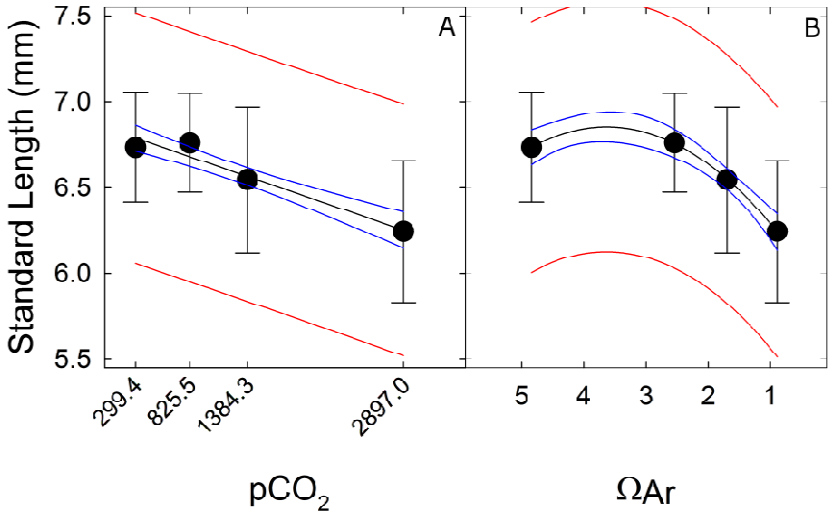

Figure 3. Standard length (SL) for *A. clarkii* with respect to pCO_2 (A) and Ω_{Arag} (B). Linear regression (black), 95% confidence interval (C.I.) (blue) and prediction interval (P.I.) (red) included for SL vs. pCO_2 ($R^2 = 0.20$, $p < 0.001$), and quadratic regression and intervals included for SL vs. Ω_{Arag} ($R^2 = 0.22$, $p < 0.001$).

A. clarkii otolith circularity index was compared to Ω_{Arag} using linear regression. Variation in otolith circularity index is related to Ω_{Arag} though the relation was not significant for astersci ($p > 0.05$). In sagittae, circularity index creased with decreasing aragonite saturation state meaning that the sagittae become more elliptical with increasing pCO_2 (Fig. 4). We found differences in side with the effect of Ω_{Arag} on circularity index stronger on the left than on the right across treatments (right: $R^2 = 0.0949$, $y = 0.010x + 0.7065$, $n = 217$, $F = 23.65$, $p < 0.001$; left: ($y = 0.010x + 0.6932$, $n = 217$, $F = 14.55$, $p < 0.001$, $R^2 = 0.0634$). Lapilli were more circular with Ω_{Arag}, meaning

that increasing pCO_2 resulted in more circular lapilli (Fig. 4). Right lapilli exhibited significant relation between Ω_{Arag} and circularity index ($y = -0.015x + 0.794$, $n = 215$, $F = 23.05$, $p < 0.001$) but the relation did not explain a large portion of the variance ($R^2 = 0.0976$). Left lapilli results were consistent with the right lapilli ($y = -0.0145x + 0.7900$, $n = 212$, $F = 16.79$, $p < 0.001$, $R^2 = 0.0740$). We found no significant relation between asterisci circularity index and Ω_{Arag} (right: $y = -0.0016x + 0.5239$, $n = 185$, $F = 0.1018$, $p = 0.7501$, $R^2 = 0.0006$; left: $y = 0.0034x + 0.4905$, $n = 193$, $F = 0.5266$, $p = 0.4689$, $R^2 = 0.0027$, Fig 4). Slopes were not significantly different between all left and right otoliths of similar type (ANCOVA, $p > 0.05$).

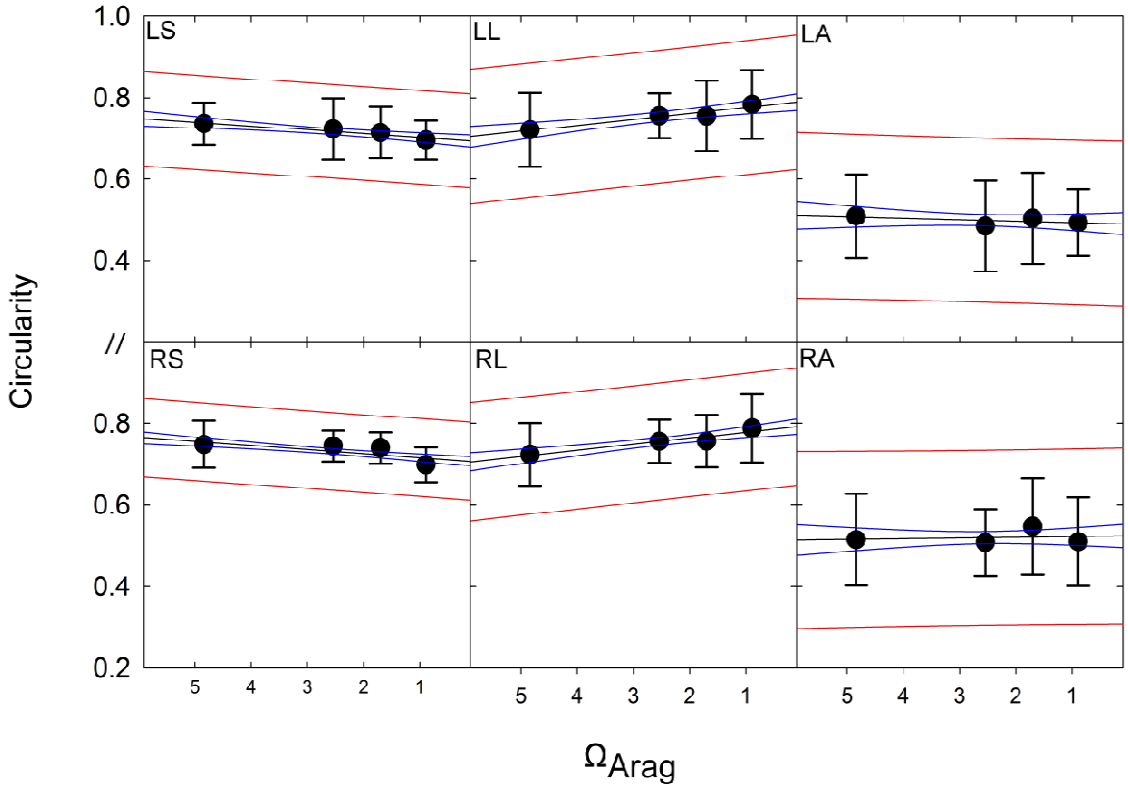

Figure 4. Circularity indices of *A. clarkii* otoliths compared to Ω_{Arag} (linear regression line - black), 95% C.I.(blue) and P.I.(red) for each otolith type (side/type: L - left, R - right, S - sagitta, L - lapillus, A - asteriscus).

We analyzed otolith area to compare against shape analysis studies. In contrast, we normalized otolith area to SL to remove somatic growth effects from the integrated effect of Ω_{Arag} on area. We found significant, but weak, negative linear relations between normalized area and Ω_{Arag} ($p < 0.001$; $R^2 < 0.10$, Fig 5) for all otolith types, but found no significant differences between the left and ride sides (ANCOVA, $p > 0.05$). Particularly,

sagittae area showed a significant negative relation to Ω_{Arag} ($p < 0.001$) as discussed in other teleost literature (Munday et al., 2011; Checkley et al., 2009).

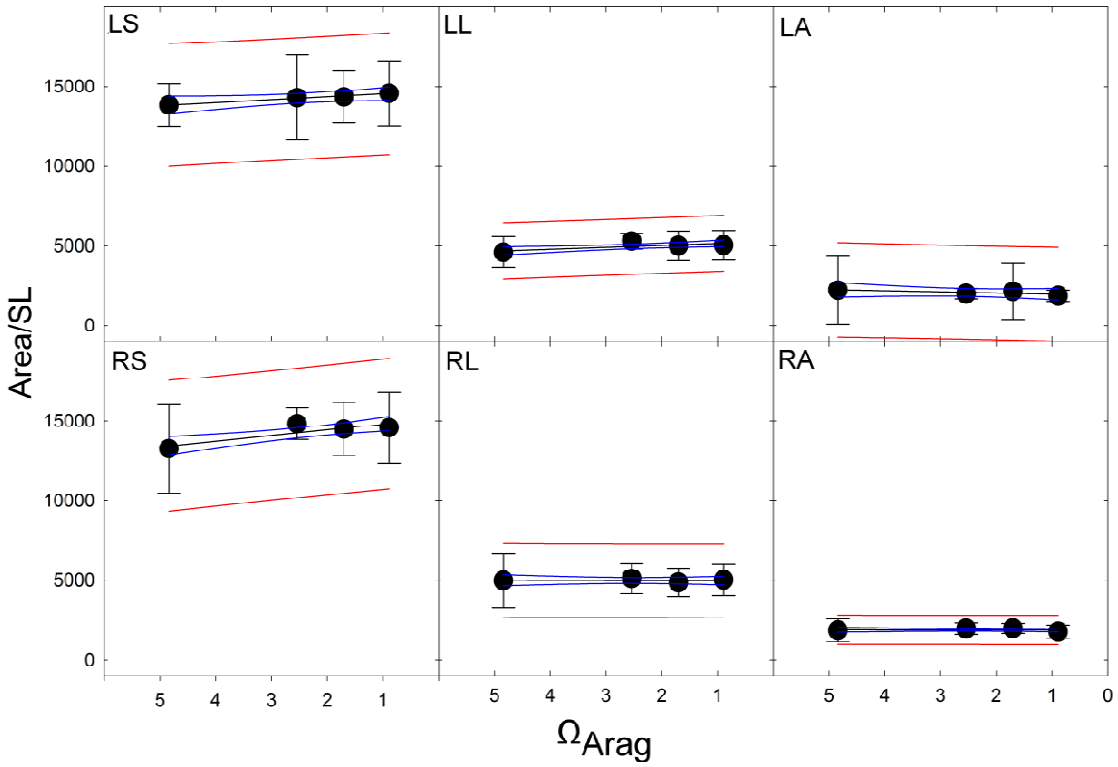

Figure 5. Normalized area measurements calculated by area/standard length. Represented are linear regression (black), 95% C.I.(blue) and P.I.(red) for each otolith type (side/type: L - left, R - right, S - sagitta, L - lapillus, A - asteriscus).

While area measurements can indicate overall mineralization rate, complex morphologies may render this calculation inaccurate. We therefore analyzed automated perimeter traces as in comparable literature. Comparison of SL-normalized perimeter to Ω_{Arag} showed results similar to those seem for SL-normalized area. All regression slopes

were significant ($p < 0.001$) but explained little of the overall variation ($R^2 < 0.1$, Fig 6). Slopes were also not significantly different between otoliths from the left and right side (ANCOVA, $p > 0.05$). SL-normalized perimeter regressions exhibited similar slope results to the SL-normalized area regressions as well, including the negative slope for sagittal perimeter against Ω_{Arag}.

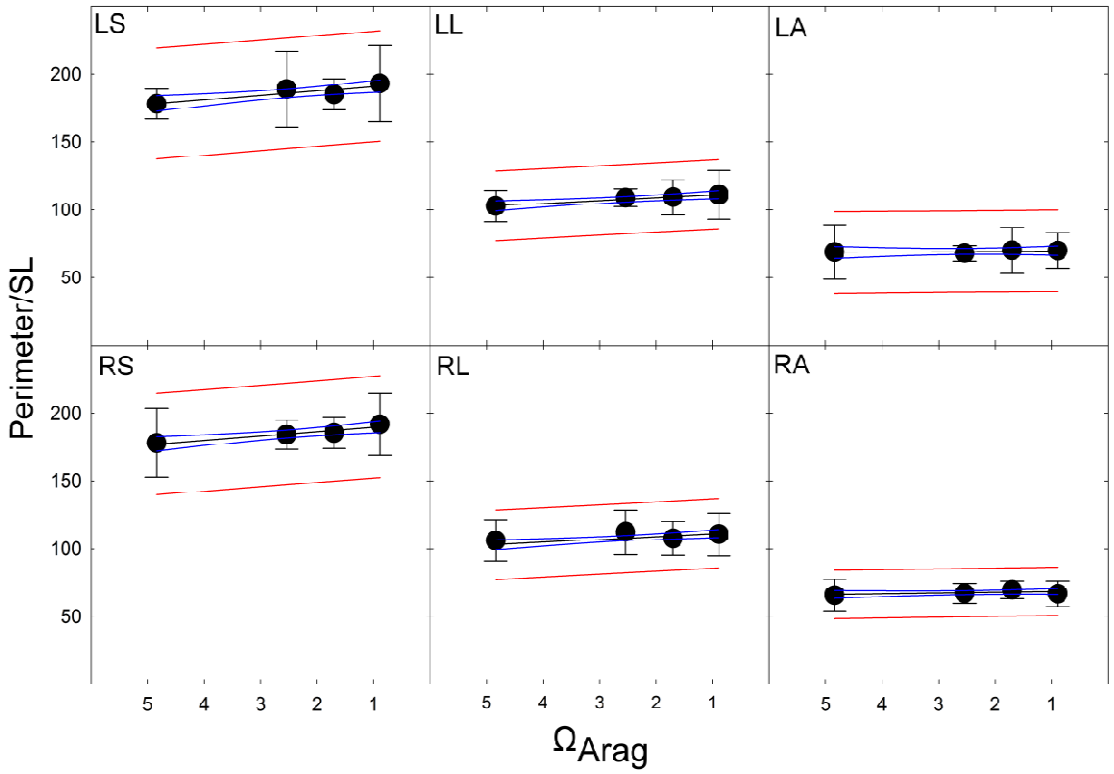

Figure 6. Normalized perimeter measurements calculated by perimeter/standard length. Represented are linear regression (black), 95% C.I.(blue) and P.I.(red) for each otolith type (side/type: L - left, R - right, S - sagitta, L - lapillus, A - asteriscus).

When comparing circularity index and Ω_{Ar}, with standard length as a covariate, the results contrast with the results from *A. percula* (Munday et al., 2011). Our results show a high significance to the relation between circularity index and pH treatment ($p < 0.0001$, $F_{3,337}=14.6770$) but low significance between circularity index and SL ($p = 0.2632$, $F_{1,337} = 1.2561$, Fig 7). There is no detectable interaction between SL and pH treatment ($p = 0.1128$, $F_{1,337} = 2.5282$) in my data. Munday et al., (2011) *A. percula* data showed low significance to the relation between otolith circularity and pH treatment ($p = 0.288$, $F_{2,45} = 1.280$) but a significant SL interaction with pH treatment ($p < 0.001$, $F_{1,45} = 40.84$) (Munday et al., 2011). The comparison between *A. clarkii* and *A. percula* suggest intragenus similarities in impact of OA on otolith morphology, though conflicting results on interaction between somatic growth and morphology.

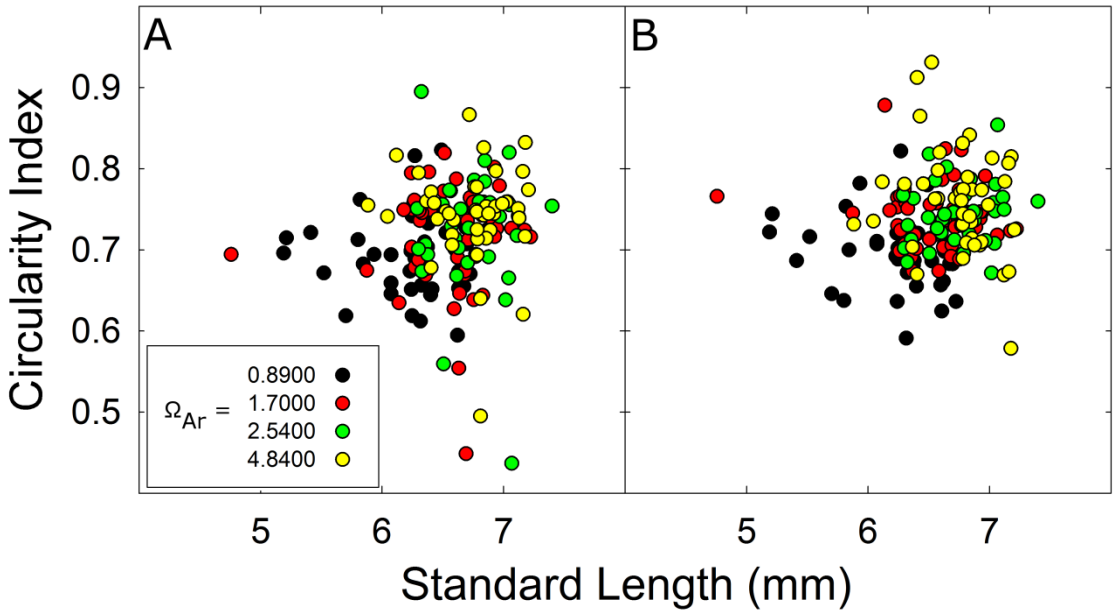

Figure 7. Scatterplot of standard length of individual vs. sagittal otolith circularity index by side (left, L; right, R) and grouped by treatment Ω_{Arag}.

Discussion

In this study we developed the otolith circularity index metric to enable interstudy comparison. Using the MATLAB tools developed in this study we provide a method for generating an accurate, repeatable metric for circularity from clean otolith images. Moreover the tools allow for objective measurement of morphometrics such as perimeter and area of all 6 otoliths at a rate of about 30 seconds/image. When comparing this method to those of 2-5 minute individual manual ROI analyses, large scale studies benefit from increased throughput and result in objective measurements. Additionally, commercial image analysis software used in the Munday et al., 2011, comparative study

(Optimas 6.5) is no longer available, increasing the need for an open-source tool available on a widely used platform such as MATLAB.

Though the image tools used in this study provide accurate and reproducible results and allow for rapid processing of images there are some drawbacks to using these tools. Due to the automated nature of the toolkit, it is important to have clean images before using the software. Therefore, some of our images were preprocessed to increase image contrast and brightness and which eroded superfluous particulates and reinforced contrasting edges, as is common in other image analysis studies (i.e. Psenner, 1993; Haralick et al., 1987). Also, we incorporated particle size filters in the final object analysis to remove any object whose calculated area did not fall within the expected as determined from preliminary tests (e.g., to remove particles too small to be otoliths). We edited the code of the analysis toolkit and replaced hard-coded values, such as minimum area filters. By replacing the current dialog driven interface with a graphical user interface (GUI), newer versions of this toolkit will not require editing of the code. Lastly, we optimized image processing and data storage to support processing of high resolution images. We believe the circularity index metric and software designed here renders exact perimeter traces are unnecessary. It is therefore possible to resize images to fit the needs of the study, thus reducing both processing and storage requirements. In the GUI version of the toolkit we will add interactive resizing dialogs to speed optimization for large images.

Somatic growth of *A. clarkii* decreased significantly under high pCO_2. This result is in direct contrast to Munday et al (2011) who found no significant difference in *A.*

percula standard length with respect to treatment group. The Munday et al. (2011) study included fewer replicates than our study: 3 pseudo-replicated aquariums using flow-through, pre-dosed water from header tanks versus individually controlled, independent tanks for full replication used in our study. Both studies included treatments at ambient pH, 7.8 and 7.6. Our fish began to display settlement coloration in day 8, four days earlier than in the Munday et al. (2011) study. Our fish, unlike those in the Munday et al. (2011) study, reached settlement age at a time similar to what is seen in the wild (8 days; (Fisher et al., 2000; Fisher and Bellwood, 2003; Thresher et al., 1989)). We attribute this difference to the fact that, in our study, prey item selection included a more natural diet (copepods versus rotifers and artemia in Munday et al., 2011) (Gordon et al., 2000; Olivotto et al., 2008). We found significant relations between SL and both pCO_2 and Ω_{Arag} though neither parameter explained the majority of the SL variance. Although both pCO_2 and Ω_{Arag} are related through the acid-base chemistry of carbonate, we expect to see differences associated with the physiology of the fish. Ameliorating blood acidosis induced by maintaining equilibrium between water pCO_2 and the blood pCO_2 has a direct energetic cost (Pörtner et al., 2004; Cech et al., 2002; Ishimatsu et al., 2008). The blood pCO_2 will directly impact the pCO_2 of the endolymph through transmission of hydrogen ion across the endolymphatic membrane required to maintain the pH gradient within the endolymph that enables crystallization of aragonite (Tohse et al., 2006). As such, pCO_2 in the water will have an indirect relation to the saturation state of aragonite within the endolymph. Our data suggest that variance in somatic growth, SL, over the length of our experiment (~8 days) is best explained by individual variability, though between 15-20%

of the variance in somatic growth can be attributed to pCO_2. Decreases in somatic growth with increasing pCO_2, even at the level observed in this study, may have profound impacts on survival. The effect of ocean acidification induced delayed settlement is not well studied for teleosts, though literature exists for marine invertebrates. Many studies have shown impacts on growth (e.g. Ries et al., 2009; Ross et al., 2011) while others go on to discuss impacts on feeding efficiency and higher rates of starvation (e.g. Kurihara et al., 2007; Timmins-Schiffman et al., 2012). Common effects are plausible between pelagic larvae, and we expect similar results of higher predation, lower feeding efficiency, and decreases in general population fitness in the context of our somatic growth results. Any fitness changes across genera will have a profound effect on the distribution of species within marine communities.

The circularity index of sagittae and lapilli is linearly related to Ω_{Arag}. Although the amount of variance in circularity index explained is low (<10%), the relation is significant. Higher pCO_2 directly impacts otolith circularity index such that, for lapilli, we saw a shift towards less circular sagittae and more circular lapilli under OA conditions. These changes could have profound ecological significance. The primary function of the sagittal otolith is hearing (Popper and Fay, 1993; Popper et al., 2003; Braun and Coombs, 2000; Bass and McKibben, 2003). The interaction of the sagittae with the macula is critical to its function and we expect that an increase in elliptical shape will impact its function. The lapilli also assists in hearing, but its primary function is gravisensing (Riley & Moorman, 2000). The lapilli functions much like a buoy moving up and down within the utricle (Whitfield et al., 2002; Fekete, 2003). Its function is

enabled by its elliptical shape which, if it becomes more circular, will change its function and response to horizontal stimuli (Gauldie, 1993). Changes in the circularity of the sagittae (vertical stimuli) and lapilli (horizontal orientation) will impact function though it is unclear how. We do know that otolith morphology changes over the life history of a fish, particularly in early life stages (Brown et al., 2001; Megalofonou, 2006; Vignon, 2012; Secor and Dean, 1989; Wilson and McCormick, 1999) so changes in circularity could have profound consequences for survival. Our results show that small, but significant, changes in sagittal and lapillar circularity index are associated with decreased Ω_{Arag}. There is, however, no apparent relation between circularity index of the sagittae or lapilli and somatic growth. The lack of relation between somatic growth and otolith circularity indicates an independent mechanism. In the context of olfaction studies (Munday et al., 2009; Nilsson et al., 2012), it appears as though blood pH, as opposed to pCO2 or Ω_{Arag} are directly responsible. While gravitation sense becomes necessary for navigation cues once clownfish become demersal, feeding events while at pelagic larvae stage require proper musculature and olfactory development.

When comparing the regression slope coefficients for circularity index versus Ω_{Arag} to regression slope coefficientts of normalized area and perimeter versus Ω_{Arag}, sagittae show different relations than lapilli and asterisci. Under decreasing Ω_{Arag}, sagittal otoliths became less circular but are larger in overall two-dimensional area and perimeter. Conversely lapilli became more circular under decreasing Ω_{Arag} with no detectable change in area or perimeter. Asteriscii results were inconclusive.

Changes in otolith morphology may translate to changes in behavior associated with changes in the function of the otoliths. In our experiment, while not quantified, we did see evidence that swim behavior changed with increasing pCO_2. In the highest pCO_2 treatment (2900 ppmv; pH = 7.3), settlement stage fish swam at constant speed in large arcing paths. Fish in control aquariums (pCO_2 = 300 ppmv; pH = 8.2) exhibited instances of station keeping followed by darting, feeding behaviors. These observations support the suggestion that otolith morphological changes impact behavior though further experimentation is required to quantify the impacts. Based on the work of Riley and Moorman (2000) and others (Bignami et al., 2013; Hardison et al., 2005; Hilbig et al., 2002), we attribute the observed differences in swimming behavior to higher pCO_2 impacts on otolith circularity index. If behavioral changes can be attributed to otolith morphological changes such as seen here, fish survival may decline due to difficulties in navigation which will directly impact feeding, settlement, and predator avoidance.

Genetic studies suggest that there are redundancies that enable fish to recover from disturbances to this vestibular system (Hughes et al., 2004). Thus additional research is needed to determine the extent of which long term effects persist. In the context of OA and the mechanistic understanding of blood pH/pCO_2 regulation (Tohse et al., 2006) it is possible that, under long-term exposure to OA, vestibular recovery may be inhibited. Further work must focus on the mineralogy and crystal habit of the otolith to more fully understand long term influences in shape and thereby function.

Conclusions

A. clarkii standard length was lower in larvae reared at higher pCO_2. Sagittal otolith circularity index decreased with decreasing Ω_{Arag} whereas lapilli circularity index increased with decreasing Ω_{Arag}. Since lapilli are vital for the proper function of the vestibular organ, we conclude that increased circularity index will impact gravisensor functionality. We know that Ω_{Arag} is the parameter that defines whether aragonite is stable. Therefore the fact that decreasing Ω_{Arag} directly impacts otolith morphology in *A. clarkii* larvae suggests that OA could have profound impacts on survival. The impacts we observed in this study showed that OA impacts pre-settlement larvae otolith morphology. We do not know whether the otoliths recover post-settlement. Future studies will explore the post-settlement impacts of OA on larval otolith morphology. We suspect that, since the disturbance to the carbonate system was external to the fish, the persistence of OA conditions would preclude recovery of the otolith system. In the context of otolith function modeling under OA (Bignami et al., 2013), these changes in morphology suggest functional changes between multiple species. This functional change may cause large scale changes in species distribution across many communities.

To more further understand the functional changes associated with shape, studies of the sulcus-macula interaction zone must focus on microstructural changes. Little is known with regards to the mineralogy and crystal habit of the this important biomechanical sensor and forthcoming work will attempt to illuminate changes along this interaction area.

References

Bass, A.H., and McKibben, J.R., 2003, Neural mechanisms and behaviors for acoustic communication in teleost fish: Progress in Neurobiology, v. 69, p. 1–26, doi: 10.1016/S0301-0082(03)00004-2.

Beier, M., Anken, R.H., and Rahmann, H., 2002, Susceptibility to abnormal (kinetotic) swimming fish correlates with inner ear carbonic anhydrase-reactivity: Neuroscience Letters, v. 335, no. 1, p. 17–20, doi: http://dx.doi.org/10.1016/S0304-3940(02)01151-5.

Beier, M, & Anken, R. (2006). On the role of carbonic anhydrase in the early phase of fish otolith mineralization. *Advances in Space Research*, *38*(6), 1119–1122. doi:http://dx.doi.org/10.1016/j.asr.2005.10.027

Bignami, S., Spongaugle, S., and Cowen, 2013, Response to ocean acidification in larvae of a large tropical marine fish , Rachycentron canadum: Global Change Biology, v. 19, p. 996–1006, doi: 10.1111/gcb.12133.

Borelli, G., Guibbolini, M.E., Mayer-Gostan, N., Priouzeau, F., De Pontual, H., Allemand, D., Puverel, S., Tambutte, E., and Payan, P., 2003, Daily variations of endolymph composition: relationship with the otolith calcification process in trout: J Exp Biol, v. 206, no. 15, p. 2685–2692, doi: 10.1242/jeb.00479.

Braun, C.B., and Coombs, S., 2000, The overlapping roles of the inner ear and lateral line: the active space of dipole source detection.: Philosophical transactions of the Royal Society of London. Series B, Biological sciences, v. 355, p. 1115–1119, doi: 10.1098/rstb.2000.0650.

Broecker, W. S., Peng, T.-H., & Beng, Z. (1982). *Tracers in the Sea*. Lamont-Doherty Geological Observatory, Columbia University.

Brown, A., Busby, M., and Mier, K., 2001, Walleye pollock Theragra chalcogramma during transformation from the larval to juvenile stage: otolith and osteological development: Marine Biology, v. 139, no. 5, p. 845–851, doi: 10.1007/s002270100641.

Byrne, R. H. (1987). Standardization of standard buffers by visible spectrometry. *Analytical Chemistry*, *59*(10), 1479–1481. doi:10.1021/ac00137a025

Campana, S.E., and Thorrold, S.R., 2001, Otoliths, increments, and elements: keys to a comprehensive understanding of fish populations?: Canadian Journal of Fisheries and Aquatic Sciences, v. 58, no. 1, p. 30–38.

Cech, J.J., Crocker, J., and Crocker, C.E., 2002, Physiology of sturgeon: effects of hypoxia and hypercapnia: Journal of Applied Ichthyology, v. 18, p. 320–324, doi: 10.1046/j.1439-0426.2002.00362.x.

Checkley, D.M., Dickson, A.G., Takahashi, M., Radich, J.A., Eisenkolb, N., Asch, R., and Checkley, D.M., 2009, Elevated CO2 enhances otolith growth in young fish: Science, v. 324, no. 5935, p. 1683, doi: 324/5935/1683 [pii] 10.1126/science.1169806.

Comeau, S., Carpenter, R.C., and Edmunds, P.J., 2014, Effects of irradiance on the response of the coral Acropora pulchra and the calcifying alga Hydrolithon reinboldii to temperature elevation and ocean acidification: Journal of Experimental Marine Biology and Ecology, v. 453, p. 28–35, doi: 10.1016/j.jembe.2013.12.013.

Cruz, S., Shiao, J.-C., Liao, B.-K., Huang, C.-J., and Hwang, P.-P., 2009, Plasma membrane calcium ATPase required for semicircular canal formation and otolith growth in the zebrafish inner ear: v. 212, no. 5, p. 639–647, doi: 10.1242/jeb.022798.

Cummings, V., Hewitt, J., Van Rooyen, A., Currie, K., Beard, S., Thrush, S., Norkko, J., Barr, N., Heath, P., Halliday, N.J., Sedcole, R., Gomez, A., McGraw, C., and Metcalf, V., 2011, Ocean acidification at high latitudes: potential effects on functioning of the Antarctic bivalve Laternula elliptica. (J. A. Gilbert, Ed.): PloS one, v. 6, no. 1, p. e16069, doi: 10.1371/journal.pone.0016069.

Dickson, A.G., and Goyet, C., 1994, Handbook of Methods for the Analysis of the Various Parameters of the Carbon Dioxide System in Sea Water . Edited by: Handbook of methods for the analysis of the various parameter of the carbon dioxide system in sea water version 2, v. 1994.

Dickson, A. G., Sabine, C. L., & Christian, J. R. (2007). *Guide to best practices for ocean CO2 measurements*. *PICES Special Publication 3* (Vol. 3, p. 191).

Esbaugh, A., Heuer, R., and Grosell, M., 2012, Impacts of ocean acidification on respiratory gas exchange and acid–base balance in a marine teleost, Opsanus beta: Journal of Comparative Physiology B, v. 182, no. 7, p. 921–934, doi: 10.1007/s00360-012-0668-5.

Fabry, V.J., Seibel, B.A., Feely, R.A., and Orr, J.C., 2008, Impacts of ocean acidification on marine fauna and ecosystem processes: ICES Journal of Marine Science: Journal du Conseil , v. 65 , no. 3 , p. 414–432, doi: 10.1093/icesjms/fsn048.

Feely, R. A., Sabine, C. L., Lee, K., Berelson, W., Kleypas, J., Fabry, V. J., & Millero, F. J. (2004). Impact of Anthropogenic CO2 on the CaCO3 System in the Oceans. *Science* , *305* (5682), 362–366. doi:10.1126/science.1097329

Fekete, D.M., 2003, Developmental biology. Rocks that roll zebrafish: Science, v. 302, no. 5643, p. 241–242, doi: 10.1126/science.1091171 302/5643/241 [pii].

Fisher, R., and Bellwood, D., 2003, Undisturbed swimming behaviour and nocturnal activity of coral reef fish larvae: Marine Ecology Progress Series, v. 263, p. 177–188, doi: 10.3354/meps263177.

Fisher, R., Bellwood, D., and Job, S., 2000, Development of swimming abilities in reef fish larvae: Marine Ecology Progress Series, v. 202, p. 163–173, doi: 10.3354/meps202163.

Frommel, A.Y., Stiebens, V., Clemmesen, C., and Havenhand, J., 2010, Effect of ocean acidification on marine fish sperm (Baltic cod: Gadus morhua): Biogeosciences, v. 7, no. 12, p. 3915–3919, doi: 10.5194/bg-7-3915-2010.

Gordon, A.K., Kaiser, H., Britz, P.J., and Hecht, T., 2000, Effect of Feed Type and Age-at-weaning on Growth and Survival of Clownfish Amphiprion percula (Pomacentridae): Aquarium Sciences and Conservation, v. 2, no. 4, p. 215–226, doi: 10.1023/A:1009652021170.

Haralick, R.M., Sternberg, S.R., and Zhuang, X., 1987, Image analysis using mathematical morphology: Pattern Analysis and Machine Intelligence, IEEE Transactions on, , no. 4, p. 532–550.

Hardison, A.L., Lichten, L., Banerjee-Basu, S., Becker, T.S., and Burgess, S.M., 2005, The zebrafish gene claudinj is essential for normal ear function and important for the formation of the otoliths: Mechanisms of Development, v. 122, no. 7-8, p. 949–958.

Hilbig, R., Anken, R.H., Sonntag, G., Höhne, S., Henneberg, J., Kretschmer, N., and Rahmann, H., 2002, Effects of altered gravity on the swimming behaviour of fish: Advances in Space Research, v. 30, no. 4, p. 835–841.

Hoegh-Guldberg, O., Mumby, P.J., Hooten, A.J., Steneck, R.S., Greenfield, P., Gomez, E., Harvell, C.D., Sale, P.F., Edwards, A.J., Caldeira, K., Knowlton, N., Eakin, C.M., Iglesias-Prieto, R., Muthiga, N., et al., 2007, Coral Reefs Under Rapid

Climate Change and Ocean Acidification: Science , v. 318 , no. 5857 , p. 1737–1742, doi: 10.1126/science.1152509.

Hughes, I., Blasiole, B., Huss, D., Warchol, M. E., Rath, N. P., Hurle, B., … Ornitz, D. M. (2004). Otopetrin 1 is required for otolith formation in the zebrafish Danio rerio. *Developmental Biology*, *276*(2), 391–402. doi:http://dx.doi.org/10.1016/j.ydbio.2004.09.001

Ishimatsu, A., Hayashi, M., and Kikkawa, T., 2008, Fishes in high-CO2, acidified oceans: Mar Ecol Prog Ser, v. 373, p. 295–302.

Kroeker, K. J., Micheli, F., Gambi, M. C., & Martz, T. R., 2011. Divergent ecosystem responses within a benthic marine community to ocean acidification. *Proceedings of the National Academy of Sciences* , *108* (35), 14515–14520. doi:10.1073/pnas.1107789108

Kurihara, H., Kato, S., and Ishimatsu, A., 2007, Effects of increased seawater pCO2 on early development of the oyster Crassostrea gigas: Aquatic Biology, v. 1, p. 91–98, doi: 10.3354/ab00009.

Lombarte, A., & Castellón, A., 1991. Interspecific and intraspecific otolith variability in the genus Merluccius as determined by image analysis. *Canadian journal of zoology*, *69*(9), 2442–2449.

Lychakov, D. V, and Rebane, Y. T. 2005. Fish otolith mass asymmetry: morphometry and influence on acoustic functionality. *Hear Res*, *201*(1-2), 55–69. doi:S0378-5955(04)00283-7 [pii] 10.1016/j.heares.2004.08.017

Lychakov, D. V, Rebane, Y.T., Lombarte, A., Fuiman, L.A., and Takabayashi, A., 2006. Fish otolith asymmetry: morphometry and modeling: Hear Res, v. 219, no. 1-2, p. 1–11, doi: S0378-5955(06)00117-1 [pii] 10.1016/j.heares.2006.03.019.

Megalofonou, P., 2006, Comparison of otolith growth and morphology with somatic growth and age in young-of-the-year bluefin tuna: Journal of Fish Biology, v. 68, p. 1867–1878, doi: 10.1111/j.1095-8649.2006.01078.x.

Millero, F. J., Zhang, J.-Z., Fiol, S., Sotolongo, S., Roy, R., Lee, K., & Mane, S., 1993. The use of buffers to measure the pH of seawater. *Marine Chemistry*. doi:10.1016/0304-4203(93)90199-X

Munday, P.L., Dixson, D.L., Donelson, J.M., Jones, G.P., Pratchett, M.S., Devitsina, G. V, and Døving, K.B., 2009, Ocean acidification impairs olfactory discrimination and

homing ability of a marine fish: Proceedings of the National Academy of Sciences, v. 106, no. 6, p. 1848–1852, doi: 10.1073/pnas.0809996106.

Munday, P.L., Hernaman, V., Dixson, D.L., and Thorrold, S.R., 2011, Effect of ocean acidification on otolith development in larvae of a tropical marine fish: Biogeosciences, v. 8, no. 6, p. 1631–1641, doi: 10.5194/bg-8-1631-2011.

Nilsson, G.E., Dixson, D.L., Domenici, P., McCormick, M.I., Sørensen, C., Watson, S.-A., and Munday, P.L., 2012, Near-future carbon dioxide levels alter fish behaviour by interfering with neurotransmitter function: Nature Climate Change, v. 2, p. 201–204, doi: 10.1038/nclimate1352.

Olivotto, I., Capriotti, F., Buttino, I., Avella, A.M., Vitiello, V., Maradonna, F., and Carnevali, O., 2008, The use of harpacticoid copepods as live prey for Amphiprion clarkii larviculture: Effects on larval survival and growth: Aquaculture, v. 274, p. 347–352, doi: 10.1016/j.aquaculture.2007.11.027.

Payan, P., Edeyer, A., de Pontual, H., Borelli, G., Boeuf, G., and Mayer-Gostan, N., 1999, Chemical composition of saccular endolymph and otolith in fish inner ear: lack of spatial uniformity: Am J Physiol, v. 277, no. 1 Pt 2, p. R123–31.

Payan, P., Kossmann, H., Watrin, A., Mayer-Gostan, N., and Boeuf, G., 1997, Ionic composition of endolymph in teleosts: origin and importance of endolymph alkalinity: J Exp Biol, v. 200, no. Pt 13, p. 1905–1912.

Pickering, A. D. (1993). Growth and stress in fish production. *Aquaculture*, *111*(1–4), 51–63. doi:http://dx.doi.org/10.1016/0044-8486(93)90024-S

Pierrot, D., Lewis, E., & Wallace, D. (2006). *Program developed for CO2 system calculations* (ORNL/CDIAC.). Carbon Dioxide Information Analysis Center, Oak Ridge National Laboratory, U.S. Department of Engergy, Oak Ridge, Tennessee. doi:10.3334/CDIAC/otg.CO2SYS_XLS_CDIAC105a

Popper, A.N., and Fay, R.R., 1993, Sound detection and processing by fish: critical review and major research questions.: Brain, behavior and evolution, v. 41, p. 14–38, doi: 10.1159/000316111.

Popper, A.N., Fay, R.R., Platt, C., and Sand, O., 2003, Sound detection mechanisms and capabilities of teleost fishes, *in* Sensory Processing in Aquatic Environments, p. 3–38.

Pörtner, H.O., Langenbuch, M., and Reipschläger, A., 2004, Biological Impact of Elevated Ocean CO2 Concentrations: Lessons from Animal Physiology and Earth

History: Journal of Oceanography, v. 60, p. 705–718, doi: 10.1007/s10872-004-5763-0.

Psenner, R., 1993, Determination of size and morphology of aquatic bacteria by automated image analysis: Handbook of methods in aquatic microbiology. Lewis Publishers, Boca Raton, Florida,, p. 339–346.

Riebesell, U., Zondervan, I., Rost, B., Tortell, P.D., Zeebe, R.E., and Morel, F.M.M., 2000, Reduced calcification of marine plankton in response to increased atmospheric CO2: Nature, v. 407, no. 6802, p. 364–367.

Ries, J.B., Cohen, A.L., and McCorkle, D.C., 2009, Marine calcifiers exhibit mixed responses to CO2-induced ocean acidification: Geology, v. 37, no. 12, p. 1131–1134.

Riley, B.B., and Moorman, S.J., 2000, Development of utricular otoliths, but not saccular otoliths, is necessary for vestibular function and survival in zebrafish: Journal of Neurobiology, v. 43, no. 4, p. 329–337.

Riley, N. A. (1941). Projection sphericity. *Journal of Sedimentary Research* , *11* (2), 94–95. doi:10.1306/D426910C-2B26-11D7-8648000102C1865D

Ross, P.M., Parker, L., O'Connor, W.A., and Bailey, E.A., 2011, The Impact of Ocean Acidification on Reproduction, Early Development and Settlement of Marine Organisms: Water, v. 3, no. 4, p. 1005–1030, doi: 10.3390/w3041005.

Secor, D.H., and Dean, J.M., 1989, Somatic growth effects on the otolith – fish size relationship in young pond-reared striped bass, *Morone saxatilis*: Canadian Journal of Fisheries and Aquatic Sciences, v. 46, p. 113–121, doi: 10.1139/f89-015.

Thresher, R.E., Colin, P.L., and Bell, L.J., 1989, Planktonic duration, distribution and population structure of western and central Pacific damselfishes (Pomacentridae): Copeia, v. 1989, p. 420–434, doi: 10.2307/1445439.

Timmins-Schiffman, E., O'Donnell, M.J., Friedman, C.S., and Roberts, S.B., 2012, Elevated pCO2 causes developmental delay in early larval Pacific oysters, Crassostrea gigas: Marine Biology,, doi: 10.1007/s00227-012-2055-x.

Tohse, H., Murayama, E., Ohira, T., Takagi, Y., & Nagasawa, H. (2006). Localization and diurnal variations of carbonic anhydrase mRNA expression in the inner ear of the rainbow trout Oncorhynchus mykiss. *Comparative Biochemistry and Physiology Part B: Biochemistry and Molecular Biology*, *145*(3-4), 257–264.

Tuset, V. M., Rosin, P. L., & Lombarte, A. (2006). Sagittal otolith shape used in the identification of fishes of the genus Serranus. *Fisheries Research*, *81*(2–3), 316–325. doi:http://dx.doi.org/10.1016/j.fishres.2006.06.020

Vignon, M., 2012, Ontogenetic trajectories of otolith shape during shift in habitat use: Interaction between otolith growth and environment: Journal of Experimental Marine Biology and Ecology, v. 420-421, p. 26–32, doi: 10.1016/j.jembe.2012.03.021.

Walther, G.-R., Post, E., Convey, P., Menzel, A., Parmesan, C., Beebee, T.J.C., Fromentin, J.-M., Hoegh-Guldberg, O., and Bairlein, F., 2002, Ecological responses to recent climate change: Nature, v. 416, no. 6879, p. 389–395.

Whitfield, T.T., Riley, B.B., Chiang, M.-Y., and Phillips, B., 2002, Development of the zebrafish inner ear: Developmental Dynamics, v. 223, no. 4, p. 427–458.

Widdicombe, S., & Needham, H. R. (2007). Impact of CO~ 2-induced seawater acidification on the burrowing activity of Nereis virens and sediment nutrient flux. *Marine Ecology-Progress Series*, *341*, 111.

Wilcox-Freeburg, E., Rhyne, A., Robinson, W. E., Tlusty, M., Bourque, B., Hannigan, R. E., & Wilcox Freeburg, E. (2013). A comparison of two pH-stat carbon dioxide dosing systems for ocean acidification experiments. *Limnology and Oceanography Methods*, *11*, 485–494.

Wilcox-Freeburg, E., Rhyne, A.L., and Hannigan, R.E., 2013, A Picture Is Worth One Thousand Words: Image Analysis Tools For Otolith Studies, *in* Larval Fish Conference 2013, Miami, FL.

Wilson, D.T., and McCormick, M.I., 1999, Microstructure of settlement-marks in the otoliths of tropical reef fishes: Marine Biology, v. 134, p. 29–41, doi: 10.1007/s002270050522.

Supplemental information

MATLAB image analysis methodology

MATLAB code used for image analysis is available over GitHub (github.com/edfreeburg/MATLAB-image-analysis). To use the code, download to a directory currently in your PATH. Use MATLAB help to add directories to your PATH if necessary. Run the code by typing "Morpho.m" into your MATLAB command line. Navigate to the directory where images are being stored for analysis. The script will process the images and move them to a subdirectory labeled "Processed" to assist the user in refraining from processing the same sample multiple times. Once all samples are processed, each sample will have an independent *.xls file.

CHAPTER 4

THE SHAPE OF THINGS TO COME: OCEAN ACIDIFICATION CAUSES FISH EARSTONE MINERALIZATION CHANGE

Abstract

Ocean acidification is expected to severely impact marine calcifiers, and as such, reef fish are currently the subject of intense study. While initial work showed enhanced growth of the otolith in acidified conditions (Bignami et al., 2013; Checkley et al., 2009), little is known about how this impacts otolith gravisensor function in relation to its sensory maculae. As a first step towards understanding the impact of OA on otolith structure and function, I assessed the general crystal habit of the otolith. Core habit development was closely correlated to Ω_{Ar} for two species of clownfish, *Amphiprion clarkii* ($R^2 = 0.65$, $p < 0.001$) and *A. frenatus* ($R^2 = 0.76$, $p < 0.001$). In the context of recent work, I believe these changes in core habit indicate a significant functional change. If functional change occurs, fishes may experience drastic declines in survival. Herein, I describe the first dataset looking specifically into otolith core development with respect to Ω_{Ar}.

Introduction

The oceans are acidifying as atmospheric CO_2 is absorbed into the ocean (Feely et al., 2004). The process of ocean acidification (OA) consequently changes the carbonate

system equilibria resulting in declining aragonite saturation state, Ω_{Ar}. This change has a direct effect on calcifying organisms. However, organismal response varies among marine species (Ries et al., 2009; Widdicombe and Needham, 2007; Checkley et al., 2009; Kroeker et al., 2011; Fabry et al., 2008).

Reef fishes are affected by ocean acidification (Munday et al., 2011; Munday et al., 2009; Munday et al., 2010; Nilsson et al., 2012; Dixson et al., 2010). A critical organismal system, the otoliths (earstones) used for gravitational sensing, are affected by carbonate equilibria state. Since calcification of otoliths occurs internally in a system isolated from the open ocean, the impact of OA on otolith growth and mineralogy is expected to be distinct from impacts on external calcifiers like corals and other marine invertebrates. For this reason, it is important to study the mineralization of fish otoliths to more fully understand the impacts of OA on calcification. Studies of otoliths and OA have, thus far, focused on otolith size, shape, and density (Checkley et al., 2009; Munday et al., 2011; Bignami et al., 2013). As the primary gravisensor in fish, the interaction of the otolith with the sensory macula is of great importance to the survival of the individual. Therefore otolith morphology, particularly at the site of macular interaction, and mineralogy, through differences in density between calcium carbonate polymorphs, must be evaluated.

Changed otolith morphology may have an impact on otolith function. The otolith acts as a buoy, free floating in an extracellular endolymphatic fluid while interacting with hair cell maculae. Change in the shape of the otolith may change its response to orientation change. The otolith interacts with the sensory maculae along colliculum

trench (Nolf, 1985). Since the macula interacts with the otolith along the otolith surface, morphology has a clear impact on otolith function. Vestibular function, in the context of otolith malformation, has been discussed [i.e. (Söllner et al., 2003; Riley and Moorman, 2000; Fekete, 2003)]. Imaging the whole otolith at high resolution allows for the characterization of core development along the colliculum. Due to the potential impacts of changed otolith-maculae interaction on vestibular function, I studied the effects of OA on otolith core development and core crystal habit.

Materials and Methods

Fish were grown in pH-stat OA treatment tanks at a density of approximately 25 individuals per 40 L aquarium. Target pH was set for 7.3, 7.6, 7.8, and a control with no set-point (pH = 8.18 ± 0.03) with 3 replicates for each treatment pH for a total of 12 individually controlled aquaria (Wilcox-Freeburg et al., 2013). *Isocrysis* spp cell density was measured using a Coulter Counter (Beckman Coulter, Inc, Brea, CA). Aquariums were dosed twice per day to a final *Isocrysis* concentration of 40,000 cells/mL. *Pseudodiaptomus* spp were provided as live food. Densities of copepod nauplii were dosed to 5/mL while adults were dosed to 1/mL. Light cycle was held at 14 hour on, 10 hours off. Fish were sacrificed when the majority of fish in a given aquarium had reached settlement age (8 days post hatch). All 6 otoliths (2 pairs of sagittae, lapilli, and asterisci) were extracted using a dissection scope and rinsed in 98% ethanol, allowed to dry and placed on aluminum scanning electron microscope (SEM) stubs for analysis.

Following SEM imaging, otoliths were analyzed for morphological characteristics using MATLAB image analysis software (version 8.2.0.701 2013b; software download link and instructions for use are available in the supplement). Circularity was calculated from major and minor axis evaluations and variance in circularity analyzed using linear regression against the pH treatment group. SEM images of the otoliths were scored using a rubric that assessed core crystal development on a range from 1 (no clear core structure) to 5 (clear, grouped large crystals with little organization). Each otolith, for both *A clarkii* (n=434) and *A. frenatus* (n = 57), was scored once by 6 different readers, each of whom was trained on a subset of images that were omitted from the final test group. Values for each sample were averaged, and regressed against the pCO_2 treatment group. Specific methodology used in this study is available in the supplemental materials.

Upon initial inspection, otoliths exhibit varying surface textural features. In the artificial bone-tissue interaction literature, results indicate a strong binding affinity between tissues and artificial bone at specific roughness characteristics (Chappard et al., 2003; Stupp and Ciegler, 1992; Grant et al., 2007). These optimal roughness studies indicate a close relationship between tissues and their hard substrate. In the context of this data, I believe roughness characteristics of the otolith also closely correspond to macula function. Therefore, an additional MATLAB script was written to quantify surface roughness characteristics. This study represents the first attempt at developing a roughness characteristic analysis set and apply it to the field of OA-biomineralization.

Results

Standard length (SL) is a standard measurement taken from the tip of the snout to the termination of the hypural plates. SL was measured for all *A. clarkii* and *A. frenatus.* SL was regressed against Ω_{Ar}. A second order relation between SL and Ω_{Ar} was detected for *A. clarkii* ($p < 0.0001$, $F_{3,203} = 27.802$, $R^2 = 0.215$, Fig 1A). The correlation is significant but does not account for the majority of the variance. *A. frenatus* somatic growth (SL) was uncorrelated to Ω_{Ar} ($p = 0.4268$, $F_{2,28} = 0.6503$, Fig 1B).

The circularity index of *A. clarkii* sagittal otoliths decreased significantly as Ω_{Ar} decreased ($p < 0.001$, Fig 2A) but the correlation was low for left sagittal otoliths ($R^2 = 0.0634$). The right sagittal otolith of *A. clarkii* exhibited a similar trend ($p < 0.001$, Fig 2B). Significant trends are not detected for *A. frenatus* (Fig 2C, D). In contrast to *A. clarkii*, the regressions for both *A. frenatus* sagittal otoliths exhibit insignificant correlation (left: $p = 0.8385$, $F_{2,25} = 0.0424$; right: $p = 0.3263$, $F_{2,28} = 0.9981$).

A general negative relation between core crystal development score and Ω_{Ar} was also observed for *A. clarkii* (Fig 3A). The slope of the trend line and correlation were significant ($F_{1,354} = 648.0753$, $p < 0.001$, $R^2 = 0.648$). A similar association was detected for *A. frenatus* ($F_{1,61} = 189.9739$, $p < 0.001$, $R^2 = 0.763$, Fig 3B). *A. clarkii* otolith surface roughness was highly variable (Fig 4). Regressions run on each *A. frenatus* otolith type against Ω_{Ar} were only significant for right sagittal otoliths ($p = 0.0241$, $F_{2,103} = 5.2407$, Fig 4D) while all others had insignificant regression outcomes ($p > 0.05$).

Discussion and Conclusion

Past studies have relied on 2D imaging techniques and area assessments (Munday et al., 2011; Checkley et al., 2009). While Munday et al. (2011) do discuss otolith morphological parameters to explain complex responses to OA, Checkley et al. (2009) relied only on otolith area data. Depending on the species of fish, quantifying the mass of larval otoliths is very difficult (*A. clarkii* sagitta length < 400µm). Assumptions made by Checkley et al. (2009) and others regarding increased mineralization rate ignore the possibility of changed mineralogy. Indeed, maintaining a constant mineralization rate while switching from aragonite [aragonitic sagittae = 2.93 g/cm^3] to vaterite [vateritic sagittae = 2.65 g/cm^3 (Campana and Thorrold, 2001)] could explain up to a 10% increase in volume seen by Checkley et al. (2009). In pioneering work by Bignami et al. (2013) otolith surface area and volume were measured and compared to relative otolith density using micro-computed tomography (µCT). This was the first direct exploration of otolith density (cobia; *Rachycentron canadum*) and the first to do so under OA. Bignami et al. (2013) showed an increase in relative otolith density (+6%) attributed to a shift away from aragonite deposition. I developed additional scoring techniques to more accurately assess the impacts of OA on otolith mineralogy and to changes in morphology.

Results from the circularity analysis correlate with observations in previous studies showing little relation between pH treatment and otolith circularity. Although the slope is significant, the correlation between pCO_2 treatment and otolith circularity is too low to be of consequence. It is likely, therefore, that other unaccounted for factors control

the circularity of the otolith or that the variation is primarily due to individual differences rather than environmentally induced differences. We do not know what the baseline individual variation in otolith circularity is in these species of fish.

We found that sagittae from fish grown at high pCO_2 were more prone to have prominent, protruding structures, indicating a change from normal aragonite mineralogy and/or habit (visible external shape of individual crystals or aggregates). Aragonite habit is typically orthorhombic but also occurs as prismatic whereas vaterite habit is hexagonal. Both polymorphs can occur as amorphous with poorly developed habits. In the data presented here, I find significant changes in aragonite habit, especially in the core region where macular contact occurs. At increasing pCO_2, the habit change towards larger, prismatic crystal development near the core provides higher surface area for enhanced mineralization (Fig 3). At low pCO_2, crystal habit around the core was significantly more amorphous, indicating protein dominated mineralization.

Generally, clownfishes exhibit a major behavioral change as they settle, moving from pelagic to demersal habitats and show strong attraction to structure. Otolith function, dependent on macular interaction with the otolith surface, is imperative for settlement and navigation (Hardison et al., 2005; Riley and Moorman, 2000). Significant changes in core development, therefore, may be detrimental to the ongoing survival of reef fishes. Indeed, the observed shift toward aragonite prismatic crystal mineralization should significantly change the otolith-macula interaction.

Recently, otoliths from a highly migratory fish (*R. canadum,* Cobia) grown in acidified conditions [pH = 8.13 to 7.04 (Bignami et al., 2013)] exhibited an increase in

sagittal density. This relative density increase may be explained by the core crystal habit data presented here. Since mineralization of the otolith is protein-mediated, lattice proteins may not be incorporated at the same rate, resulting in increased mineralization on the face of existing crystals. This may explain the observed lack of ordered crystal structure in high pCO_2 treatments. Another important aspect of the observed crystal formation at high pCO_2 are the deep grooves formed in the core of the otolith. To date, physiomechanical simulations of macula transduction in response to otolith orientation change have not been reported. The only function modeling reports use an oscillator model to describe macula transduction (Bignami et al., 2013; Lychakov and Rebane, 2005; De Vries, 1950; Lychakov and Rebane, 2000) whose inputs include otolith area and shape, but no 3D surface topographic data. Calculation of physical responses using a more sophisticated 3D model will better inform assessments of functional assessments.

Hearing models predicted a marked decrease in the lower limit of hearing sensitivity with response to the observed relative density increase in *R. canadum* (Bignami et al., 2013). This inherent change in sound sensitivity may also result in other sensory changes. In the context of these results, it is imperative to more fully understand the ramifications of changed otolith composition, structure, and morphology to function of the system. In other fish species, altered otolith formation corresponds to changes in swimming and general navigation behavior (Beier, 1998; Hilbig et al., 2002). Although these behavioral changes occurred in response to complete failure of the otolith system, it is likely that there is a gradational response with changes in Ω_{Ar}. In the context of OA, these results of other otolith studies as well as the data presented here, expose a need to

more fully understand the physiomechanical properties of the otolith and the ramifications of changed mineralogy on function.

I believe I have discovered a potential driver for catastrophic gravisense failure. The significance of behavioral changes induced by otolith malformation may be high given that fish with pelagic estuarine larval stages are already experiencing extremes in low pH, such as those found in upwelling zones along the US Pacific Northwest coastline (Hauri et al., 2013; Feely et al., 2008; Feely et al., 2010).

Table 1. Carbonate chemistry showing average (±SD where applicable) and model output from CO2SYS data output as collected over the period of the experiment. All water chemistry parameters were collected using standard methods (Dickson et al., 2007; Millero et al., 1993). pH was measured on the total scale using UV spectroscopy (Byrne, 1987). Salinity (S), temperature (T), pH_T, and total alkalinity (A_T) were measured directly. Using the CO2SYS excel macro (Pierrot et al., 2006), carbonate chemistry parameters were calculated using the above measurements.

pH_T	S ppt	T °C	A_T µmol kg^{-1}	DIC µmol kg^{-1}	pCO_2 µatm	CO_2 µmol kg^{-1}	HCO_3^- µmol kg^{-1}	CO_3^{2-} µmol kg^{-1}	Ω_{Ar}
8.16 (0.04)	35	28.2(0.4)	2440(147)	2018	299.4	7.83	1709.99	300.12	4.84
7.80 (0.01)	35	28.2(0.4)	2440(152)	2237	825.5	21.60	2058.15	157.68	2.54
7.60 (0.01)	35	28.3(0.4)	2432(140)	2318	1384.3	36.14	2176.54	105.58	1.70
7.30 (0.01)	35	28.2(0.4)	2418(140)	2415	2897.0	75.82	2284.16	55.34	0.89

.

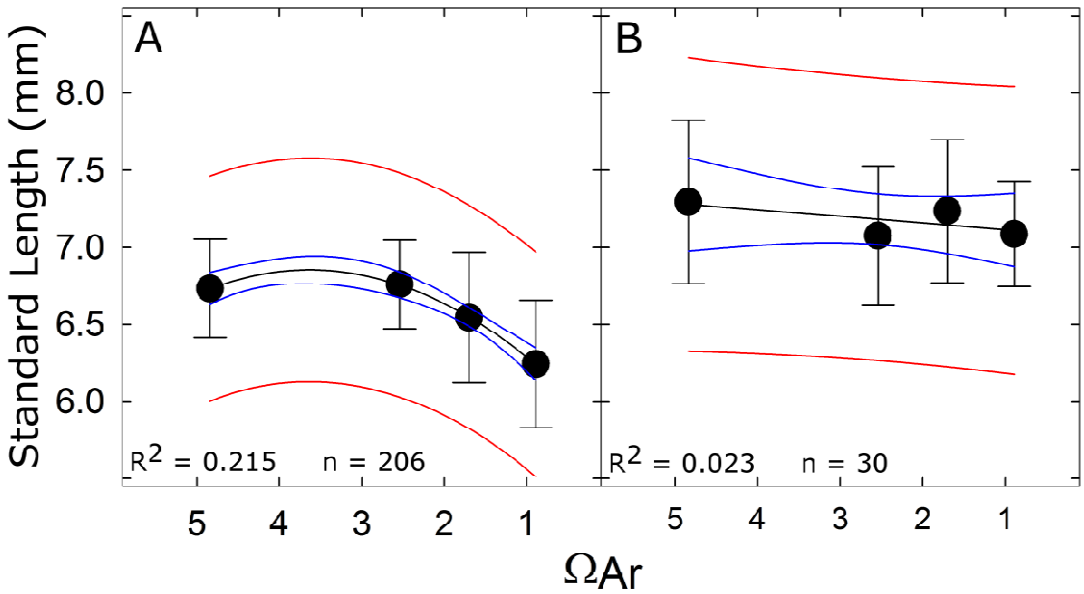

Fig 1. Somatic growth (standard length) and relation to modeled aragonite saturation state (Ω_{Ar}) comparisons between *A. clarkii* (A) and *A. frenatus* (B). Mean ± S.D. are included as dot and tails, respectively. Regression (black), 95% C.I. (blue), and 95% P.I. (red) are also included. *A. clarkii* exhibited a significant 2nd order relationship to Ω_{Ar} ($p < 0.0001$, $F_{2,203} = 27.8023$, $SL = 0.591*\Omega - 0.081*\Omega^2 + 5.779$, A). *A. frenatus* exhibited no significant linear correlation ($p = 0.427$, $F_{2,28} = 0.6503$, $SL = 0.043*\Omega + 7.0731$, B).

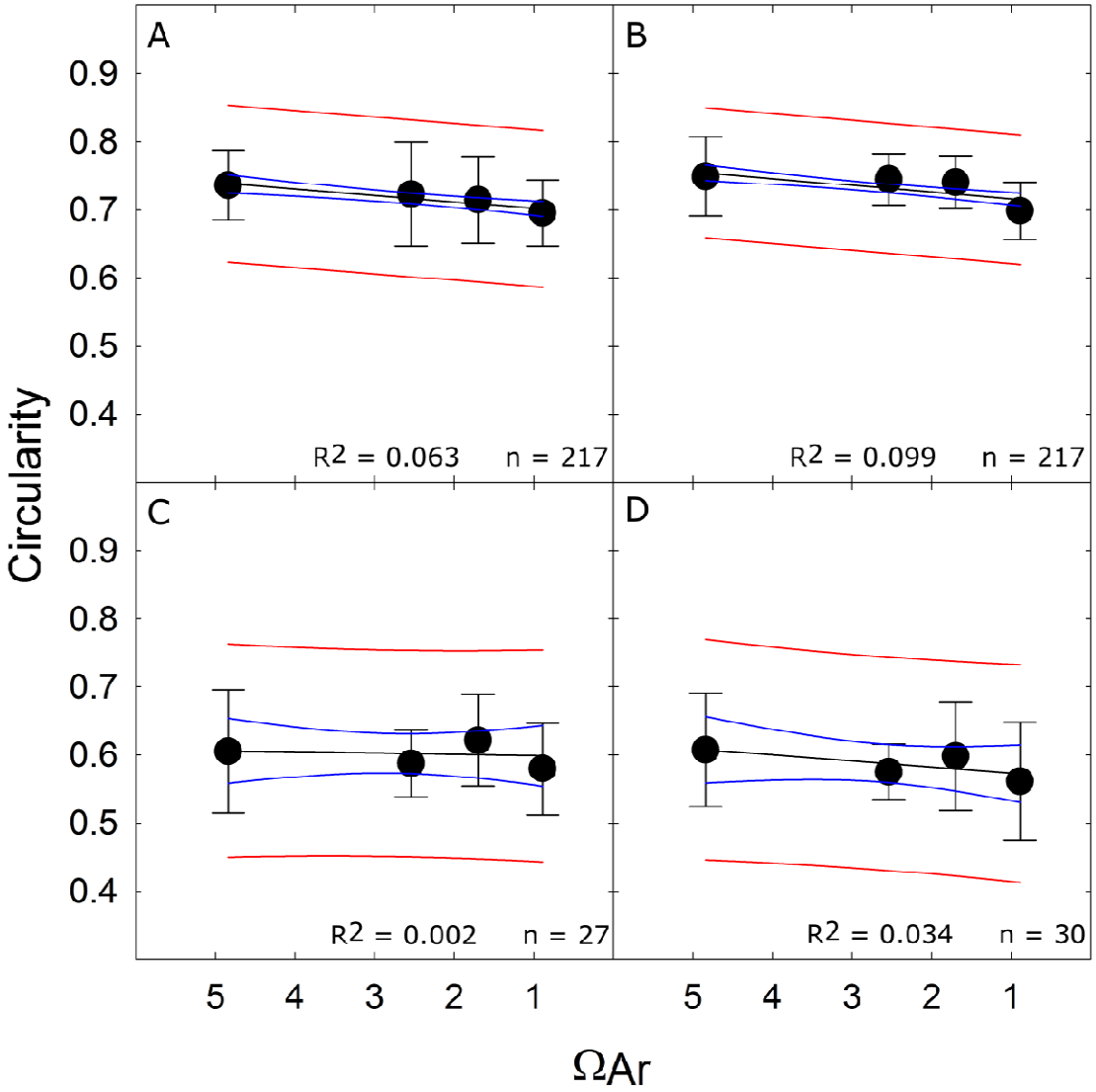

Fig. 2. Circularity index and modeled aragonite saturation state (Ω_{Ar}) for *A. clarkii* for left (A) and right (B) and *A. frenatus* for left (C) and right (D) sagittal otoliths vs. Ω_{Ar}, including linear regression results exhibiting 95% confidence intervals (blue) and 95% prediction interval (red). *A. clarkii* results are significant (left: CircIndex = 0.0093*Ω + 0.0093, $p < 0.001$, $F_{2,215} = 14.55$; right: CircIndex = 0.0099*Ω + 0.7065, $p < 0.0001$, $F_{2,215} = 23.6467$) while *A. frenatus* correlation are not ($p > 0.05$).

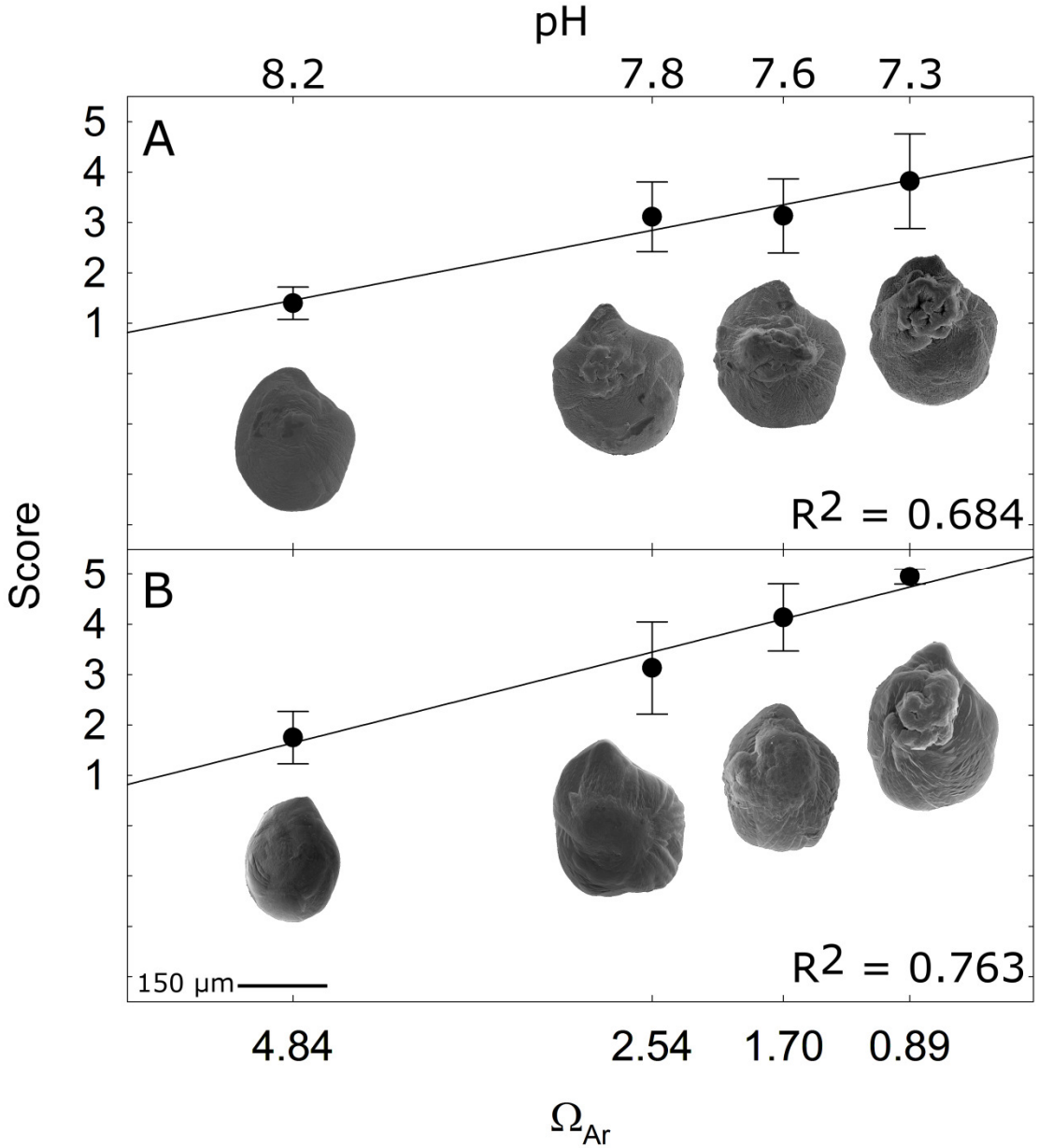

Fig 3. Core development score and modeled aragonite saturation state (Ω_{Ar}) linear regression results with embedded SEM imagery of otoliths for *A. clarkii* (A) and *A. frenatus* (B), including regression line (black). Examples are taken from each pCO_2 treatment group. All samples are of equal scale with the scale bar representing 150 µm. *A. clarkii* score regression was significant (score = $-0.6043*\Omega_{Ar} + 4.3813$, $F_{1,354} = 648.0753$, $p < 0.001$, A). *A. frenatus* score regression was also significant (score = $-0.7837*\Omega_{Ar} + 5.4391$, $F_{1,61} = 189.9739$, $p < 0.001$, B). Slopes were significantly different between species as well (ANCOVA, Ω_{Ar}-Species interaction term, $F_{3,411} = 7.788$ $p = 0.0055$).

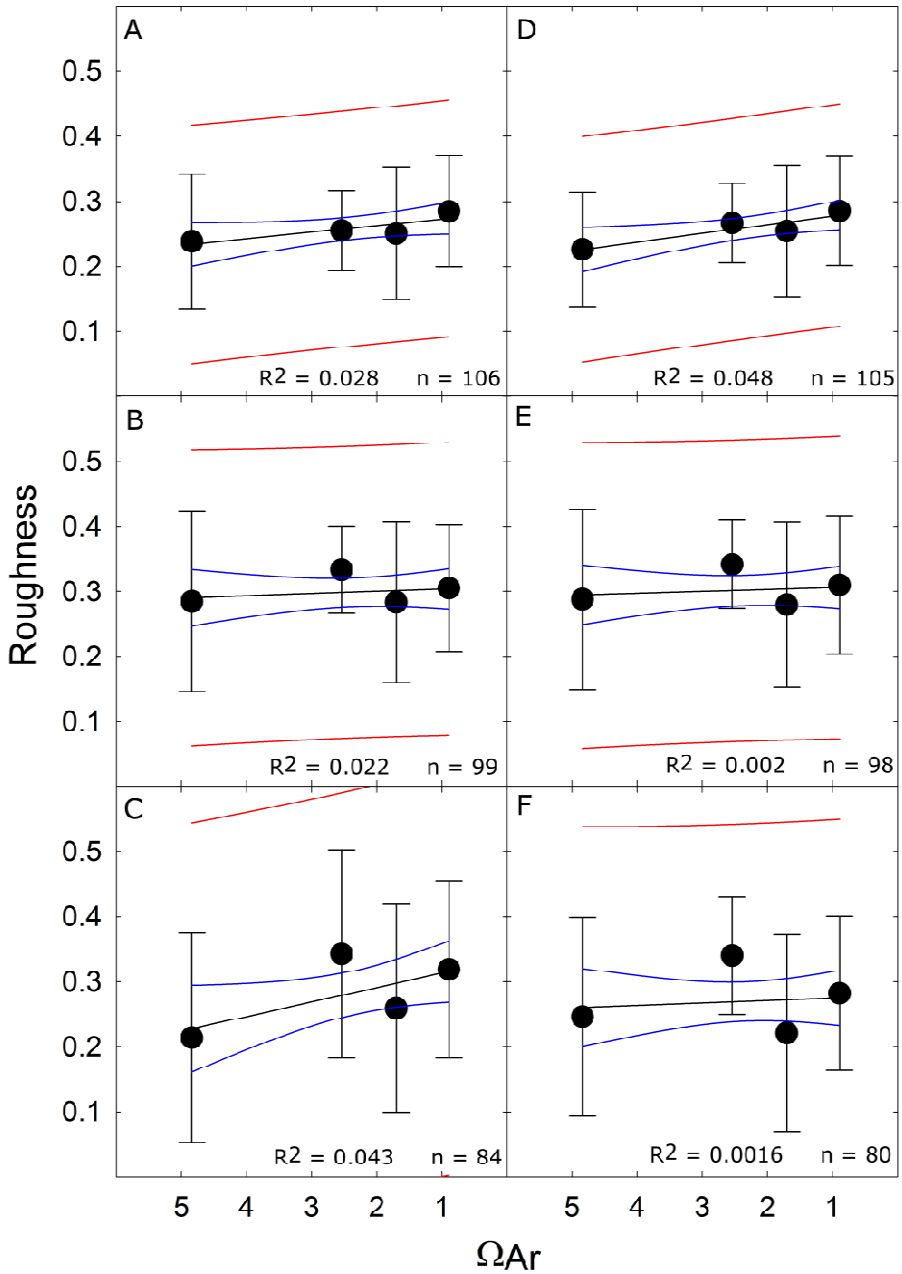

Fig 4. Roughness assessment compared to modeled aragonite saturation state (Ω_{Ar}) output, including mean ± S.D (dot, tails), regression (black), 95% C.I. (blue), and 95% P.I.(red). The only regression that was significant was for the right sagittal otoliths (Roughness = $-0.0133*\Omega_{Ar} + 0.291$, $p = 0.00241$, $F_{2,103} = 5.2407$, D).

References and Notes:

Beier, M., 1998, On the influence of altered gravity on the growth of fish inner ear otoliths: Acta Astronautica, v. 44, no. 7-12, p. 585–591.

Bignami, S., Spongaugle, S., and Cowen, 2013, Response to ocean acidification in larvae of a large tropical marine fish , Rachycentron canadum: Global Change Biology, v. 19, p. 996–1006, doi: 10.1111/gcb.12133.

Borelli, G., Guibbolini, M.E., Mayer-Gostan, N., Priouzeau, F., De Pontual, H., Allemand, D., Puverel, S., Tambutte, E., and Payan, P., 2003, Daily variations of endolymph composition: relationship with the otolith calcification process in trout: J Exp Biol, v. 206, no. 15, p. 2685–2692, doi: 10.1242/jeb.00479.

Campana, S.E., and Thorrold, S.R., 2001, Otoliths, increments, and elements: keys to a comprehensive understanding of fish populations?: Canadian Journal of Fisheries and Aquatic Sciences, v. 58, no. 1, p. 30–38.

Chappard, D., Degasne, I., Hure, G., Legrand, E., Audran, M., and Basle, M.F., 2003, Image analysis measurements of roughness by texture and fractal analysis correlate with contact profilometry: Biomaterials, v. 24, no. 8, p. 1399–1407.

Checkley, D.M., Dickson, A.G., Takahashi, M., Radich, J.A., Eisenkolb, N., Asch, R., and Checkley, D.M., 2009, Elevated CO2 enhances otolith growth in young fish: Science, v. 324, no. 5935, p. 1683, doi: 10.1126/science.1169806.

Dickson, A.G., Sabine, C.L., and Christian, J.R., 2007, Guide to best practices for ocean CO2 measurements.

Dixson, D.L., Munday, P.L., and Jones, G.P., 2010, Ocean acidification disrupts the innate ability of fish to detect predator olfactory cues: Ecology Letters, v. 13, no. 1, p. 68–75, doi: 10.1111/j.1461-0248.2009.01400.x.

Fabry, V.J., Seibel, B.A., Feely, R.A., and Orr, J.C., 2008, Impacts of ocean acidification on marine fauna and ecosystem processes: ICES Journal of Marine Science: Journal du Conseil , v. 65 , no. 3 , p. 414–432, doi: 10.1093/icesjms/fsn048.

Feely, R.A., Alin, S.R., Newton, J., Sabine, C.L., Warner, M., Devol, A., Krembs, C., and Maloy, C., 2010, The combined effects of ocean acidification, mixing, and respiration on pH and carbonate saturation in an urbanized estuary: Estuarine, Coastal and Shelf Science, v. 88, no. 4, p. 442–449, doi: http://dx.doi.org/10.1016/j.ecss.2010.05.004.

Feely, R.A., Sabine, C.L., Hernandez-Ayon, J.M., Ianson, D., and Hales, B., 2008, Evidence for Upwelling of Corrosive "Acidified" Water onto the Continental Shelf: Science , v. 320 , no. 5882 , p. 1490–1492, doi: 10.1126/science.1155676.

Feely, R.A., Sabine, C.L., Lee, K., Berelson, W., Kleypas, J., Fabry, V.J., and Millero, F.J., 2004, Impact of Anthropogenic CO2 on the CaCO3 System in the Oceans: Science , v. 305 , no. 5682 , p. 362–366, doi: 10.1126/science.1097329.

Fekete, D.M., 2003, Developmental biology. Rocks that roll zebrafish: Science, v. 302, no. 5643, p. 241–242, doi: 10.1126/science.1091171.

Grant, J.A., Bishop, N.E., Götzen, N., Sprecher, C., Honl, M., and Morlock, M.M., 2007, Artificial composite bone as a model of human trabecular bone: The implant–bone interface: Journal of biomechanics, v. 40, no. 5, p. 1158–1164.

Hardison, A.L., Lichten, L., Banerjee-Basu, S., Becker, T.S., and Burgess, S.M., 2005, The zebrafish gene claudinj is essential for normal ear function and important for the formation of the otoliths: Mechanisms of Development, v. 122, no. 7-8, p. 949–958.

Hauri, C., Gruber, N., Vogt, M., Doney, S.C., Feely, R.A., Lachkar, Z., Leinweber, A., McDonnell, A.M.P., Munnich, M., and Plattner, G.-K., 2013, Spatiotemporal variability and long-term trends of ocean acidification in the California Current System: Biogeosciences, v. 10, no. 1, p. 193–216, doi: 10.5194/bg-10-193-2013.

Hilbig, R., Anken, R.H., Sonntag, G., Höhne, S., Henneberg, J., Kretschmer, N., and Rahmann, H., 2002, Effects of altered gravity on the swimming behaviour of fish: Advances in Space Research, v. 30, no. 4, p. 835–841.

Kroeker, K.J., Micheli, F., Gambi, M.C., and Martz, T.R., 2011, Divergent ecosystem responses within a benthic marine community to ocean acidification: Proceedings of the National Academy of Sciences , v. 108 , no. 35 , p. 14515–14520, doi: 10.1073/pnas.1107789108.

Lychakov, D. V, and Rebane, Y.T., 2005, Fish otolith mass asymmetry: morphometry and influence on acoustic functionality: Hear Res, v. 201, no. 1-2, p. 55–69, doi: S0378-5955(04)00283-7 [pii] 10.1016/j.heares.2004.08.017.

Lychakov, D. V, and Rebane, Y.T., 2000, Otolith regularities: Hearing Research, v. 143, no. 1–2, p. 83–102, doi: http://dx.doi.org/10.1016/S0378-5955(00)00026-5.

Millero, F.J., Zhang, J.-Z., Fiol, S., Sotolongo, S., Roy, R., Lee, K., and Mane, S., 1993, The use of buffers to measure the pH of seawater: Marine Chemistry, v. 44, p. 143–152, doi: 10.1016/0304-4203(93)90199-X.

Munday, P.L., Dixson, D.L., Donelson, J.M., Jones, G.P., Pratchett, M.S., Devitsina, G. V, and Døving, K.B., 2009, Ocean acidification impairs olfactory discrimination and homing ability of a marine fish: Proceedings of the National Academy of Sciences, v. 106, no. 6, p. 1848–1852, doi: 10.1073/pnas.0809996106.

Munday, P.L., Dixson, D.L., McCormick, M.I., Meekan, M., Ferrari, M.C.O., and Chivers, D.P., 2010, Replenishment of fish populations is threatened by ocean acidification: Proceedings of the National Academy of Sciences, v. 107, no. 29, p. 12930–12934, doi: 10.1073/pnas.1004519107.

Munday, P.L., Hernaman, V., Dixson, D.L., and Thorrold, S.R., 2011, Effect of ocean acidification on otolith development in larvae of a tropical marine fish: Biogeosciences, v. 8, no. 6, p. 1631–1641, doi: 10.5194/bg-8-1631-2011.

Nilsson, G.E., Dixson, D.L., Domenici, P., McCormick, M.I., Sørensen, C., Watson, S.-A., and Munday, P.L., 2012, Near-future carbon dioxide levels alter fish behaviour by interfering with neurotransmitter function: Nature Climate Change, v. 2, p. 201–204, doi: 10.1038/nclimate1352.

Pierrot, D., Lewis, E., and Wallace, D., 2006, Program developed for CO2 system calculations: Carbon Dioxide Information Analysis Center, Oak Ridge National Laboratory, U.S. Department of Engergy, Oak Ridge, Tennessee.

Ries, J.B., Cohen, A.L., and McCorkle, D.C., 2009, Marine calcifiers exhibit mixed responses to CO2-induced ocean acidification: Geology, v. 37, no. 12, p. 1131–1134.

Riley, B.B., and Moorman, S.J., 2000, Development of utricular otoliths, but not saccular otoliths, is necessary for vestibular function and survival in zebrafish: Journal of Neurobiology, v. 43, no. 4, p. 329–337.

Söllner, C., Burghammer, M., Busch-Nentwich, E., Berger, J., Schwarz, H., Riekel, C., and Nicolson, T., 2003, Control of Crystal Size and Lattice Formation by Starmaker in Otolith Biomineralization: Science , v. 302 , no. 5643 , p. 282–286, doi: 10.1126/science.1088443.

Stupp, S.I., and Ciegler, G.W., 1992, Organoapatites: materials for artificial bone. I. Synthesis and microstructure: Journal of biomedical materials research, v. 26, no. 2, p. 169–183.

Widdicombe, S., and Needham, H.R., 2007, Impact of CO~ 2-induced seawater acidification on the burrowing activity of Nereis virens and sediment nutrient flux: Marine Ecology-Progress Series, v. 341, p. 111.

Wilcox-Freeburg, E., Rhyne, A., Robinson, W.E., Tlusty, M., Bourque, B., Hannigan, R.E., and Wilcox Freeburg, E., 2013, A comparison of two pH-stat carbon dioxide dosing systems for ocean acidification experiments: Limnology and Oceanography Methods, v. 11, p. 485–494.

Supplemental materials

A1: Experimental methods

Experiment apparatus was constructed as indicated in Wilcox Freeburg et al. (2013). 12 experimental 40L glass aquariums were deployed for the research. The sides and back of the tank were painted flat black with epoxy resin paint and the front was covered with removable 6 mil plastic sheeting. Direct high output fluorescent overhead lighting was maintained on a 14 hour diurnal cycle. pCO_2 was controlled using a DigitalAquatics Reef Keeper Elite reef tank controller. Individual tanks were pH monitored using single junction refillable glass electrodes calibrated on the total hydrogen scale pH_T (Byrne, 1987; Millero et al., 1993). Aquariums were aerated using externally supplied house air. CO_2 was pulse dosed using solenoid valves when pH drifted above setpoint. pH was also manually assessed using a handheld meter calibrated to pH_T synthetic seawater buffers, as above. Total alkalinity (A_T) was monitored twice daily for each aquarium following standard methods (EPA #310.1). Salinity was measured using a conductivity electrode immediately calibrated prior to measurement. Temperature was measured using an alcohol thermometer (±0.1ºC). These values were input into CO2SYS for carbonate series modeling for DIC, pCO_2, $[CO_3^{2-}]$, $[HCO_3^-]$, and Ω_{Ar} (Pierrot et al., 2006). Aquarium seawater was held static with 25% water changes every other day.

Fish were initially dosed at a density of 1 individual per liter (40/aquarium). Following hatch, fish were randomly distributed into the experimental aquariums. pH was then manually dosed to experimental levels over a period of 2 hours. Fish were

grown in a background of *Isochrysis* spp. Algae density was measure by Coulter Counter (Coulter Instruments, Inc) and was dosed to hold density to 40,000 cells/mL. Native *Pseudodiaptomus* spp. copepods were collected and selected into monoculture. This population was then used to dose experimental aquariums at a density of 4 nauplii and 1 adult per mL.

Fish were grown until coloration and behavior shifted to those typically seen in juveniles (8 days). Fish were sacrificed using a lethal dose of tricaine methanesulfonate. Fish were then placed on 1mm gratings and photographed under a dissection microscope. Fish were then rinsed and stored in 95% ethanol.

A2: Otolith extraction method

Otoliths were removed from the fish using microsurgical techniques. Fish were transferred to a glass petri dish and submerged in 70% ethanol. Under a dissection microscope, fish heads were removed from the body posterior to the gills. Heads were laterally transected. Microforceps were used to displace the brain and manipulate tissue surrounding the otoconia. Crossed polarizers were used to take advantage of the optically active otolith mineral phase (Fig A2.1). Otoliths were then moved to a clean petri dish, washed of any superficial material and photographed in a repeated orientation (Figure A2.2).

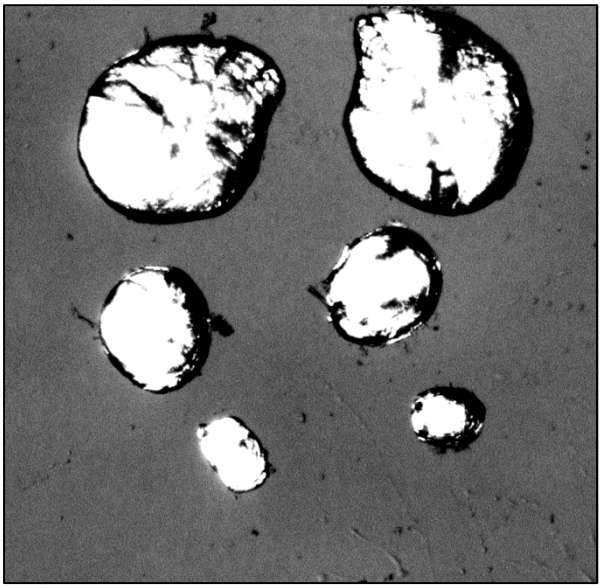

Fig A2.1. Example photograph of crossed-polizer view of otoliths. Contrast is high in the photograph due to camera auto-exposure settings.

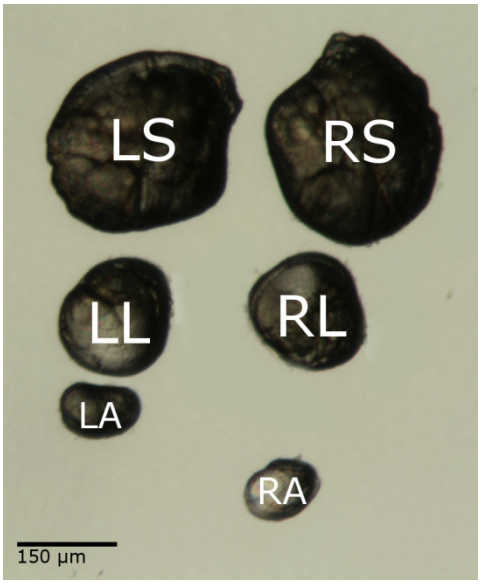

Figure A2.2. Example photograph with superimposed otolith side and type.

A3: Otolith core score training guide

The following guide was given to every person responsible for scoring images. Due to time restraints, almost all of the participants stopped their scoring after finishing up the core development section (characteristic #4). The complete guide is attached herein for use in future work.

CHARACTERISTIC #1 - CRYSTAL HABIT

Crystal habit has to do with shape of a crystal. You should focus on the whole otolith though most of the crystal structure will be in the "core" of the otolith. Below are the habits and pictures of the "ideal" shape.

Orthorhombic	Hexagonal	Acicular	acrystalline	Amorphous
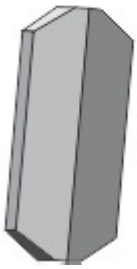	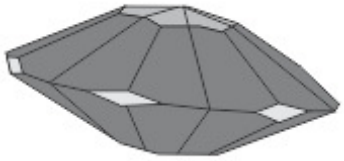	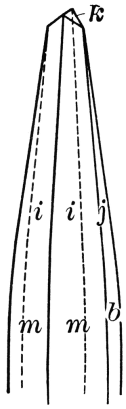	No obvious crystals	Small "blubs" of material

To Score the images, identify the DOMINANT habit:

1 = orthorhombic
2 = acicular
3 = hexagonal
4 = acrystalline (no crystals)
5 = amorphous

CHARACTERISTIC #2 – MINEROLOGY

Here we will use crystal habit to identify relative percentages of minerals using the following key:

Aragonite

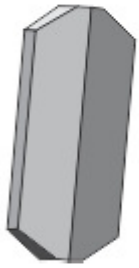

Vaterite

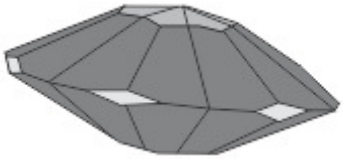

Score images as follows:

1 = completely aragonite
2= vaterite ≤ 33%
3 = vaterite 33% to 66%
4 = ≥ 66% vaterite.
5 = no visible crystals

CHARACTERISTIC #3 - % VISIBLE MINERALS

Using your best estimate, what is the relative % of visible crystals? Enter into Box.

ESTIMATING PERCENTAGES

Below are images with the relative % of dark material noted. When you look at these figures examine the balance of white space to dark space use the balance to estimate % dark.

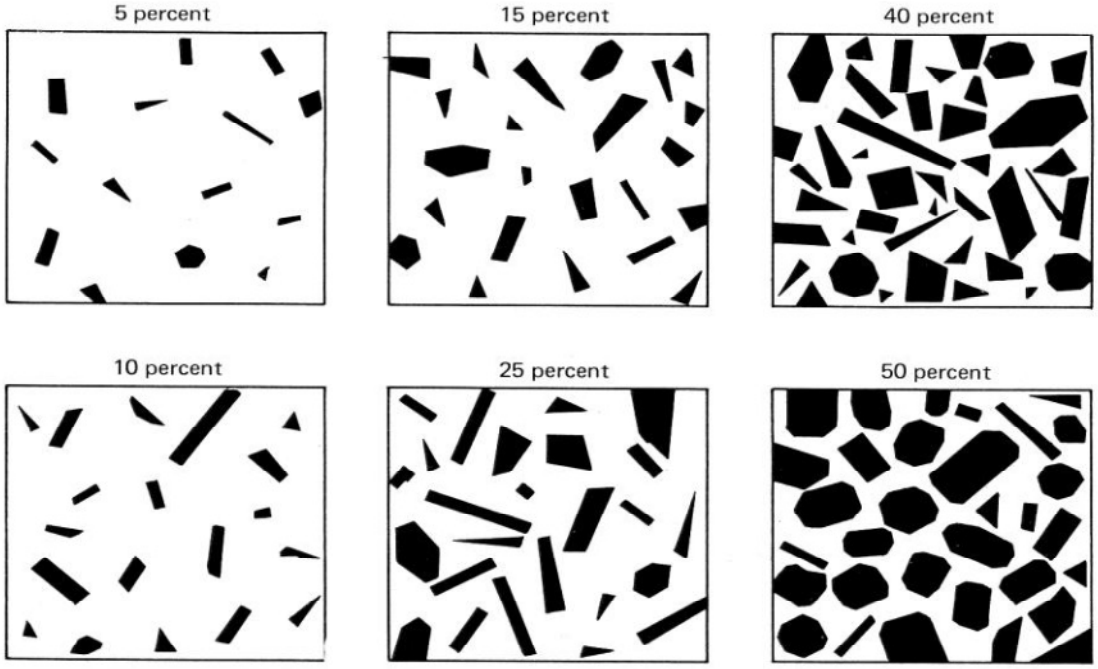

Using the above figure as an example you will be asked to evaluate the % of a particular characteristic in images of fish ear stones (otoliths).

CHARACTERISTIC #4 - CORE DEVELOPMENT

Rank core crystal development using the scheme shown below (1-5)

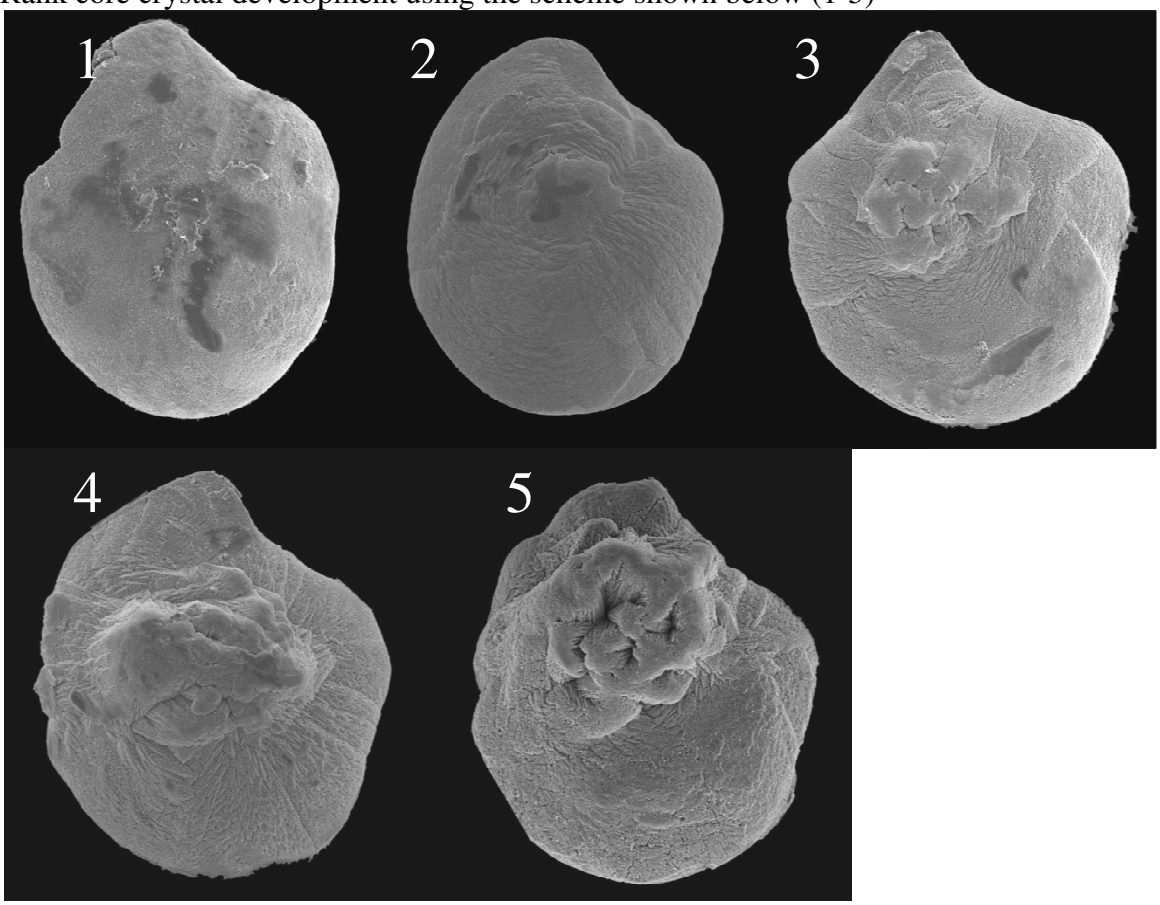

TRAINING IMAGES

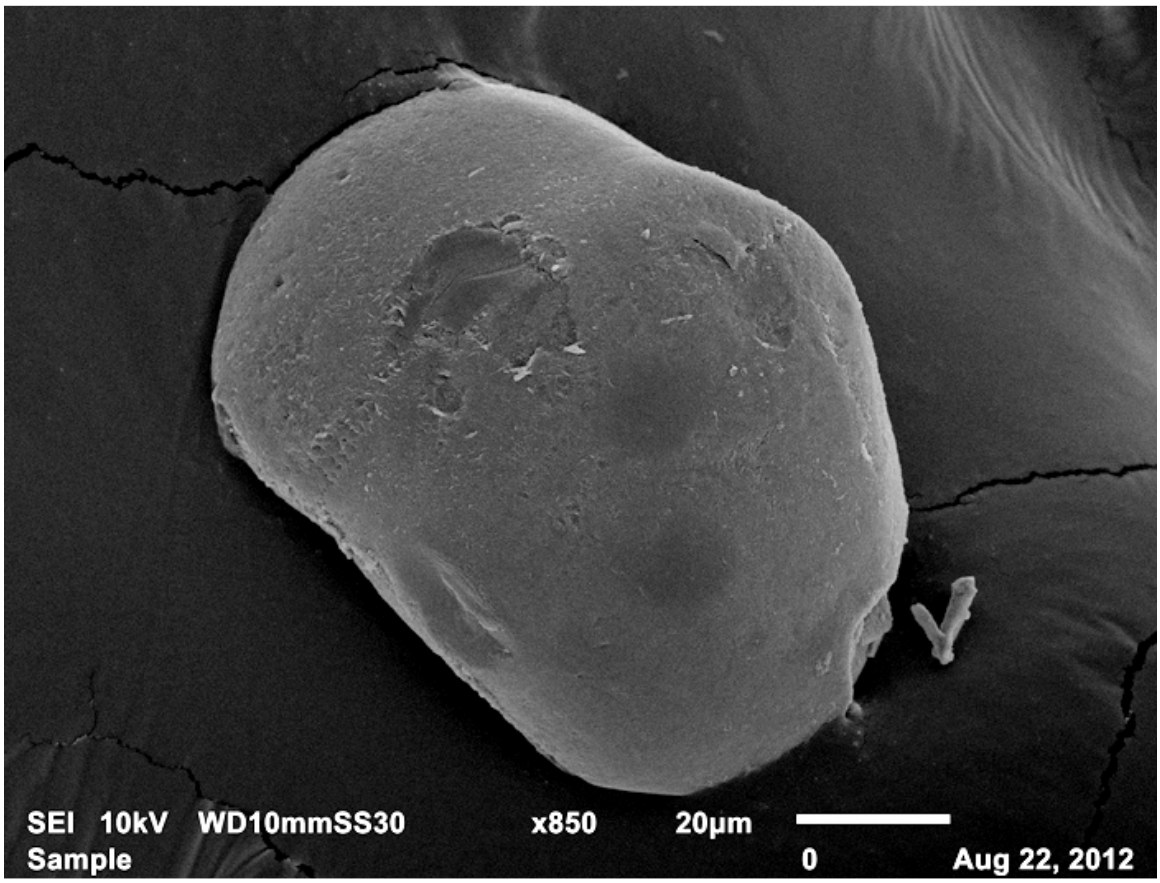

COMMENTS: No clear visible crystals. Gouge on surface is from tweezers. Flecks on surface are from carbon coating.

HABIT SCORE: 5 MINERAL SCORE: 4 % SCORE: 0% CORE: 1

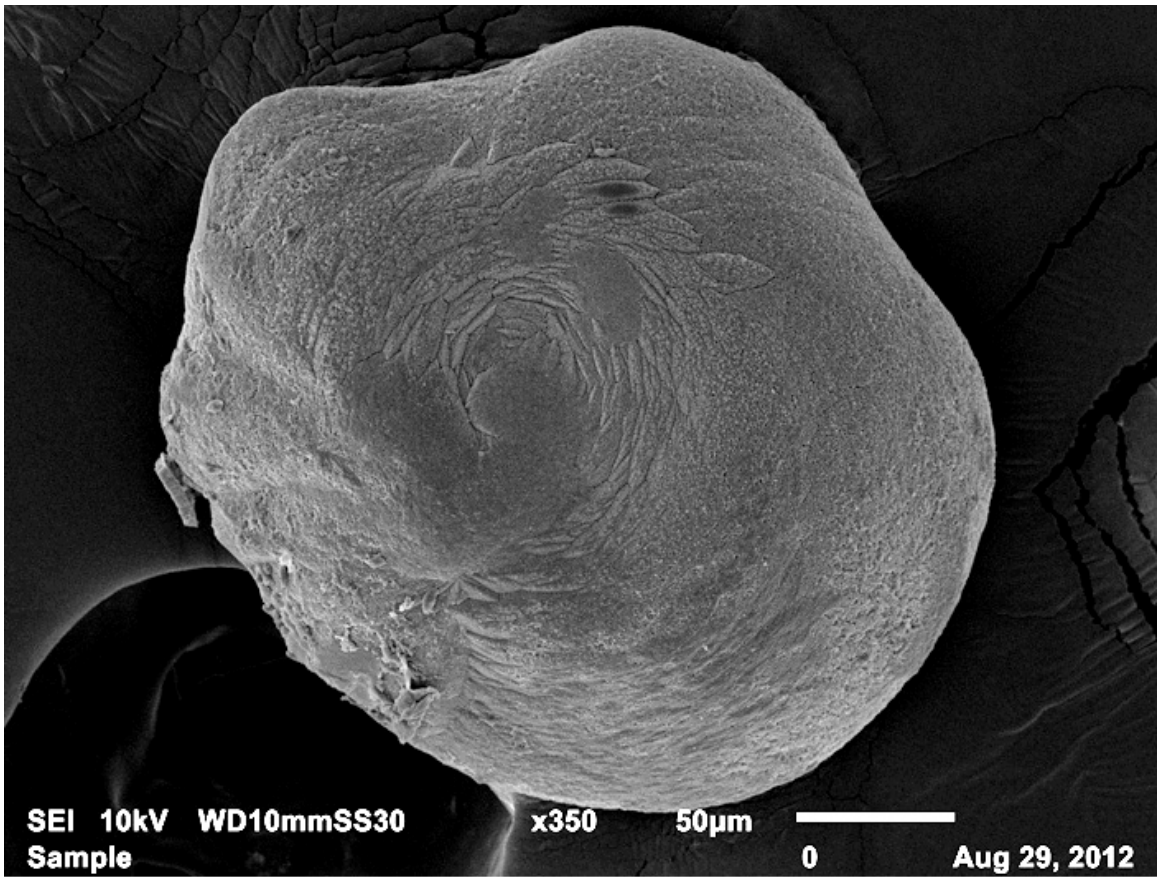

COMMENTS: Flecks on surface are from carbon coating. Curved area represents core of otolith. When you see structure score in this area.
HABIT SCORE: 1 MINERAL SCORE: 1 % SCORE: 90% CORE: 2

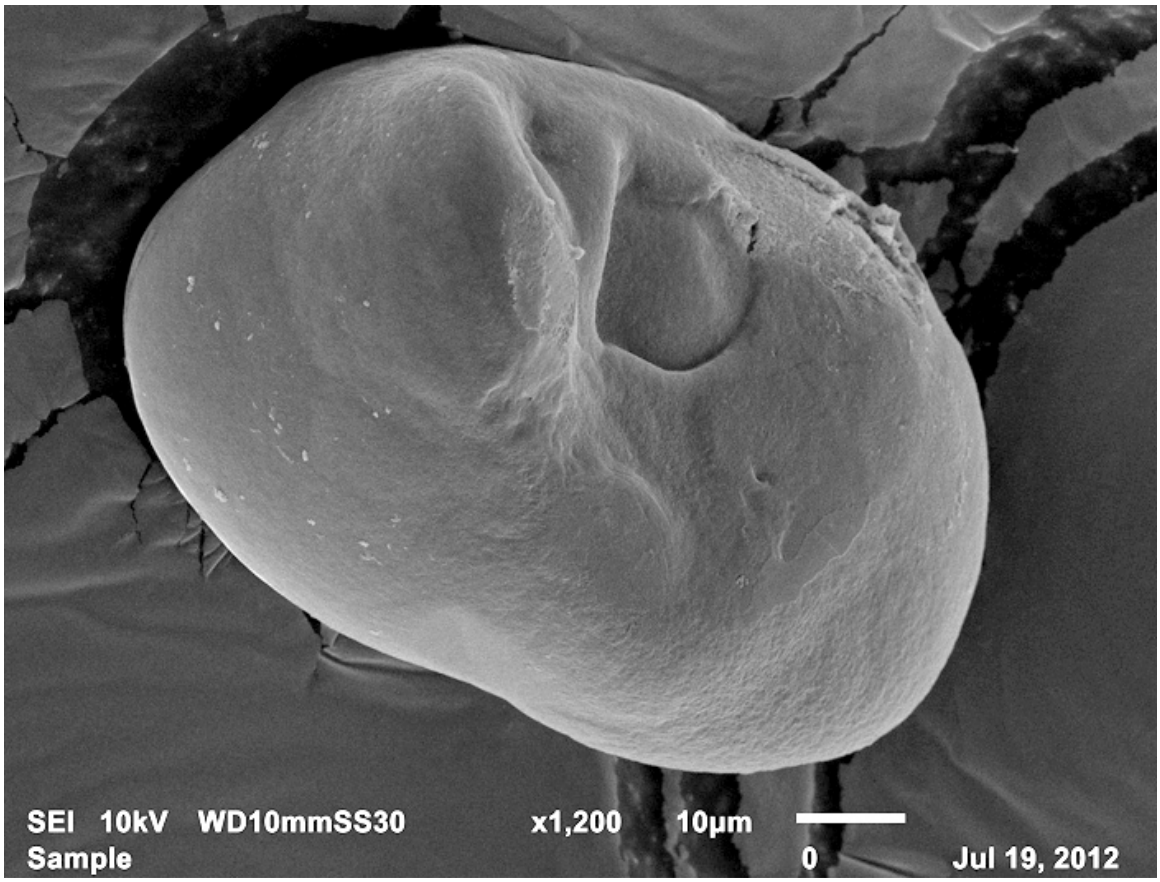

COMMENTS: No clear visible crystals except on upper right. Flecks on surface are from carbon coating.

HABIT SCORE: 5 MINERAL SCORE: 4 % SCORE: 2% CORE: 1

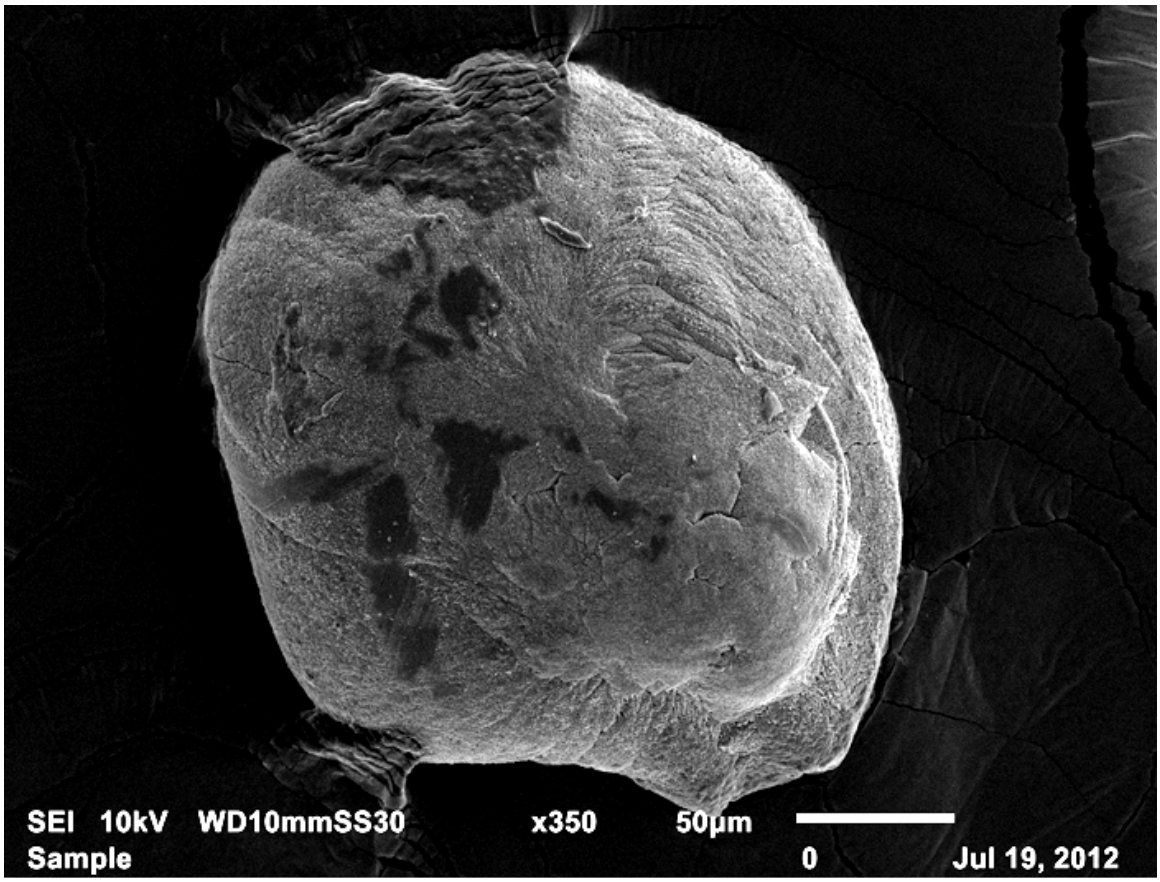

COMMENTS: Dark streaks – tweezer marks. Crystals visible upper right quadrant.
HABIT SCORE: 1 MINERAL SCORE: 1 % SCORE: 90% CORE: 3

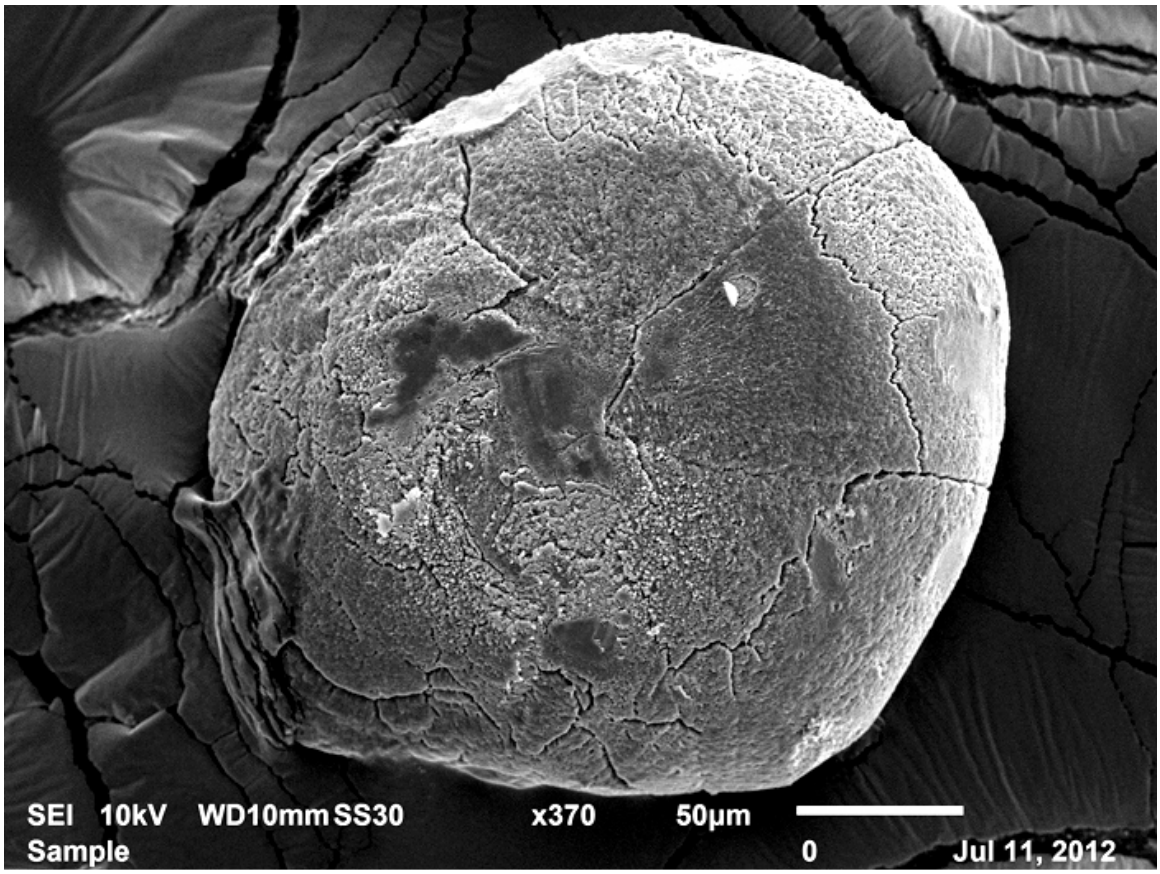

COMMENTS: Crystals visible on upper right and center. Gouge on surface is from tweezers.

HABIT SCORE: 5 MINERAL SCORE: 4 % SCORE: 75% CORE: 1

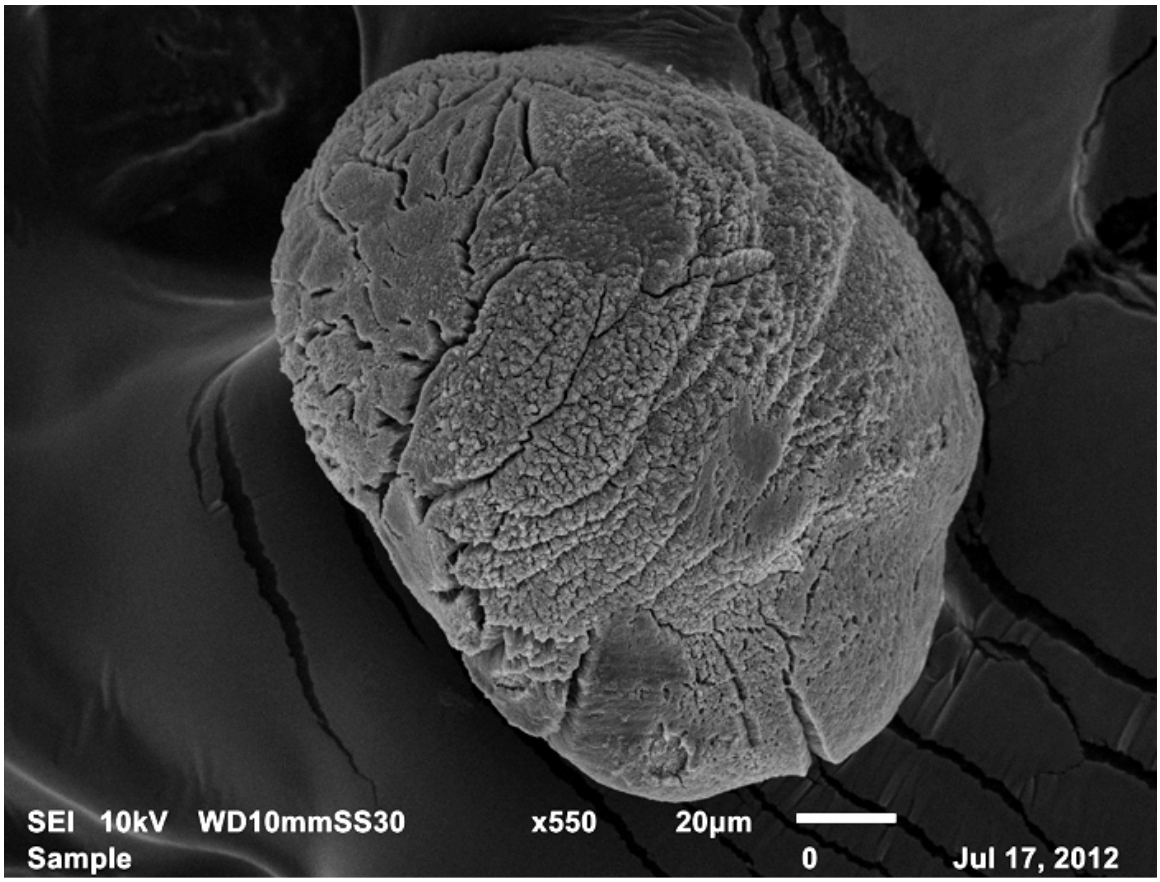

COMMENTS: Dark regions on surface from tweezers. Cracks are caused by dessication. Shape of crystals is pointed and in some cases “flat topped” suggesting some vaterite.
HABIT SCORE: 2 MINERAL SCORE: 2 % SCORE: 60% CORE: 2

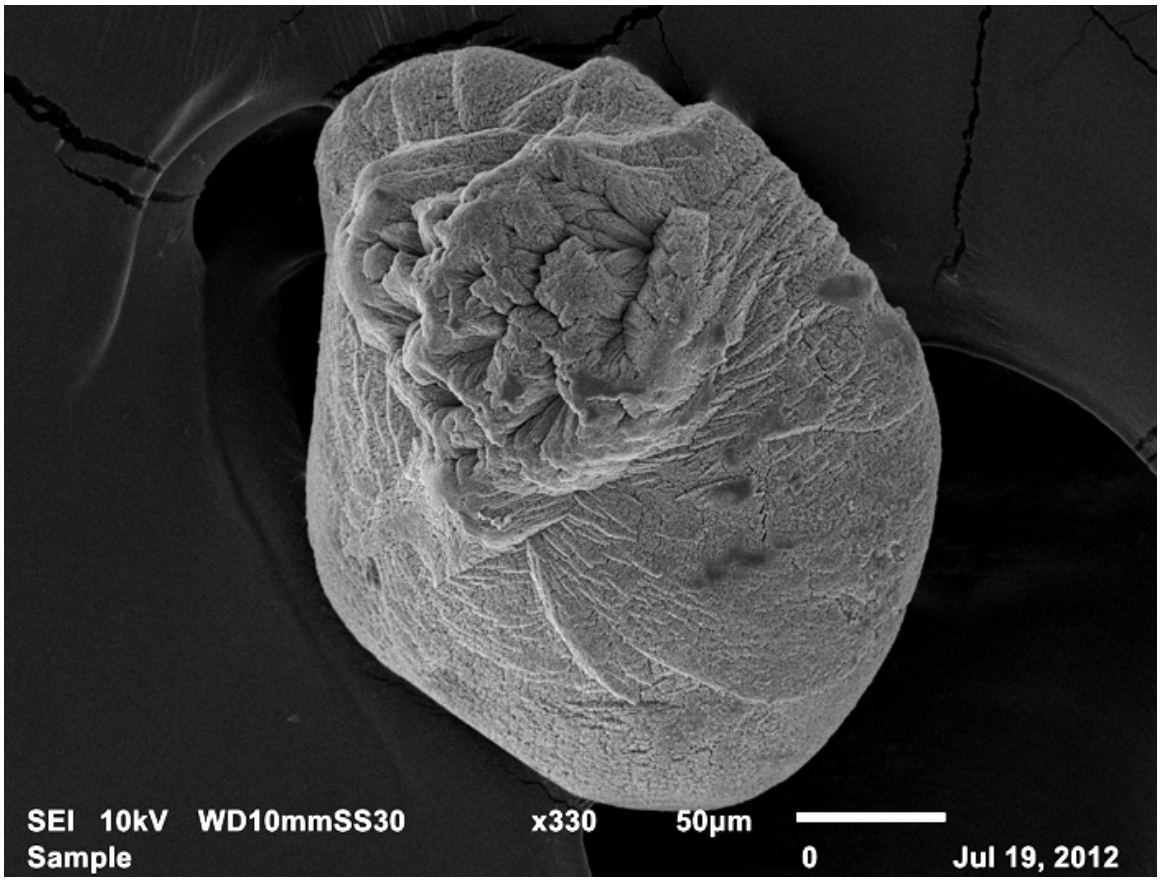

COMMENTS: This is a textbook example of otolith structure with a clearly visible core to the otolith showing beautiful prismatic aragonite.

HABIT SCORE: 1 MINERAL SCORE: 1 % SCORE: 90% CORE: 5

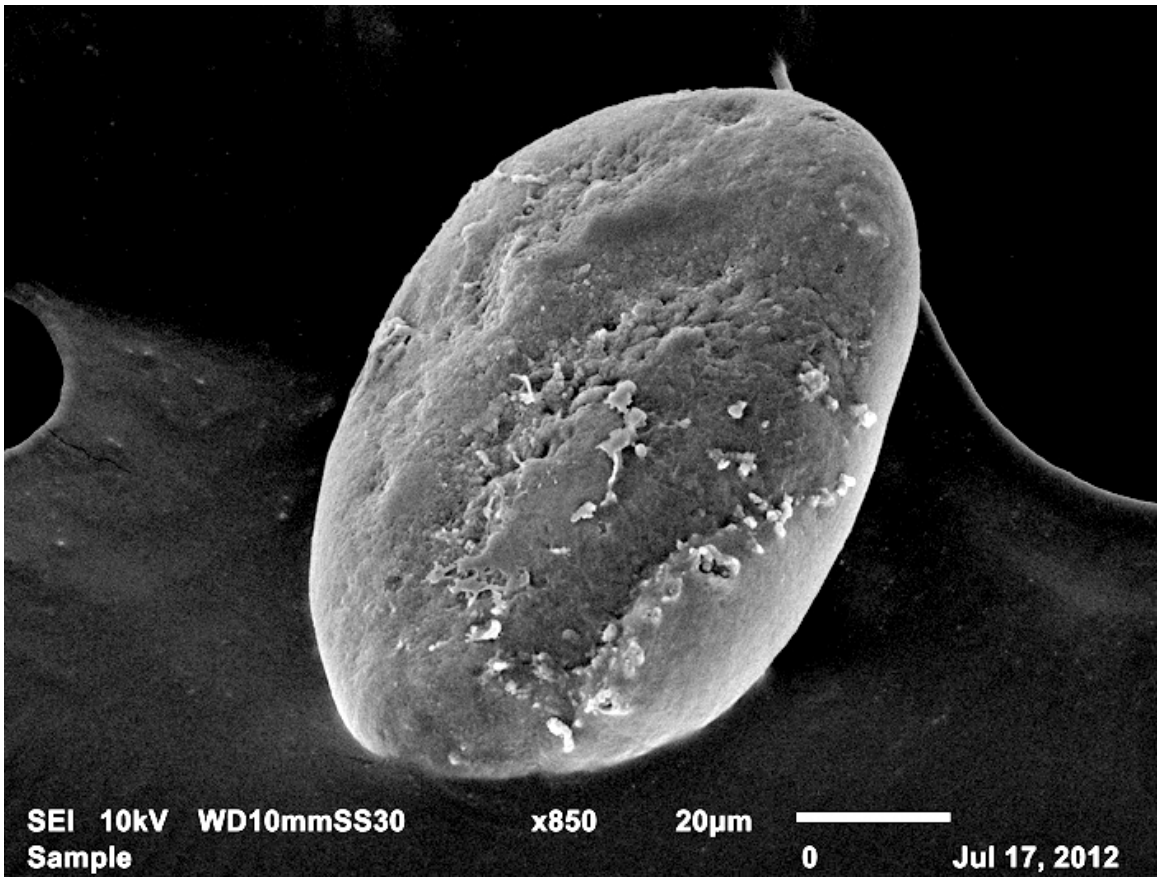

COMMENTS: Very little visible structure. Flecks on surface are from carbon coating and also could be amorphous material. Center region looks vateritic.

HABIT SCORE: 5 MINERAL SCORE: 2 % SCORE: 10% CORE: 2

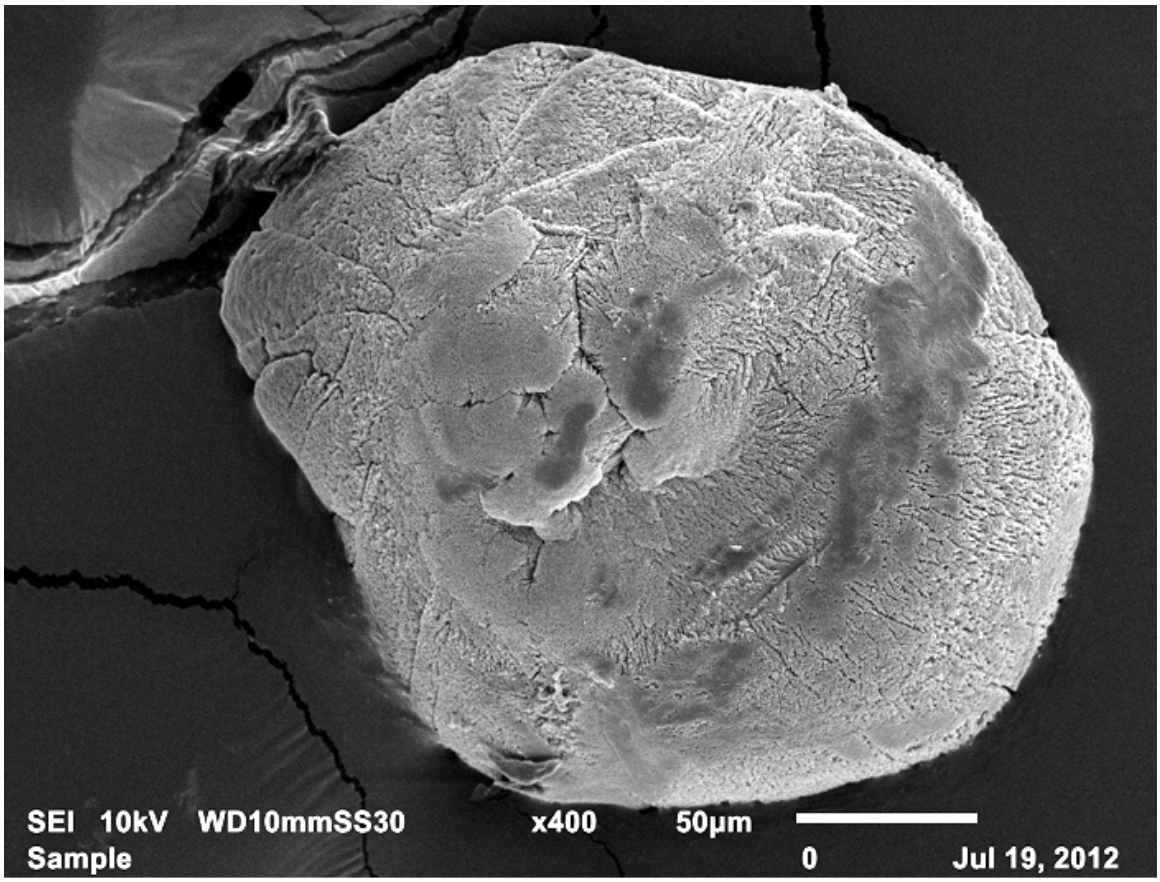

COMMENTS: Dark regions are from tweezers. Crystal habit visible on right side. Though prismatic in center the majority is not prismatic.

HABIT SCORE: 2 MINERAL SCORE: 1 % SCORE: 90% CORE: 3

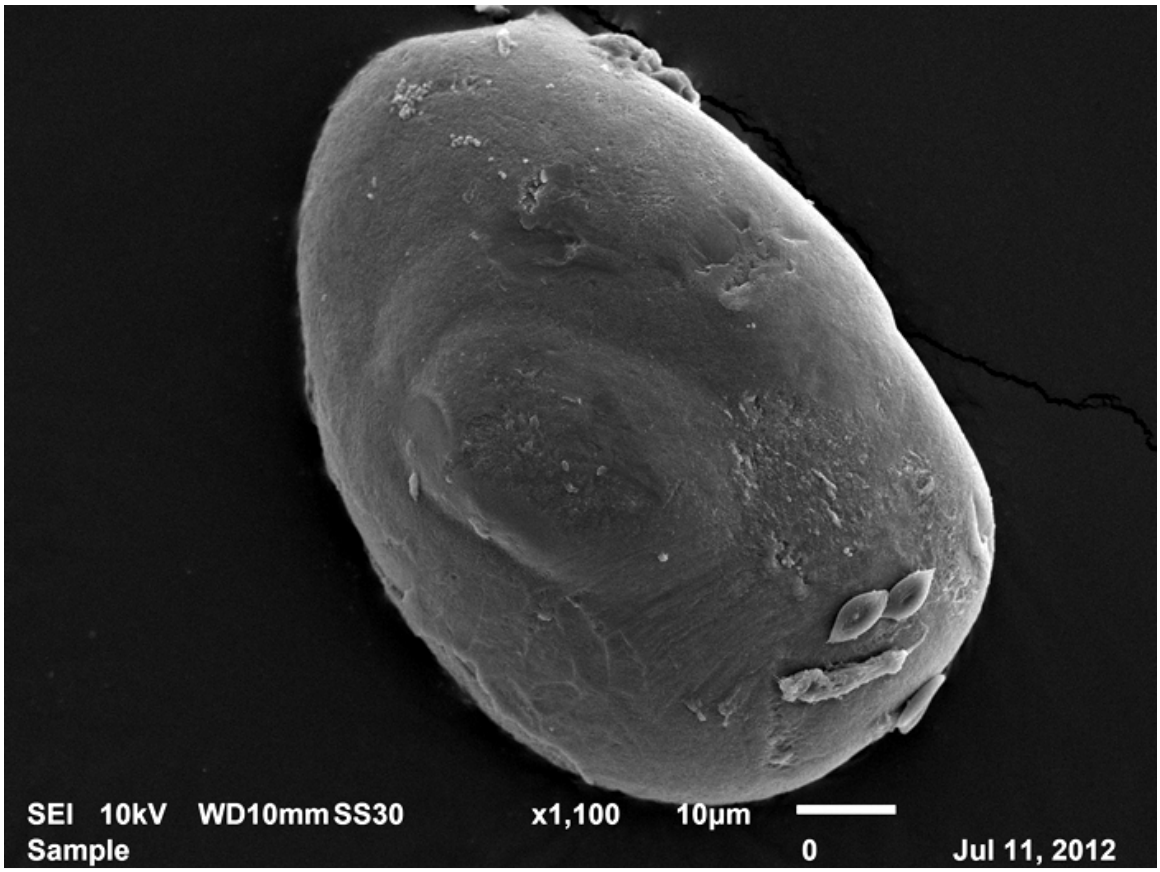

COMMENTS: Little visible structure. Debris on surface from carbon tape. Upper left shows amorphous mineralogy. Mineralogy center looks like vaterite.

HABIT SCORE: 5 MINERAL SCORE: 2 % SCORE: 2%

CORE:2

A4: Example image from core scoring website

Qualtrics (Qualtrics, L.L.C) enterprise survey resources allowed for the use of crowd-sourced analysis. Although this data was not publically available, several scientists and non-scientists alike were trained using the attached manual and given a link to score otoliths individually. Using the web interface, otoliths were displayed on screen and scored using the slider on the webpage (Fig A4.1).

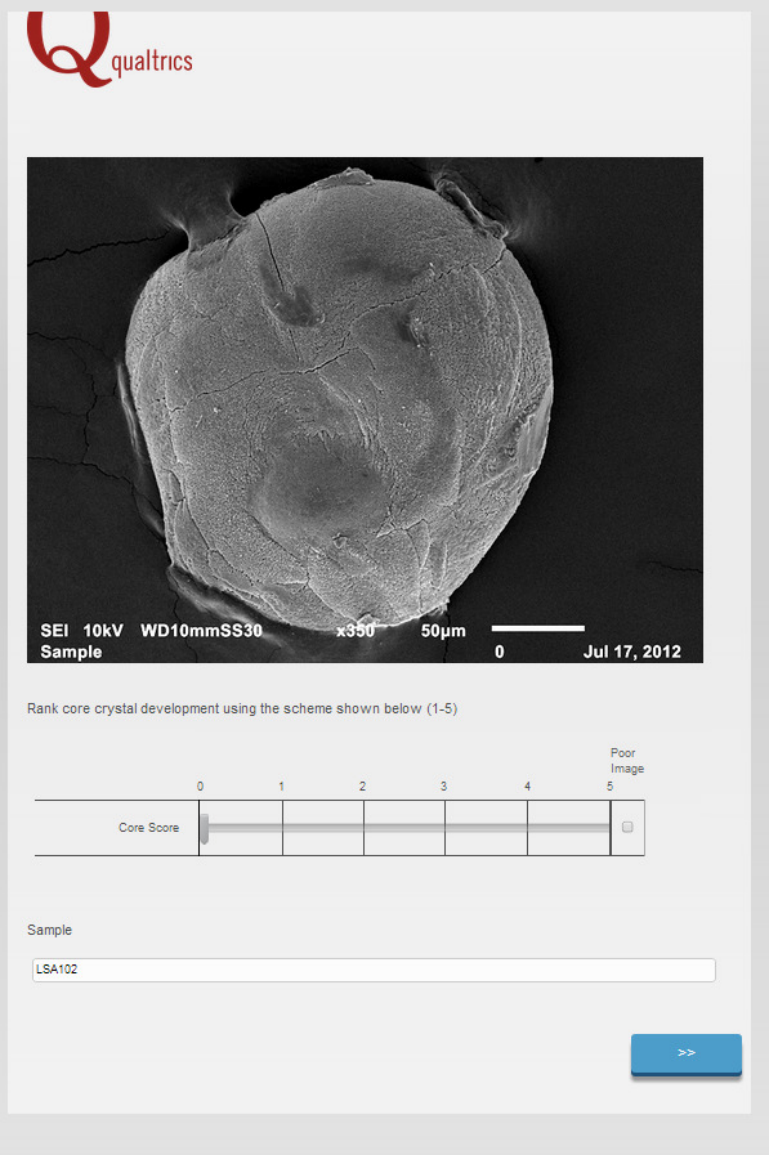

Fig A4.1 Website screenshot of otolith core scoring page.

A5: MATLAB image analysis toolset instructions

The MATLAB image analysis toolset used in this study is available online (github.com/edfreeburg/ MATLAB-roughness-image-analysis/) and is also added to this supplement (SA4). All modules used in this script are included in the image analysis toolbox, or freely available on the MATLAB file exchange (mathworks.com/matlabcentral/fileexchange/) or on Stack Overflow (stackoverflow.com).

This toolset is mainly prompt driven, so its use is obvious when deployed. Run the script by calling the script name in the command line of MATLAB. Following script start, a standard prompt will appear allowing one to navigate to the directory where all images are stored for analysis. The script will loop over every image in the folder, so making subset folders is highly suggested.

The image is then automatically background subtracted and displayed for approval (Fig SA5.1). Following this procedure, the script uses a local normalizing routine to remove of all "gradient" lighting effects that are inherent in SEM imagery. After image flattening, a nearest neighbor standard deviation calculation is carried out over a scanning window across the image. This standard deviation finds areas of particularly different grayscale values in close proximity, or rough areas. Using a hard-coded threshold value, the image is then converted to binary and box counted. The result is displayed, morphometrics calculated on the image mask, and summary data is stored locally. Following analysis of

all images in the folder, a summary *.xls file will be created and saved that contains all data collected for the analysis.

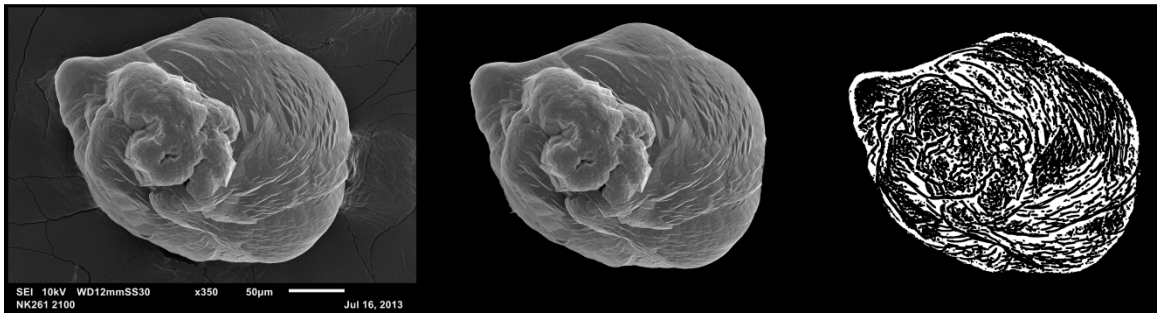

Figure A5.1. Example image, background subtraction, and final processed image proof (left to right).

A6: MATLAB image analysis morphology toolset code

Direct download available at:
http://github.com/edfreeburg/MATLAB-Image-Analysis/

```
%% Load sample
clear all;
close all;
loop = 0;
while loop == 0;
    load('C:\MATLAB\LUP.mat');
    if LUP == 0;
        LUP = 'C:\';
    end
    ftypes = {'*.jpg','JPEG';'*.bmp','Bitmap';'*.tif','TIF'};
    [Filename, PATH] = uigetfile(ftypes,'Select image:',LUP);
    RPF = [PATH,Filename];
    cd 'C:\MATLAB';
    LUP = PATH;
    save LUP.mat LUP;
    I = imread(RPF);
    %%
    [D1, FileNm, D2] = fileparts(RPF);
    IC = size(I);
    ICb = size(IC);
    if ICb(1,2) == 3
        L = rgb2gray(I);
    else L = I;
    end
    %% Threshold/binarize
    K = medfilt2(L,[3 3]);
    imshow(I);
    % Select method of thresholding
    button = questdlg('Select thresholding method:',...
        'Select thresholding method:','Manual','Low Contrast(Auto)','Manual');
    switch button
        case 'Manual'
            MethT = 1;
        case 'Low Contrast(Auto)'
            MethT = 2;
    end
    close all;
    repro = 0;
    rep_adj = 0;
    try1 = 20;
    try2 = 40;
    while repro == 0;
        J = rangefilt(K);
        if MethT == 1;
            try1 = try1;
            J(J < try1) = 0;                    % Threshhold binary calculation
            J(J > try2) = 0;
```

```
            J(J >= try1) = 1;
            J = logical(J);
            M = J;
        else
            lvlM = graythresh(K);
            M = im2bw(K,lvlM);                    % Threshold autocalculation
            J = rangefilt(M);
        end

        imshow(J)
        s = size(J);
        X = [];
        button_repro = questdlg('Reprocessing required?','Reprocessing
required?','Yes','Reset','No','No');
        switch button_repro
            case 'Yes'
                repro = 0;
                MethT = 1;
                try1_str = num2str(try1);
                try2_str = num2str(try2);
                rep_adj = inputdlg([{'Low'}, {'High'}],'Range:',1,[{try1_str}, {try2_str}]);
                try1 = str2double(rep_adj{1,1});
                try2 = str2double(rep_adj{2,1});
            case 'Reset'
                repro = 0;
                try1 = 20;
                try2 = 40;
            case 'No'
                repro = 1;
        end
    end


    %% Calculate parameters

    for row = 1:25:s(1)                 % Identification of objects (rowscan)
       for col=1:s(2)
          if J(row,col),
             break;
          end
       end
       contour = bwtraceboundary(J, [row, col], 'SW', 8, Inf, 'counterclockwise');
       if(~isempty(contour))
          X = [X; {contour}];
       else
          hold on; plot(col, row,'rx','LineWidth',2);
       end
    end

    for row = s(1):-25:1                 % Identification of objects (descending rowscan)
       for col=s(2):-1:1
          if J(row,col),
             break;
```

```
      end
   end
   contour = bwtraceboundary(J, [row, col], 'NE', 8, Inf, 'clockwise');
   if(~isempty(contour))
      X = [X; {contour}];
   else
      hold on; plot(col, row,'rx','LineWidth',2);
   end
end

for col = 1:25:s(2)                % Identification of objects (columnscan)
   for row=1:s(1)
      if J(row,col),
         break;
      end
   end

   contour = bwtraceboundary(J, [row, col], 'NE', 8, Inf, 'counterclockwise');
   if(~isempty(contour))
      X = [X; {contour}];
   else
      hold on; plot(col, row,'rx','LineWidth',2);
   end
end


for col = s(2):-25:1                % Identification of objects (descending columnscan)
   for row=s(1):-1:1
      if J(row,col),
         break;
      end
   end

   contour = bwtraceboundary(J, [row, col], 'SW', 8, Inf, 'clockwise');
   if(~isempty(contour))
      X = [X; {contour}];
   else
      hold on; plot(col, row,'rx','LineWidth',2);
   end
end



z1 = size(X);
md = [];
c = 0;
for row = 1:z1(1,1);              % Deleting multiple object hits.
    md = [md; size(X{row,1})];
end
[junk, idx] = unique(md,'rows');
Xa = X(sort(idx,1));

z2 = size(Xa);                    % Delete erroneous object hits.
```

```
md2 = [];
for row = 1:z2(1,1);
    md2 = [md2; size(Xa{row,1})];
end
md2 = md2(:,1);
fa = find(md2>100);
Xb = Xa(fa,:);                    % Resultant x-y pair traces.

z3 = size(Xb);
hold on
for obj1 = 1:z3(1,1);
    Pl = Xb{obj1,1};                % Plot reduced set
    plot(Pl(:,2),Pl(:,1),'g','LineWidth',2);
    CntCoord_lb = mean(Pl);
    lblObj = num2str(obj1);
    text(CntCoord_lb(2),CntCoord_lb(1),lblObj,'HorizontalAlignment',...
        'center','Color',[0 1 0],'BackgroundColor',[0 0 0],...
        'FontSize',24);
end

button2 = questdlg('Erroneous extra volume data?');  % Remove error volumes
switch button2
    case 'Yes'
        b2 = 1;
    case 'No'
        b2 = 0;
    case 'Cancel'
        b2 = 2;
end
redc = [];
redr = [];
if b2 == 1;
    erd = impoly;
    pos = getPosition(erd);
    c = pos(:,1);
    r = pos(:,2);
    BWi = (roipoly(M,c,r));
    [redc, redr] = find(BWi==1);
end


BW = [];
for item = 1:z3(1,1);
    c = [];
    r = [];
    A = Xb{item,1};                      % Define ROIs.
    c = A(:,2);
    r = A(:,1);
    BW = [BW; {roipoly(M,c,r)}];
end


%% Appropriately label individual objects
```

```
prompt_obj = [];
def_answ = [];
for item = 1:z3(1,1);
    int_obj = [];
    int_obj = 'Object ';
    itm_x = num2str(item);
    int_obj = [int_obj, itm_x];
    prompt_obj = [prompt_obj; {int_obj}];
    def_answ = [def_answ; {FileNm}];
end

options.Resize='on';
options.WindowStyle='normal';
obj_label = inputdlg(prompt_obj,Filename,1,def_answ,options);




%%
zs = size(M);
sr = size(redr);
Mask1 = zeros(zs(1),zs(2));
STATS = [];                % Calculate all properties using regionprops
for obj = 1:z3(1,1);
    CObj = BW{obj,1};
    for erdc = 1:sr(1);
        CObj(redc(erdc), redr(erdc)) = 0;  % Subtract exclusion area
    end
    STATS = [STATS; regionprops(CObj, 'all')];
    Mask1 = Mask1 + CObj;  % Mask generation
end


OUT = {'Obj #' 'Area' 'Perimeter' 'Major Axis' 'Minor Axis'};
countr_lbl = 0;
for obj = 1:size(STATS,1);
    if STATS(obj).Area>1000;
        countr_lbl = countr_lbl + 1;
        Ar = STATS(obj).Area;
        Peri = STATS(obj).Perimeter;
        MajAL = STATS(obj).MajorAxisLength;
        MinAL = STATS(obj).MinorAxisLength;
        ObjL = obj_label(countr_lbl);
        ObjC = [ObjL, Ar, Peri, MajAL, MinAL];
        OUT = [OUT; ObjC];
    end
end
if b2 == 1;
    figure, imshow(Mask1);
end

button = questdlg('Save data?','Save?');
switch button
```

```
        case 'Yes'
            b = 1;
        case 'No'
            b = 0;
        case 'Cancel'
            b = 2;
    end
    %%
    if b == 1;
        FileOut = [PATH FileNm '.xls'];
        xlswrite(FileOut, OUT);
    end
    %%
    cd(PATH);
    mkdir('Processed');
    movefile(Filename(),'Processed');

    %%
    loopq = questdlg('Process another sample?','Process another sample?','Yes','No','Cancel','Yes');
    switch loopq
        case 'Yes'
            loop = 0;
        case 'No'
            loop = 1;
        case 'Cancel'
            loop = 2;
    end
end
```

A7: MATLAB image analysis roughness toolset code

Direct download available at:
http://github.com/edfreeburg/MATLAB-roughness-image-analysis/

```
%-----------------------------------------------------------%
%                                                           %
%   SEM Image Texture Analysis                              %
%   Eric Wilcox-Freeburg                                    %
%   Rev 0.2a    Last Modified 02/30/13                      %
%                                                           %
%   Notes: Histogram equalization should yield balanced     %
%   images.  Appears to be a gradient effect still across   %
%   the images, making the edges erroneously "smooth" due   %
%   to low contrast between values along those regions.     %
%   MATLAB help has an example of gradient reduction.       %
%                                                           %
%   Want to add pattern recognition to analyze sample for   %
%   patterns as opposed to box counting methods.            %
%                                                           %
%-----------------------------------------------------------%


clear all;
close all;

%% Point directory for batch processing
ftypes = {'*.jpg','JPEG';'*.bmp','Bitmap';'*.tif','TIF'};
[Filename, PATH, FIndx] = uigetfile(ftypes,'Select image:','C:\MATLAB');
RPF = [PATH,Filename];
switch FIndx;
    case 1;
        FTa = '*.jpg';
    case 2;
        FTa = '*.bmp';
    case 3;
        FTa = '*.tif';
end
cd(PATH);

items = dir(FTa);           % Index images of same file type
params = dir('*.txt');      % Identify parameter files if saved (JEOL format)


%%
OUTComp = [];                           % Preallocate compiled output matrix
for samp = 1:size(items);
    close all;
%% Load image (index by lit in cell array items().name)
    I = imread(items(samp).name);
    [D1, FileNm, D2] = fileparts(items(samp).name);
```

```
%% Histogram equalization
    if size(I,3)==3;
         I = .2989*I(:,:,1)+.5870*I(:,:,2)+.1140*I(:,:,3);
    end
    Ir = imresize(I, [NaN 2048]);
    Eim = histeq(Ir);
    BW1 = im2bw(Eim, 0.66);

    %%
    BWao = bwareaopen(BW1,8000);
    nhood = true(9);
    closeBWao = imclose(BWao,nhood);        % Smooth
    roughMask = imfill(closeBWao,'holes');  % Fill in holes in mask
    I2 = Ir;
    I2(~roughMask) = NaN;                   % Background subtracted raw image
    imshow(I2);

    %%
    button3 = questdlg(items(samp).name,'Skip?','Skip','Cont','Cont');  % Remove error volumes
%%
    switch button3
        case 'Skip'
            b3 = 1;
        case 'Cont'
            b3 = 0;
    end
    %%
    if b3 == 0;
        %% Remove extraneous features.
            button2 = questdlg('Erroneous extra volume data?');  % Remove error volumes
            switch button2
                case 'Yes'
                    b2 = 1;
                case 'No'
                    b2 = 0;
                case 'Cancel'
                    b2 = 2;
            end

        %% Loop to create multiple ROIs for deletion
            delc = [];
            delr = [];
            while b2 == 1;
                imshow(roughMask);
                redc = [];
                redr = [];
                if b2 == 1;
                    erd = impoly;
                    pos = getPosition(erd);
                    c = pos(:,1);
                    r = pos(:,2);
                    BWi = (roipoly(roughMask,c,r));
                    [redc, redr] = find(BWi==1);
```

```
                end
                delc = [delc; redc];
                delr = [delr; redr];
                imshow(I2);
                    button2 = questdlg('Additional erroneous extra volume data?');  % Remove error
volumes
                    switch button2
                        case 'Yes'
                            b2 = 1;
                        case 'No'
                            b2 = 0;
                        case 'Cancel'
                            b2 = 2;
                    end
            end

        %% subtract from roughMask
            zs = size(Ir);
            sr = size(delr);
            Mask1 = zeros(zs(1),zs(2));
            for erdc = 1:sr(1);
                roughMask(delc(erdc), delr(erdc)) = 0;  % Subtract exclusion area
            end
        %% construct new mask
            roughMask = bwareaopen(roughMask,8000);
            I2(~roughMask) = NaN;                   % Background subtracted raw image
            imshow(I2);


        %%
        sigma1 = 10;
        sigma2 = 20;
        Igrad=localnormalize(I2,sigma1,sigma2);
        Imean=mean(Igrad(roughMask));
        imshow(Igrad)

        %% Analyze standard deviation of pixel-neighbors ~ texture
            S = stdfilt(Igrad, nhood);
            S = (S./Imean).*100;                    % RSD
            S2 = S>90;                                    % High RSD = high roughness?
            S3 = (~S2);                             % Inverts to give "smoothness" and removes otolith
edge.
            S3(~roughMask) = 0;                     % Removes background
            imshow(S3);


        %% Calculate object statistics
            PxCount = sum(sum(S3));                 % # of "smooth" pixels
            STATS = regionprops(roughMask,'all');   % Calculates eccentricity
            AreaCount = sum(sum(roughMask));        % Area of ROI
            SmRat = PxCount/AreaCount;              % "Smoothness" ratio.
            Ecc = STATS(1).Eccentricity;            % Pull eccentricity data for fitted elipse.
```

```
        %% Save data to temporary matrix, append to compiled matrix
            OutTemp = {FileNm SmRat Ecc};
            OUTComp = [OUTComp; OutTemp];

        %% Save figures to files
            imwrite(I2,[FileNm '_bcksubt.bmp'],'bmp');  % Save background subtracted figure
            imwrite(S3,[FileNm '_proc.bmp'],'bmp');     % Save processed image
        %% Generate ellipse overlay
            EOv = fig('units','pixels','width',zs(2),'height',zs(1));
            imshow(S3)
            hold on
            phi = linspace(0,2*pi,50);
            cosphi = cos(phi);
            sinphi = sin(phi);

            for k = 1:length(STATS)
                xbar = STATS(k).Centroid(1);
                ybar = STATS(k).Centroid(2);

                a = STATS(k).MajorAxisLength/2;
                b = STATS(k).MinorAxisLength/2;

                theta = pi*STATS(k).Orientation/180;
                R = [ cos(theta)   sin(theta)
                    -sin(theta)   cos(theta)];

                xy = [a*cosphi; b*sinphi];
                xy = R*xy;

                x = xy(1,:) + xbar;
                y = xy(2,:) + ybar;

                plot(x,y,'r','LineWidth',2);
            end
            hold off
            %%
            export_fig(EOv, [FileNm '_overlay.bmp'], '-bmp');
    else
    end
end

%% Create header for output file
header = {'Sample' 'Smoothness Ratio' 'Eccentricity'};
OUTx = [header; OUTComp];
xlswrite('Summary.xls', OUTx, 1);
```

CHAPTER 5

SUMMARY, DISCUSSION, AND CONCLUSIONS

Summary

Following an exhaustive search of the literature, no clearly described pH-stat CO_2-dosing controller was found. It was necessary to first engineer a system that exhibited both high precision and accuracy of pH control. Following significant development, the Reef Keeper Elite system available from Digital Aquatics, L.L.C., was able to maintain pH with great precision (±0.01 pH units) across the study range (8.0 - 7.3) (Wilcox-Freeburg et al., 2013). Additionally, the flexible software built into the controller allowed for the use of custom synthetic seawater based pH buffer systems for enhanced accuracy (Byrne, 1987; Millero et al., 1993). Additionally, the system has been running for over a year collecting data every three seconds to provide a truly continuous pH record. The cost-effective nature of the system (~$408/aquarium replication) allows for low-cost adoption and entry into the field of study.

Fin-fish are a central food source for humans around the world with global catch estimated at over 88 million tons per year (FAO, 2010). As such, an understanding into the impacts of ocean acidification (OA) on fish physiology is paramount. In fish, the main sensory structure for providing hearing, gravitation, and acceleration sense, are the otoliths and so they represent a crucial organ system for the survival of fish. As a

carbonate structure, these structures are susceptible to OA. The impacts of changed carbonate balance on otolith mineralogy must be studied to elucidate the possible changes to function. However, standardized metrics and functional morphological models have not been established. Indeed, studies that highlighted morphology characteristics measured area normalized to control otolith area (Checkley et al., 2009) or calculated circularity index using a metric with no normalized output yielding values greater than 10 (Munday et al., 2011). To help standardize the measurement of morphology characteristics, I developed a set of MATLAB image analysis scripts to objectively and autonomously calculate morphology characteristics, freely available via GitHub (github.com/edfreeburg/MATLAB-Image-Analysis).

To more fully understand intra-genus variability, I completed trials with Clark's clownfish, *Amphiprion clarkii*, and tomato clownfish, *Amphiprion frenatus*. Using the objective analysis tools developed for MATLAB, I generated data exhibiting linear relationships of high significance between otolith circularity index and pH treatment. These first datasets show possible common effects on otolith circularity index. When compared to *Amphiprion percula* results in previous work (Munday et al., 2011), similar trends were found. Unfortunately, the raw data from the Munday et al. (2011) study are not available and so I was unable to investigate the erroneously high circularity index values (15-25). Of particular importance in my study was the significant relations between otolith circularity and aragonite saturation state for *A. clarkii* lapilli. This is the first data presented for lapilli which is the otolith that serves as the key gravitational sensor in fish (Riley and Moorman, 2000). Although the regression coefficient was low,

the high significance of the coefficient suggests an increase in circularity index with respect to acidifying conditions. Given that function is highly dependent upon maculae interaction (Hardison et al., 2005) with the otoliths and that otolith shape and density are assumed to have high correlation to function (Bignami et al., 2013), the change in morphology I found may be indicative of functional change.

In order to more fully understand otolith mineralization changed under OA, otoliths were imaged using scanning electron microscopy (SEM). These electron micrographs allowed for the collection high precision imagery showing crystal form and general habit. The otolith interacts with the sensory maculae along colliculum trench (Nolf, 1985). Imaging the whole otolith at high resolution allowed for the characterization of core development along the colliculum. I developed a rubric-based web scoring survey to crowd-source the analysis of the otoliths, garnering many replicated readings (6 individual readers). After removing statistical outliers, the resultant core scoring data was regressed against pH treatment. The resultant regression exhibited both high significance and correlation, indicating a confident relation between core development and treatment pH. This is the first data to show significant core structural changes in the otolith and I hope to continue this work in the future to establish behavioral endpoints for fitness evaluation.

Discussion

I believe through the development of the pH-stat CO_2-dosing control system, I have provided the OA research community a powerful tool to supplement field studies with single-variable experiments to bolster our understanding of the intricate processes

that feed into the complex physiological changes and thereby interspecies interactions in response to OA. While single-variable studies will not explain large scale regime shifts at the community level, such studies remain paramount to our mechanistic understanding at the individual level. Modeling efforts informing policy decisions are, themselves, informed by laboratory experimentation and field study verification. Therefore, I believe I have developed a sound foundation for the future of OA science.

In the context of the interspecies *A. clarkii* and *A. frenatus* experimentation, I believe these new data corroborates what was seen in *A. percula* suggesting that the impacts of OA will be similar for other members of this genus. I found similar trends in circularity for *A. clarkii* and *A. frenatus* as found in *A. percula* (Munday et al., 2011) but the raw data for the *A. percula* study are not available so no direct comparison of data was possible. Through the comparison of three species within the genus, I believe otolith impacts of OA are comparable and therefore recommend further transgenus experimentation. I found anecdotal evidence that swim behaviors change between species associated with pH treatment. This evidence indicates slower, less directed swim behavior under low pH conditions. It is possible, therefore, that these fish are exhibiting signs of stress including sensory inhibition of their otolith maculae. I did not carry out comprehensive behavioral analyses due to the inability to appropriately characterize standardized methods of analysis.

I believe the trends towards more circular otoliths with OA may have an impact in gravitation sensing. As indicated above, anecdotal evidence suggested inhibition of otolith function resulting in changed swim behavior. This behavioral change appears to

follow morphological trends in lapilli for *A. clarkii* as more circular otoliths should impact the buoy-like nature of the otolith. Signal transduction from the otolith to the maculae is necessarily changed when otolith shape is changed. I believe these are the first data to be collected to offer mechanistic understanding into functional change seen anecdotally. Behavioral change of a lesser magnitude was reported in fish grown exposed to microgravity, roughly analogous to otolith function inhibition (Hilbig et al., 2002; Anken et al., 1998). We believe the behavioral shifts seen anecdotally imply otolith functional change.

Using rubric-based core development scoring methods, we were able to produce significant results specifically analyzing the region responsible for otolith-maculae interaction. These results are the first showing highly correlated and significant results between pH treatment group and core development. In the context of otolith functional work regarding matrix protein/mineralogy (Hardison et al., 2005), we believe we have exposed functional change in macular sensory transduction with respect to otolith core development. This work should form the basis by which further otolith function investigation progresses.

Conclusions

Significant advances to both the fields of Ocean Acidification and otolith studies have been achieved through this dissertation work:

1. A well-described, cost-effective, precise and accurate pH-stat CO_2 dosing controller is now a published standard method (Wilcox-Freeburg et al., 2013).

2. Otolith morphology tools for objective, autonomous analysis exists in a freely distributed format.
3. Intra and interspecies analysis of otoliths yielded significant correlation between circularity and pH treatment group, indicating a common intragenus response
4. Core development has been described in the context of OA for the first time, including significant and highly correlated linear response to pH.

Suggestions for Future Research

Due to the low significance of the regression for *A. frenatus*, additional trials are suggested. Indeed, a large portion of the original stocking did not survive to settlement. While this may be unrelated to experimental parameters, it is important to increase the confidence of this result. Additional intergenus work should also be carried out using the same experimental regimes. There are many additional questions to be investigated such as the impact of long larval periods on otolith development and individual survival. Additionally, it is important to understand the spectrum of responses to OA by making intergenus comparisons. Since clownfish, or damselfish in general, do not represent an important food product, extrapolating the sensory results from these first to economically important species should be prioritized.

Software development for core development analysis is ongoing. Early attempts have yielded data that does not corroborate the scoring method. Since drastic changes in core development are obvious, this software needs to be more finely tuned. We suggest that the software development to continue such that a concise, portable toolkit would be developed for objective, autonomous analysis of core development yielding quantitative

evaluations for further understanding of the impacts of OA on otolith function. Complete discussion on this software's development will be included in the supplemental sections.

While the results of the core scoring study are significant, quantitative measurements must be completed to understand fully the functional interaction with the sensory maculae. 3D modeling technologies are available and we suggest future collaborations to complete these measurements for model development and insight into function.

Tying functional models to behavioral endpoints is also suggested. Standardization of a behavioral test is necessary and development of quantitative metrics will allow for the analysis of such endpoints. We suggest future experimentation and collaborations with behavioral experts to develop protocols for quantitative data collection and analysis.

By coupling these suggested research projects in the context of this dissertation research, we believe it possible to develop a more comprehensive understanding of the functional, behavioral, and possibly ecological impacts of Ocean Acidification on otolith development.

References

Anken, R.H., Ibsch, M., and Rahmann, H., 1998, Neurobiology of fish under altered gravity conditions: Brain Research Reviews, v. 28, no. 1-2, p. 9–18.

Bignami, S., Spongaugle, S., and Cowen, 2013, Response to ocean acidification in larvae of a large tropical marine fish , Rachycentron canadum: Global Change Biology, v. 19, p. 996–1006, doi: 10.1111/gcb.12133.

Byrne, R.H., 1987, Standardization of standard buffers by visible spectrometry: Analytical Chemistry, v. 59, no. 10, p. 1479–1481, doi: 10.1021/ac00137a025.

Checkley, D.M., Dickson, A.G., Takahashi, M., Radich, J.A., Eisenkolb, N., Asch, R., and Checkley, D.M., 2009, Elevated CO2 enhances otolith growth in young fish: Science, v. 324, no. 5935, p. 1683, doi: 324/5935/1683 [pii] 10.1126/science.1169806.

FAO, 2010, FAO yearbook. Fishery and aquaculture statistics.

Hardison, A.L., Lichten, L., Banerjee-Basu, S., Becker, T.S., and Burgess, S.M., 2005, The zebrafish gene claudinj is essential for normal ear function and important for the formation of the otoliths: Mechanisms of Development, v. 122, no. 7-8, p. 949–958.

Hilbig, R., Anken, R.H., Sonntag, G., Höhne, S., Henneberg, J., Kretschmer, N., and Rahmann, H., 2002, Effects of altered gravity on the swimming behaviour of fish: Advances in Space Research, v. 30, no. 4, p. 835–841.

Millero, F.J., Zhang, J.-Z., Fiol, S., Sotolongo, S., Roy, R., Lee, K., and Mane, S., 1993, The use of buffers to measure the pH of seawater: Marine Chemistry, v. 44, p. 143–152, doi: 10.1016/0304-4203(93)90199-X.

Munday, P.L., Hernaman, V., Dixson, D.L., and Thorrold, S.R., 2011, Effect of ocean acidification on otolith development in larvae of a tropical marine fish: Biogeosciences, v. 8, no. 6, p. 1631–1641, doi: 10.5194/bg-8-1631-2011.

Riley, B.B., and Moorman, S.J., 2000, Development of utricular otoliths, but not saccular otoliths, is necessary for vestibular function and survival in zebrafish: Journal of Neurobiology, v. 43, no. 4, p. 329–337.

Wilcox-Freeburg, E., Rhyne, A., Robinson, W.E., Tlusty, M., Bourque, B., Hannigan, R.E., and Wilcox Freeburg, E., 2013, A comparison of two pH-stat carbon dioxide dosing systems for ocean acidification experiments: Limnology and Oceanography Methods, v. 11, p. 485–494

REFERENCES

Aloisi, G., Gloter, A., Kruger, M., Wallmann, K., Guyot, F., and Zuddas, P., 2006, Nucleation of calcium carbonate on bacterial nanoglobules: Geology, v. 34, no. 12, p. 1017–1020, doi: 10.1130/g22986a.1.

Andreassen, J.-P., and Hounslow, M.J., 2004, Growth and aggregation of vaterite in seeded-batch experiments: AIChE Journal, v. 50, no. 11, p. 2772–2782, doi: 10.1002/aic.10205.

Anken, R.H., Ibsch, M., and Rahmann, H., 1998, Neurobiology of fish under altered gravity conditions: Brain Research Reviews, v. 28, no. 1-2, p. 9–18.

Anken, R.H., and Rahmann, H., 1999, Effect of Altered Gravity on the Neurobiology of Fish: Naturwissenschaften, v. 86, no. 4, p. 155–167, doi: 10.1007/s001140050591.

Arai, T., Hirata, T., and Takagi, Y., 2007, Application of laser ablation ICPMS to trace the environmental history of chum salmon Oncorhynchus keta: Marine Environmental Research, v. 63, no. 1, p. 55–66.

Bass, A.H., and McKibben, J.R., 2003, Neural mechanisms and behaviors for acoustic communication in teleost fish: Progress in Neurobiology, v. 69, p. 1–26, doi: 10.1016/S0301-0082(03)00004-2.

Bath, G.E., Thorrold, S.R., Jones, C.M., Campana, S.E., McLaren, J.W., and Lam, J.W.H., 2000, Strontium and barium uptake in aragonitic otoliths of marine fish: Geochimica et Cosmochimica Acta, v. 64, no. 10, p. 1705–1714.

Beier, M., 1998, On the influence of altered gravity on the growth of fish inner ear otoliths: Acta Astronautica, v. 44, no. 7-12, p. 585–591.

Beier, M., and Anken, R., 2006, On the role of carbonic anhydrase in the early phase of fish otolith mineralization: Advances in Space Research, v. 38, no. 6, p. 1119–1122, doi: http://dx.doi.org/10.1016/j.asr.2005.10.027.

Beier, M., Anken, R.H., and Rahmann, H., 2002, Susceptibility to abnormal (kinetotic) swimming fish correlates with inner ear carbonic anhydrase-reactivity: Neuroscience Letters, v. 335, no. 1, p. 17–20, doi: http://dx.doi.org/10.1016/S0304-3940(02)01151-5.

Berman, A., 2008, Biomineralization of Calcium Carbonate: The Interplay with Biosubstrates, *in* Sigel, A., Sigel, H., and Sigel, R.K.O. eds., Metal Ions in Life Sciences, Wiley, West Sussex PO19 8SQ, England, p. 167–205.

Beier, M, & Anken, R. (2006). On the role of carbonic anhydrase in the early phase of fish otolith mineralization. *Advances in Space Research*, *38*(6), 1119–1122. doi:http://dx.doi.org/10.1016/j.asr.2005.10.027

Berge, J.A., Bjerkeng, B., Pettersen, O., Schaanning, M.T., and Øxnevad, S., 2006, Effects of increased sea water concentrations of CO_2 on growth of the bivalve *Mytilus edulis* L: Chemosphere, v. 62, p. 681-687.Bignami, S., Spongaugle, S., and Cowen, 2013, Response to ocean acidification in larvae of a large tropical marine fish , Rachycentron canadum: Global Change Biology, v. 19, p. 996–1006, doi: 10.1111/gcb.12133.

Bignami, S., Spongaugle, S., and Cowen, 2013, Response to ocean acidification in larvae of a large tropical marine fish , Rachycentron canadum: Global Change Biology, v. 19, p. 996–1006, doi: 10.1111/gcb.12133.

Borelli, G., Guibbolini, M.E., Mayer-Gostan, N., Priouzeau, F., De Pontual, H., Allemand, D., Puverel, S., Tambutte, E., and Payan, P., 2003, Daily variations of endolymph composition: relationship with the otolith calcification process in trout: J Exp Biol, v. 206, no. 15, p. 2685–2692, doi: 10.1242/jeb.00479.

Braun, C.B., and Coombs, S., 2000, The overlapping roles of the inner ear and lateral line: the active space of dipole source detection.: Philosophical transactions of the Royal Society of London. Series B, Biological sciences, v. 355, p. 1115–1119, doi: 10.1098/rstb.2000.0650.

Broecker, W. S., Peng, T.-H., & Beng, Z. (1982). *Tracers in the Sea*. Lamont-Doherty Geological Observatory, Columbia University.

Brown, A., Busby, M., and Mier, K., 2001, Walleye pollock Theragra chalcogramma during transformation from the larval to juvenile stage: otolith and osteological development: Marine Biology, v. 139, no. 5, p. 845–851, doi: 10.1007/s002270100641.

Byrne, R.H., 1987, Standardization of standard buffers by visible spectrometry: Analytical Chemistry, v. 59, no. 10, p. 1479–1481, doi: 10.1021/ac00137a025.

Campana, S.E., and Thorrold, S.R., 2001, Otoliths, increments, and elements: keys to a comprehensive understanding of fish populations?: Canadian Journal of Fisheries and Aquatic Sciences, v. 58, no. 1, p. 30–38.

Cech, J.J., Crocker, J., and Crocker, C.E., 2002, Physiology of sturgeon: effects of hypoxia and hypercapnia: Journal of Applied Ichthyology, v. 18, p. 320–324, doi: 10.1046/j.1439-0426.2002.00362.x.

Campana, S.E., Thorrold, S.R., Jones, C.M., Günther, D., Tubrett, M., Longerich, H., Jackson, S., Halden, N.M., Kalish, J.M., Piccoli, P., Pontual, H. de, Troadec, H., Panfili, J., Secor, D.H., et al., 1997, Comparison of accuracy, precision, and sensitivity in elemental assays of fish otoliths using the electron microprobe, proton-induced X-ray emission, and laser ablation inductively coupled plasma mass spectrometry:.

Campbell, J.L., Babaluk, J.A., Cooper, M., Grime, G.W., Halden, N.M., Nejedly, Z., Rajta, I., and Reist, J.D., 2002, Strontium distribution in young-of-the-year Dolly Varden otoliths: Potential for stock discrimination: Nuclear Instruments and Methods in Physics Research Section B: Beam Interactions with Materials and Atoms, v. 189, no. 1-4, p. 185–189.

Carlström, D., 1963, A crystallographic study of vertebrate otoliths: Biol Bull, v. 125, p. 441–463.

Casanova, D., Cirera, J., Llunell, M., Alemany, P., Avnir, D., and Alvarez, S., 2004, Minimal distortion pathways in polyhedral rearrangements: Journal of the American Chemical Society, v. 126, no. 6, p. 1755–1763.Chappard, D., Degasne, I., Hure, G., Legrand, E., Audran, M., and Basle, M.F., 2003, Image analysis measurements of roughness by texture and fractal analysis correlate with contact profilometry: Biomaterials, v. 24, no. 8, p. 1399–1407.

Checkley, D.M., Dickson, A.G., Takahashi, M., Radich, J.A., Eisenkolb, N., Asch, R., and Checkley, D.M., 2009, Elevated CO2 enhances otolith growth in young fish: Science, v. 324, no. 5935, p. 1683, doi: 324/5935/1683 [pii] 10.1126/science.1169806.

Chittaro, P.M., Usseglio, P., Fryer, B.J., and Sale, P.F., 2006, Spatial variation in otolith chemistry of Lutjanus apodus at Turneffe Atoll, Belize: Estuarine, Coastal and Shelf Science, v. 67, no. 4, p. 673–680.

Coghlan, S.M., Lyerly, M.S., Bly, T.R., Williams, J., Bowman, D., and Hannigan, R., 2007, Otolith Chemistry Discriminates among Hatchery-Reared and Tributary-Spawned Salmonines in a Tailwater System:.

Comeau, S., Carpenter, R.C., and Edmunds, P.J., 2014, Effects of irradiance on the response of the coral Acropora pulchra and the calcifying alga Hydrolithon

reinboldii to temperature elevation and ocean acidification: Journal of Experimental Marine Biology and Ecology, v. 453, p. 28–35, doi: 10.1016/j.jembe.2013.12.013.

Cruz, S., Shiao, J.-C., Liao, B.-K., Huang, C.-J., and Hwang, P.-P., 2009, Plasma membrane calcium ATPase required for semicircular canal formation and otolith growth in the zebrafish inner ear: v. 212, no. 5, p. 639–647, doi: 10.1242/jeb.022798.

Cummings, V., Hewitt, J., Van Rooyen, A., Currie, K., Beard, S., Thrush, S., Norkko, J., Barr, N., Heath, P., Halliday, N.J., Sedcole, R., Gomez, A., McGraw, C., and Metcalf, V., 2011, Ocean acidification at high latitudes: potential effects on functioning of the Antarctic bivalve Laternula elliptica. (J. A. Gilbert, Ed.): PloS one, v. 6, no. 1, p. e16069, doi: 10.1371/journal.pone.0016069.

Dauphin, Y., and Dufour, E., 2003, Composition and properties of the soluble organic matrix of the otolith of a marine fish: Gadus morhua Linne, 1758 (Teleostei, Gadidae): Comp Biochem Physiol A Mol Integr Physiol, v. 134, no. 3, p. 551–561, doi: S1095643302003586 [pii].

Dauphin, Y., and Dufour, E., 2008, Nanostructures of the aragonitic otolith of cod (Gadus morhua): Micron, v. 39, no. 7, p. 891–896.de Putron, S.J., McCorkle, D.C., Cohen, A.L., and Dillon, A., 2011, The impact of seawater saturation state and bicarbonate ion concentration on calcification by new recruits of two Atlantic corals: Coral Reefs, v. 30, p. 321-328.

Dickson, A.G., and Goyet, C., 1994, Handbook of Methods for the Analysis of the Various Parameters of the Carbon Dioxide System in Sea Water . Edited by: Handbook of methods for the analysis of the various parameter of the carbon dioxide system in sea water version 2, v. 1994.

Dickson, A. G., Sabine, C. L., & Christian, J. R. (2007). *Guide to best practices for ocean CO2 measurements*. *PICES Special Publication 3* (Vol. 3, p. 191).

Dixson, D.L., Munday, P.L., and Jones, G.P., 2010, Ocean acidification disrupts the innate ability of fish to detect predator olfactory cues: Ecology Letters, v. 13, no. 1, p. 68–75, doi: 10.1111/j.1461-0248.2009.01400.x.

Doropoulos, C., Ward, S., Diaz-Pulido, G., Hoegh-Guldberg, O., and Mumby, P.J., 2012, Ocean acidification reduces coral recruitment by disrupting intimate larval-algal settlement interactions: Ecology Letters, v. 15, p. 338-346.

Dulcic, J., 1995, Estimation of age and growth of sardine, Sardina pilchardus (Walbaum, 1792), larvae by reading daily otolith increments: Fisheries Research, v. 22, no. 3-4, p. 265–277.

Edmunds, P.J., Brown, D., and Moriarty, V., 2012, Interactive effects of ocean acidification and temperature on two scleractinian corals from Moorea, French Polynesia: Global Change Biology, v. 18, p. 2173-2183.

Esbaugh, A., Heuer, R., and Grosell, M., 2012, Impacts of ocean acidification on respiratory gas exchange and acid–base balance in a marine teleost, Opsanus beta: Journal of Comparative Physiology B, v. 182, no. 7, p. 921–934, doi: 10.1007/s00360-012-0668-5.

Fabry, V.J., Seibel, B.A., Feely, R.A., and Orr, J.C., 2008, Impacts of ocean acidification on marine fauna and ecosystem processes: ICES Journal of Marine Science: Journal du Conseil , v. 65 , no. 3 , p. 414–432, doi: 10.1093/icesjms/fsn048.

Falini, G., Fermani, S., Vanzo, S., Miletic, M., and Zaffino, G., 2005, Influence on the formation of aragonite or vaterite by otolith macromolecules: European Journal of Inorganic Chemistry, , no. 1, p. 162–167, doi: DOI 10.1002/ejic.200400419.

FAO, 2010, FAO yearbook. Fishery and aquaculture statistics.

Feely, R.A., Alin, S.R., Newton, J., Sabine, C.L., Warner, M., Devol, A., Krembs, C., and Maloy, C., 2010, The combined effects of ocean acidification, mixing, and respiration on pH and carbonate saturation in an urbanized estuary: Estuarine, Coastal and Shelf Science, v. 88, no. 4, p. 442–449, doi: http://dx.doi.org/10.1016/j.ecss.2010.05.004.

Feely, R.A., Sabine, C.L., Hernandez-Ayon, J.M., Ianson, D., and Hales, B., 2008, Evidence for Upwelling of Corrosive “Acidified” Water onto the Continental Shelf: Science , v. 320 , no. 5882 , p. 1490–1492, doi: 10.1126/science.1155676.

Feely, R.A., Sabine, C.L., Lee, K., Berelson, W., Kleypas, J., Fabry, V.J., and Millero, F.J., 2004, Impact of Anthropogenic CO2 on the CaCO3 System in the Oceans: Science , v. 305 , no. 5682 , p. 362–366, doi: 10.1126/science.1097329.

Fekete, D.M., 2003, Developmental biology. Rocks that roll zebrafish: Science, v. 302, no. 5643, p. 241–242, doi: 10.1126/science.1091171.

Ferrari, M.C.O., Manassa, R.P., Dixson, D.L., Munday, P.L., McCormick, M.I., Meekan, M.G., Sih, A., and Chivers, D.P., 2012, Effects of Ocean Acidification on Learning in Coral Reef Fishes: PLoS ONE, v. 7, p. e31478.

Fisher, R., and Bellwood, D., 2003, Undisturbed swimming behaviour and nocturnal activity of coral reef fish larvae: Marine Ecology Progress Series, v. 263, p. 177–188, doi: 10.3354/meps263177.

Fisher, R., Bellwood, D., and Job, S., 2000, Development of swimming abilities in reef fish larvae: Marine Ecology Progress Series, v. 202, p. 163–173, doi: 10.3354/meps202163.

Frommel, A.Y., Stiebens, V., Clemmesen, C., and Havenhand, J., 2010, Effect of ocean acidification on marine fish sperm (Baltic cod: Gadus morhua): Biogeosciences, v. 7, no. 12, p. 3915–3919, doi: 10.5194/bg-7-3915-2010.

Gattuso, J.P., Frankignoulle, M., Bourge, I., Romaine, S., and Buddemeier, R.W., 1998, Effect of calcium carbonate saturation of seawater on coral calcification: Global and Planetary Change, v. 18, p. 37-46.

Gauldie, R.W., 1999, Ultrastructure of lamellae, mineral and matrix components of fish otolith twinned aragonite crystals: implications for estimating age in fish: Tissue Cell, v. 31, no. 2, p. 138–153, doi: S0040-8166(99)90030-7 [pii] 10.1054/tice.1999.0030.

Gazeau, F., Quiblier, C., Jansen, J.M., Gattuso, J.-P., Middelburg, J.J., and Heip, C.H.R., 2007, Impact of elevated CO_2 on shellfish calcification: Geophys. Res. Lett., v. 34, p. L07603.

Gemperline, P.J., Rulifson, R.A., and Paramore, L., 2002, Multi-way analysis of trace elements in fish otoliths to track migratory patterns: Chemometrics and Intelligent Laboratory Systems, v. 60, no. 1-2, p. 135–146.

Ghosh, P., Eiler, J., Campana, S.E., and Feeney, R.F., 2007, Calibration of the carbonate [`]clumped isotope' paleothermometer for otoliths: Geochimica et Cosmochimica Acta, v. 71, no. 11, p. 2736–2744.

Gillanders, B.M., 2005, Using elemental chemistry of fish otoliths to determine connectivity between estuarine and coastal habitats: Estuarine, Coastal and Shelf Science, v. 64, no. 1, p. 47–57.

Gillanders, B.M., and Kingsford, M.J., 2003, Spatial variation in elemental composition of otoliths of three species of fish (family Sparidae): Estuarine, Coastal and Shelf Science, v. 57, no. 5-6, p. 1049–1064.

Gordon, A.K., Kaiser, H., Britz, P.J., and Hecht, T., 2000, Effect of Feed Type and Age-at-weaning on Growth and Survival of Clownfish Amphiprion percula

(Pomacentridae): Aquarium Sciences and Conservation, v. 2, no. 4, p. 215–226, doi: 10.1023/A:1009652021170.

Grant, J.A., Bishop, N.E., Götzen, N., Sprecher, C., Honl, M., and Morlock, M.M., 2007, Artificial composite bone as a model of human trabecular bone: The implant–bone interface: Journal of biomechanics, v. 40, no. 5, p. 1158–1164.

Grant, J.A., Bishop, N.E., Götzen, N., Sprecher, C., Honl, M., and Morlock, M.M., 2007, Artificial composite bone as a model of human trabecular bone: The implant–bone interface: Journal of biomechanics, v. 40, no. 5, p. 1158–1164.

Haralick, R.M., Sternberg, S.R., and Zhuang, X., 1987, Image analysis using mathematical morphology: Pattern Analysis and Machine Intelligence, IEEE Transactions on, , no. 4, p. 532–550.

Hardison, A.L., Lichten, L., Banerjee-Basu, S., Becker, T.S., and Burgess, S.M., 2005, The zebrafish gene claudinj is essential for normal ear function and important for the formation of the otoliths: Mechanisms of Development, v. 122, no. 7-8, p. 949–958.

Hilbig, R., Anken, R.H., Sonntag, G., Höhne, S., Henneberg, J., Kretschmer, N., and Rahmann, H., 2002, Effects of altered gravity on the swimming behaviour of fish: Advances in Space Research, v. 30, no. 4, p. 835–841.

Hauri, C., Gruber, N., Vogt, M., Doney, S.C., Feely, R.A., Lachkar, Z., Leinweber, A., McDonnell, A.M.P., Munnich, M., and Plattner, G.-K., 2013, Spatiotemporal variability and long-term trends of ocean acidification in the California Current System: Biogeosciences, v. 10, no. 1, p. 193–216, doi: 10.5194/bg-10-193-2013.

Hoegh-Guldberg, O., Mumby, P.J., Hooten, A.J., Steneck, R.S., Greenfield, P., Gomez, E., Harvell, C.D., Sale, P.F., Edwards, A.J., Caldeira, K., Knowlton, N., Eakin, C.M., Iglesias-Prieto, R., Muthiga, N., et al., 2007, Coral Reefs Under Rapid Climate Change and Ocean Acidification: Science , v. 318 , no. 5857 , p. 1737–1742, doi: 10.1126/science.1152509.

Hughes, I., Blasiole, B., Huss, D., Warchol, M. E., Rath, N. P., Hurle, B., … Ornitz, D. M. (2004). Otopetrin 1 is required for otolith formation in the zebrafish Danio rerio. *Developmental Biology*, *276*(2), 391–402. doi:http://dx.doi.org/10.1016/j.ydbio.2004.09.001

Hughes, T.P., Baird, A.H., Bellwood, D.R., Card, M., Connolly, S.R., Folke, C., Grosberg, R., Hoegh-Guldberg, O., Jackson, J.B.C., Kleypas, J., Lough, J.M., Marshall, P., Nystrom, M., Palumbi, S.R., et al., 2003, Climate Change, Human Impacts, and the Resilience of Coral Reefs: Science, v. 301, no. 5635, p. 929–933, doi: 10.1126/science.1085046.

Hughes, I., Blasiole, B., Huss, D., Warchol, M.E., Rath, N.P., Hurle, B., Ignatova, E., David Dickman, J., Thalmann, R., Levenson, R., and Ornitz, D.M., 2004, Otopetrin 1 is required for otolith formation in the zebrafish Danio rerio: Developmental Biology, v. 276, no. 2, p. 391–402, doi: http://dx.doi.org/10.1016/j.ydbio.2004.09.001.

Hüssy, K., 2008, Otolith shape in juvenile cod (Gadus morhua): Ontogenetic and environmental effects: Journal of Experimental Marine Biology and Ecology, v. 364, no. 1, p. 35–41.

Iglesias-Rodriguez, M.D., Halloran, P.R., Rickaby, R.E.M., Hall, I.R., Colmenero-Hidalgo, E., Gittins, J.R., Green, D.R.H., Tyrrell, T., Gibbs, S.J., von Dassow, P., Rehm, E., Armbrust, E.V., and Boessenkool, K.P., 2008, Phytoplankton Calcification in a High-CO_2 World: Science, v. 320, p. 336-340.

IPCC, 2007, Climate Change 2007: Synthesis Report: Intergovernmental Panel on Climate Change, Geneva.

Ishimatsu, A., Hayashi, M., and Kikkawa, T., 2008, Fishes in high-CO2, acidified oceans: *Mar Ecol Prog Ser*, v. 373, p. 295–302.

Kalish, J.M., 1993, Fish Otolith Chemistry: Science, v. 260, no. 5106, p. 279, doi: 260/5106/279 [pii] 10.1126/science.260.5106.279.

Kang, Y., Stevenson, A., Yau, P., and Kollmar, R., 2008, Sparc Protein is required for normal growth of zebrafish otoliths: J Assoc Res Otolaryngol, v. 9, no. 4, p. 436–451.

Kroeker, K.J., Micheli, F., Gambi, M.C., and Martz, T.R., 2011, Divergent ecosystem responses within a benthic marine community to ocean acidification: *Proceedings of the National Academy of* Sciences , v. 108 , no. 35 , p. 14515–14520, doi: 10.1073/pnas.1107789108.

Kurihara, H., Kato, S., and Ishimatsu, A., 2007, Effects of increased seawater pCO2 on early development of the oyster Crassostrea gigas: Aquatic Biology, v. 1, p. 91–98, doi: 10.3354/ab00009.

Langdon, C., Broecker, W.S., Hammond, D.E., Glenn, E., Fitzsimmons, K., Nelson, S.G., Peng, T., Hajdas, I., and Bonani, G., 2003, Effect of elevated CO2 on the community metabolism of an experimental coral reef: Global Biogeochemical Cycles, v. 17, no. 1, p. 14, doi: 10.1029/2002GB001941.

Lombarte, A., & Castellón, A., 1991. Interspecific and intraspecific otolith variability in the genus Merluccius as determined by image analysis. *Canadian journal of zoology*, *69*(9), 2442–2449.

Lychakov, D. V, and Rebane, Y.T., 2005, Fish otolith mass asymmetry: morphometry and influence on acoustic functionality: Hear Res, v. 201, no. 1-2, p. 55–69, doi: S0378-5955(04)00283-7 [pii] 10.1016/j.heares.2004.08.017.

Lychakov, D. V, and Rebane, Y.T., 2000, Otolith regularities: Hearing Research, v. 143, no. 1–2, p. 83–102, doi: http://dx.doi.org/10.1016/S0378-5955(00)00026-5.

Lychakov, D. V, Rebane, Y.T., Lombarte, A., Fuiman, L.A., and Takabayashi, A., 2006, Fish otolith asymmetry: morphometry and modeling: Hear Res, v. 219, no. 1-2, p. 1–11, doi: S0378-5955(06)00117-1 [pii] 10.1016/j.heares.2006.03.019.

Mc Dougall, A., 2004, Assessing the use of sectioned otoliths and other methods to determine the age of the centropomid fish, barramundi (Lates calcarifer) (Bloch), using known-age fish: Fisheries Research, v. 67, no. 2, p. 129–141.

Megalofonou, P., 2006, Comparison of otolith growth and morphology with somatic growth and age in young-of-the-year bluefin tuna: Journal of Fish Biology, v. 68, p. 1867–1878, doi: 10.1111/j.1095-8649.2006.01078.x.

Melancon, S., Fryer, B.J., Ludsin, S.A., Gagnon, J.E., and Yang, Z., 2005, Effects of crystal structure on the uptake of metals by lake trout (Salvelinus namaycush) otoliths: Canadian Journal of Fisheries & Aquatic Sciences, v. 62, no. 11, p. 2609–2619, doi: 10.1139/f05-161.

Miller, J.A., and Kent, A.J.R., 2009, The determination of maternal run time in juvenile Chinook salmon (Oncorhynchus tshawytscha) based on Sr/Ca and 87Sr/86Sr within otolith cores: Fisheries Research, v. 95, no. 2-3, p. 373–378.

Miller, Stephen, and Harley, 2007, Zoology: McGraw-Hill Higher Education, New York.

Millero, F.J., Zhang, J.-Z., Fiol, S., Sotolongo, S., Roy, R., Lee, K., and Mane, S., 1993a, The use of buffers to measure the pH of seawater: Marine Chemistry, v. 44, p. 143–152, doi: 10.1016/0304-4203(93)90199-X.

Millero, F.J., Zhang, J.-Z., Lee, K., and Campbell, D.M., 1993b, Titration alkalinity of seawater: Marine Chemistry, v. 44, p. 153-165.

Morales-Nin, B., 2000, Review of the growth regulation processes of otolith daily increment formation: Fisheries Research, v. 46, no. 1-3, p. 53–67.

Munday, P.L., Dixson, D.L., Donelson, J.M., Jones, G.P., Pratchett, M.S., Devitsina, G. V, and Døving, K.B., 2009, Ocean acidification impairs olfactory discrimination and homing ability of a marine fish: Proceedings of the National Academy of Sciences, v. 106, no. 6, p. 1848–1852, doi: 10.1073/pnas.0809996106.

Munday, P.L., Dixson, D.L., McCormick, M.I., Meekan, M., Ferrari, M.C.O., and Chivers, D.P., 2010, Replenishment of fish populations is threatened by ocean acidification: Proceedings of the National Academy of Sciences, v. 107, no. 29, p. 12930–12934, doi: 10.1073/pnas.1004519107.

Munday, P.L., Hernaman, V., Dixson, D.L., and Thorrold, S.R., 2011, Effect of ocean acidification on otolith development in larvae of a tropical marine fish: Biogeosciences, v. 8, no. 6, p. 1631–1641, doi: 10.5194/bg-8-1631-2011.

Murayama, E., Herbomel, P., Kawakami, A., Takeda, H., and Nagasawa, H., 2005, Otolith matrix proteins OMP-1 and Otolin-1 are necessary for normal otolith growth and their correct anchoring onto the sensory maculae: Mechanisms of Development, v. 122, no. 6, p. 791–803.

Murayama, E., Takagi, Y., Ohira, T., Davis, J.G., Greene, M.I., and Nagasawa, H., 2002, Fish otolith contains a unique structural protein, otolin-1: Eur J Biochem, v. 269, no. 2, p. 688–696, doi: 2701 [pii].

Nan, Z., Chen, X., Yang, Q., Wang, X., Shi, Z., and Hou, W., 2008a, Structure transition from aragonite to vaterite and calcite by the assistance of SDBS: Journal of Colloid and Interface Science, v. 325, no. 2, p. 331–336.

Nan, Z., Shi, Z., Yan, B., Guo, R., and Hou, W., 2008b, A novel morphology of aragonite and an abnormal polymorph transformation from calcite to aragonite with PAM and CTAB as additives: Journal of Colloid and Interface Science, v. 317, no. 1, p. 77–82.

Nehrke, G., and Van Cappellen, P., 2006, Framboidal vaterite aggregates and their transformation into calcite: A morphological study: Journal of Crystal Growth, v. 287, no. 2, p. 528–530.

Nilsson, G.E., Dixson, D.L., Domenici, P., McCormick, M.I., Sørensen, C., Watson, S.-A., and Munday, P.L., 2012, Near-future carbon dioxide levels alter fish behaviour by interfering with neurotransmitter function: Nature Climate Change, v. 2, p. 201–204, doi: 10.1038/nclimate1352.

Nolf, D., 1985, Otolithi piscium, *in* Handbook of Paleoichthyology, Gustav Fischer Verlag, Stuttgart.

Olivotto, I., Capriotti, F., Buttino, I., Avella, A.M., Vitiello, V., Maradonna, F., and Carnevali, O., 2008, The use of harpacticoid copepods as live prey for Amphiprion clarkii larviculture: Effects on larval survival and growth: Aquaculture, v. 274, p. 347–352, doi: 10.1016/j.aquaculture.2007.11.027.

Payan, P., Edeyer, A., de Pontual, H., Borelli, G., Boeuf, G., and Mayer-Gostan, N., 1999, Chemical composition of saccular endolymph and otolith in fish inner ear: lack of spatial uniformity: Am J Physiol, v. 277, no. 1 Pt 2, p. R123–31.

Payan, P., Kossmann, H., Watrin, A., Mayer-Gostan, N., and Boeuf, G., 1997, Ionic composition of endolymph in teleosts: origin and importance of endolymph alkalinity: J Exp Biol, v. 200, no. Pt 13, p. 1905–1912.

Pickering, A. D. (1993). Growth and stress in fish production. *Aquaculture*, *111*(1–4), 51–63. doi:http://dx.doi.org/10.1016/0044-8486(93)90024-S

Pelejero, C., Calvo, E., and Hoegh-Guldberg, O., 2010, Paleo-perspectives on ocean acidification: Trends Ecol Evol,, doi: S0169-5347(10)00044-3 [pii] 10.1016/j.tree.2010.02.002.

Pickering, A.D., 1993, Growth and stress in fish production: Aquaculture, v. 111, no. 1–4, p. 51–63, doi: http://dx.doi.org/10.1016/0044-8486(93)90024-S.

Pierrot, D., Lewis, E., & Wallace, D. (2006). *Program developed for CO2 system calculations* (ORNL/CDIAC.). Carbon Dioxide Information Analysis Center, Oak Ridge National Laboratory, U.S. Department of Engergy, Oak Ridge, Tennessee. doi:10.3334/CDIAC/otg.CO2SYS_XLS_CDIAC105a

Ponton, D., 2006, Is geometric morphometrics efficient for comparing otolith shape of different fish species?: J Morphol, v. 267, no. 6, p. 750–757, doi: 10.1002/jmor.10439.

Popper, A.N., and Fay, R.R., 1993, Sound detection and processing by fish: critical review and major research questions.: Brain, behavior and evolution, v. 41, p. 14–38, doi: 10.1159/000316111.

Popper, A.N., Fay, R.R., Platt, C., and Sand, O., 2003, Sound detection mechanisms and capabilities of teleost fishes, *in* Sensory Processing in Aquatic Environments, p. 3–38.

Pörtner, H.O., Langenbuch, M., and Reipschläger, A., 2004, Biological Impact of Elevated Ocean CO2 Concentrations: Lessons from Animal Physiology and Earth History: Journal of Oceanography, v. 60, p. 705–718, doi: 10.1007/s10872-004-5763-0.

Psenner, R., 1993, Determination of size and morphology of aquatic bacteria by automated image analysis: Handbook of methods in aquatic microbiology. Lewis Publishers, Boca Raton, Florida,, p. 339–346.

Rhyne, A.L., Tlusty, M.F., Schofield, P.J., Kaufman, L., Morris Jr, J.A., and Bruckner, A.W., 2012, Revealing the appetite of the marine aquarium fish trade: the volume and biodiversity of fish imported into the United States: PloS one, v. 7, no. 5, p. e35808.

Ridgwell, A., and Zeebe, R.E., 2005, The role of the global carbonate cycle in the regulation and evolution of the Earth system: Earth and Planetary Science Letters, v. 234, no. 3-4, p. 299–315.

Riebesell, U., Zondervan, I., Rost, B., Tortell, P.D., Zeebe, R.E., and Morel, F.M.M., 2000, Reduced calcification of marine plankton in response to increased atmospheric CO2: Nature, v. 407, no. 6802, p. 364–367.

Ries, J.B., Cohen, A.L., and McCorkle, D.C., 2009, Marine calcifiers exhibit mixed responses to CO2-induced ocean acidification: Geology, v. 37, no. 12, p. 1131–1134.

Riley, B.B., and Moorman, S.J., 2000, Development of utricular otoliths, but not saccular otoliths, is necessary for vestibular function and survival in zebrafish: Journal of Neurobiology, v. 43, no. 4, p. 329–337.

Riley, N. A. (1941). Projection sphericity. *Journal of Sedimentary Research* , *11* (2), 94–95. doi:10.1306/D426910C-2B26-11D7-8648000102C1865D

Ross, P.M., Parker, L., O'Connor, W.A., and Bailey, E.A., 2011, The Impact of Ocean Acidification on Reproduction, Early Development and Settlement of Marine Organisms: Water, v. 3, no. 4, p. 1005–1030, doi: 10.3390/w3041005.

Secor, D.H., and Dean, J.M., 1989, Somatic growth effects on the otolith – fish size relationship in young pond-reared striped bass, *Morone saxatilis*: Canadian Journal of Fisheries and Aquatic Sciences, v. 46, p. 113–121, doi: 10.1139/f89-015.

Sabine, C.L., Feely, R.A., Gruber, N., Key, R.M., Lee, K., Bullister, J.L., Wanninkhof, R., Wong, C.S., Wallace, D.W.R., Tilbrook, B., Millero, F.J., Peng, T.-H., Kozyr, A., Ono, T., et al., 2004, The Oceanic Sink for Anthropogenic CO2: Science, v. 305, no. 5682, p. 367.

Shi, D., Xu, Y., Hopkinson, B.M., and Morel, F.M., 2010, Effect of ocean acidification on iron availability to marine phytoplankton: Science, v. 327, no. 5966, p. 676–679, doi: science.1183517 [pii] 10.1126/science.1183517.

Söllner, C., Burghammer, M., Busch-Nentwich, E., Berger, J., Schwarz, H., Riekel, C., and Nicolson, T., 2003, Control of Crystal Size and Lattice Formation by Starmaker in Otolith Biomineralization: Science , v. 302 , no. 5643 , p. 282–286, doi: 10.1126/science.1088443.

Sorte, C.J.B., Etter, R.J., Spackman, R., Boyle, E.E., and Hannigan, R.E., 2013, Elemental Fingerprinting of Mussel Shells to Predict Population Sources and Redistribution Potential in the Gulf of Maine: PloS one, v. 8, no. 11, p. e80868.

Spero, H.J., Bijma, J., Lea, D.W., and Bemis, B.E., 1997, Effect of seawater carbonate concentration on foraminiferal carbon and oxygen isotopes: Nature, v. 390, p. 497-500.

Spanos, N., and Koutsoukos, P.G., 1998, The transformation of vaterite to calcite: effect of the conditions of the solutions in contact with the mineral phase: Journal of Crystal Growth, v. 191, no. 4, p. 783–790.

Stanley, S.M., Ries, J.B., and Hardie, L.A., 2010, Increased Production of Calcite and Slower Growth for the Major Sediment-Producing Alga Halimeda as the Mg/Ca Ratio of Seawater is Lowered to a "Calcite Sea" Level: Journal of Sedimentary Research, v. 80, no. 1, p. 6–16, doi: 10.2110/jsr.2010.011.

Stupp, S.I., and Ciegler, G.W., 1992, Organoapatites: materials for artificial bone. I. Synthesis and microstructure: Journal of biomedical materials research, v. 26, no. 2, p. 169–183.

Sumanas, S., Larson, J.D., and Miller Bever, M., 2003, Zebrafish chaperone protein GP96 is required for otolith formation during ear development: Developmental Biology, v. 261, no. 2, p. 443–455.

Takagi, Y., Tohse, H., Murayama, E., Ohira, T., and Nagasawa, H., 2005, Diel changes in endolymph aragonite saturation rate and mRNA expression of otolith matrix proteins in the trout otolith organ: Marine Ecology-Progress Series, v. 294, p. 249–256.

Thorrold, S.R., Jones, C.M., and Campana, S.E., 1997, Response of otolith microchemistry to environmental variations experienced by larval and juvenile Atlantic croaker (Micropogonias undulatus): Limnology and Oceanography, v. 42, no. 1, p. 102–111.

Thorrold, S.R., Jones, C.M., Campana, S.E., McLaren, J.W., and Lam, J.W.H., 1998, Trace element signatures in otoliths record natal river of juvenile American shad (Alosa sapidissima):.

Thresher, R.E., 1999, Elemental composition of otoliths as a stock delineator in fishes: Fisheries Research, v. 43, no. 1-3, p. 165–204.

Thresher, R.E., Colin, P.L., and Bell, L.J., 1989, Planktonic duration, distribution and population structure of western and central Pacific damselfishes (Pomacentridae): Copeia, v. 1989, p. 420–434, doi: 10.2307/1445439.

Timmins-Schiffman, E., O'Donnell, M.J., Friedman, C.S., and Roberts, S.B., 2012, Elevated pCO2 causes developmental delay in early larval Pacific oysters, Crassostrea gigas: Marine Biology,, doi: 10.1007/s00227-012-2055-x.

Tohse, H., Murayama, E., Ohira, T., Takagi, Y., & Nagasawa, H. (2006). Localization and diurnal variations of carbonic anhydrase mRNA expression in the inner ear of the rainbow trout Oncorhynchus mykiss. *Comparative Biochemistry and Physiology Part B: Biochemistry and Molecular Biology*, *145*(3-4), 257–264.

Tuset, V. M., Rosin, P. L., & Lombarte, A. (2006). Sagittal otolith shape used in the identification of fishes of the genus Serranus. *Fisheries Research*, *81*(2–3), 316–325. doi:http://dx.doi.org/10.1016/j.fishres.2006.06.020

Vignon, M., 2012, Ontogenetic trajectories of otolith shape during shift in habitat use: Interaction between otolith growth and environment: Journal of Experimental Marine Biology and Ecology, v. 420-421, p. 26–32, doi: 10.1016/j.jembe.2012.03.021.

Waldbusser, G., Voigt, E., Bergschneider, H., Green, M., and Newell, R., 2011, Biocalcification in the Eastern Oyster (*Crassostrea virginica*) in Relation to Long-term Trends in Chesapeake Bay pH: Estuaries and Coasts, v. 34, p. 221-231.

Walther, G.-R., Post, E., Convey, P., Menzel, A., Parmesan, C., Beebee, T.J.C., Fromentin, J.-M., Hoegh-Guldberg, O., and Bairlein, F., 2002, Ecological responses to recent climate change: Nature, v. 416, no. 6879, p. 389–395.

Walther, B.D., and Thorrold, S.R., 2009, Inter-annual variability in isotope and elemental ratios recorded in otoliths of an anadromous fish: Journal of Geochemical Exploration, v. In Press, .

Whitfield, T.T., Riley, B.B., Chiang, M.-Y., and Phillips, B., 2002, Development of the zebrafish inner ear: Developmental Dynamics, v. 223, no. 4, p. 427–458.

Widdicombe, S., and Needham, H.R., 2007, Impact of CO~ 2-induced seawater acidification on the burrowing activity of Nereis virens and sediment nutrient flux: Marine Ecology-Progress Series, v. 341, p. 111.

Wilcox-Freeburg, E., Rhyne, A., Robinson, W.E., Tlusty, M., Bourque, B., Hannigan, R.E., and Wilcox Freeburg, E., 2013, A comparison of two pH-stat carbon dioxide dosing systems for ocean acidification experiments: Limnology and Oceanography Methods, v. 11, p. 485–494

Wilcox-Freeburg, E., Rhyne, A.L., and Hannigan, R.E., 2013, A Picture Is Worth One Thousand Words: Image Analysis Tools For Otolith Studies, *in* Larval Fish Conference 2013, Miami, FL.

Wilson, D.T., and McCormick, M.I., 1999, Microstructure of settlement-marks in the otoliths of tropical reef fishes: Marine Biology, v. 134, p. 29–41, doi: 10.1007/s002270050522.

Wilson, R.W., Millero, F.J., Taylor, J.R., Walsh, P.J., Christensen, V., Jennings, S., and Grosell, M., 2009, Contribution of Fish to the Marine Inorganic Carbon Cycle: Science, v. 323, p. 359-362.

Yoshioka, S., Ohde, S., Kitano, Y., and Kanamori, N., 1986, Behaviour of magnesium and strontium during the transformation of coral aragonite to calcite in aquatic environments: Marine Chemistry, v. 18, no. 1, p. 35–48.

Zhang, Y., and Dawe, R.A., 2000, Influence of Mg2+ on the kinetics of calcite precipitation and calcite crystal morphology: Chemical Geology, v. 163, no. 1-4, p. 129–138.

Zhong, S., and Mucci, A., 1989, Calcite and aragonite precipitation from seawater solutions of various salinities: Precipitation rates and overgrowth compositions: Chemical Geology, v. 78, no. 3-4, p. 283–299.